CALCULATING GROUNDWATER NUTRIENT DISCHARGE TO A STREAM

CALCULATING THE GROUNDWATER CONTRIBUTION OF PHOSPHORUS AND NITROGREN TO A SMALL URBAN STREAM, BARRIE, ONTARIO

By

ALEXANDER FITZGERALD, B.Sc.

A Thesis Submitted to the School of Graduate Studies

In Partial Fulfillment of the Requirements

For the Degree Master of Science

McMaster University

MASTER OF SCIENCE (2012) McMaster University

Earth and Environmental Science Hamilton, Ontario

TITLE: Calculating the groundwater contribution of phosphorus and nitrogen to a small urban stream, Barrie, Ontario

AUTHOR: Alexander Fitzgerald

SUPERVISOR: Professor James E. Smith

NUMBER OF PAGES: xviii, 175

ABSTRACT

Excess nutrients are currently impacting the ecosystem, fisheries, and recreational use of Lake Simcoe. The objective of this study was to determine the importance of groundwater as a pathway for nutrient input during base flow periods to a landfill impacted urban stream in Barrie, Ontario, which flows directly into the lake. A conceptual model of a 28 m reach was created using sediment and water level data, and a groundwater flux map of the stream was creating using heat tracer methods. This data was combined with the shallow groundwater nutrient concentration distribution measured with multi-level piezometers and diffusion samplers to calculate nutrient discharge. Such fine-scale measurements of nutrient discharge using groundwater-based data like these have not previously been reported. The water flux results were then extrapolated to a larger 460 reach (Site B) of Dyment's Creek, and combined with groundwater contaminant data from that reach to derive a crude estimate of nutrient discharge at a larger scale. Heat tracer data estimated total groundwater discharge from Site A ranging from 10 000 to 27 000 L/d. Shallow groundwater soluble reactive phosphorus (SRP) and ammonium concentrations, with maximum values of 1058 μg/L and 37.5 mg/L, respectively, were much higher than stream concentrations of 23 μg/L (SRP) and 0.4 mg/L (ammonium). SRP and ammonium concentrations were higher under reducing conditions, which may be linked with landfill contaminants or naturally-occurring in the sediments. Estimates of total SRP discharge ranged from 3.6 to 8.1 g/d at Site A and 38 to 108 g/d at Site B, and ammonium discharge ranged from 66 to 218 g/d at Site A and 757 to 2043 at Site B. This study showed that groundwater is an important pathway for nutrients to enter Dyment's Creek, and this pathway that must be considered when addressing nutrient input to Lake Simcoe.

Acknowledgements

First, I would like to thank my supervisor Dr. James E. Smith for all of his support and wisdom over my years at McMaster. I would also like to sincerely thank Dr. James W. Roy, my unofficial co-supervisor at the National Water Research Institute at Environment Canada. Thank you for all the time you spent in our countless meetings over the last two years, and for all of your assistance without which this project would not have been possible. I deeply appreciate the opportunity my supervisors have given me, as well as the knowledge and experiences that will be invaluable for the rest of my life.

The field work would not have been possible if not for Melissa Gallina, Lee Grapentine, Urooj Kishor, Braden Kralt, Kristen Leal, and Amanda Malenica. Your great company made the field work fun, on both the nice summer days and the cold winter days. Special thanks to John Voralek- you always had a simple yet eloquent solution to my field problems, and your sense of humour made those long days feel short.

Thank you to Greg Bickerton, Susan Brown, Pamela Collins, Jerry Rajkumar, and John Spoelstra for the help in the lab at Environment Canada and teaching me all about the different instruments. I don't want to know how many DC- samples are on the sample code list.

My time at Environment Canada meant I was not often in my lab at McMaster, but when I was there my lab mates (and Jennie!) made sure I always felt welcome.

Last but not least, I like to thank my family and Kristina for their unconditional love and words of encouragement over the last few years. I could not have done this without you.

Table of Contents

List of Figures

List of Tables

List of Appendices

Note- all appendices hosted online at http://www.sendspace.com/file/i16t92

A. Stream and well levels

B. VFLUX plots

C. Site A contaminant levels

E. SRP peeper plots

E. Ammonium peeper plots

F. Site B contaminant levels

List of Symbols Used for Heat Tracer Equations

A = amplitude of temperature variation

c_s, c_w = specific heat of the soil (s) and water (w)

P = period of temperature variation

q = vertical groundwater flux

q_s = rate of fluid source

t = time

T = temperature of the soil

T_s = temperature of fluid source

v = rate of penetration of the thermal front

z = vertical distance

κ = thermal diffusivity

ρ_s, ρ_w = density of the soil (s) and water (w)

$\Delta\phi$ = time delay between the arrival of the maximum or minimum temperature between two different points

Θ = volumetric water content

1. Introduction

1.1 Lake Simcoe Protection Plan

Lake Simcoe, situated about 100 km north of Toronto, is the largest lake in southern Ontario apart from the Great Lakes. The lake is important to the local economy and environment, generating $200 million per year from recreational use and sport fishing and contains within its watershed provincially significant wetlands and woodlands (Ministry of the Environment, Ontario, 2012). In the 1970s and 1980s, a steady decrease in dissolved oxygen along the bottom of the lake was observed which has been linked to an increase in phosphorus (Nicholls, 1991). The increase in phosphorus caused an increase in phytoplankton production, the decomposition of which used up available oxygen**.** As a result of the declining dissolved oxygen, cold water fisheries, such as lake trout and whitefish, were no longer self-sustaining (Ministry of the Environment, Ontario, 2009). This led to the creation in 1990 of a multi-agency program called the Lake Simcoe Environmental Management Strategy (LSEMS), with the goal of restoring the self-sustainability of these fisheries by reducing phosphorus inputs to the lake. This program led to a reduction in phosphorus inputs to the lake from more than 100 tonnes per year before 1990 to an average of 67 tonnes per year after 1995; however, the cold water fisheries are not yet self-sustaining (Ministry of the Environment, Ontario, 2009).

In 2008, the Ontario government passed the Lake Simcoe Protection Act, outlining the Lake Simcoe Protection Plan, a new multi-agency approach to restore the ecological health of the lake (Ontario Ministry of the Environment, 2009). Phosphorus

was singled out as the most significant cause of water quality deterioration, although the levels of other nutrients, chloride, heavy metals, organic compounds, and pharmaceuticals are also a concern (Ministry of the Environment, Ontario, 2009).

Watershed streams and rivers are estimated to account for 56% of the phosphorus entering the lake (Ministry of the Environment, Ontario, 2009). Several of these streams pass through urban areas in Lake Simcoe's watershed. Elevated concentrations of phosphorus and other nutrients are often seen in urban streams due to the large number and variety of sources (Paul and Meyer, 2001; Dubrovsky et al, 2010). Groundwater is a known source of nutrients to streams and rivers (Banaszuk and Wysocka-Czybasek, 2005; Pretty et al, 2006; Jarvie et al, 2008; Schilling and Jacobson, 2008; Palmer-Felgate et al, 2010), although limited work has been done in urban areas, where the contribution with groundwater may be underrated (Shepherd et al, 2006; Kannel et al, 2008; Mayer et al, 2010; Roy and Bickerton, 2012). Quantifying the nutrient contribution of groundwater discharge to a stream may help determine if it is an important contributor to urban stream nutrient concentrations. If so, groundwater discharge of nutrients is something that needs to be addressed when attempting to reduce stream nutrient concentrations.

1.2 Objective

The objective of this study was to investigate the importance of groundwater as a pathway for nutrient input to Dyment's Creek, an urban stream located in the city of Barrie and in the Lake Simcoe watershed. This was done by quantifying the groundwater mass discharge of relevant soluble forms of phosphorus and nitrogen to a small reach,

and putting this value in the context of nutrient mass discharge of the stream at base flow conditions. The nutrient of primary focus was phosphorus because it is considered the most significant for water quality in Lake Simcoe (Ministry of the Environment, Ontario, 2009). Mass discharge estimates were facilitated through a combination of shallow groundwater sampling for nutrient concentrations and temperature-based groundwater flux measurements. While nutrient discharge can be estimated from a difference in stream concentrations between two points, this does not take into nutrient uptake along the reach, so direct measurements are preferred. There have been few studies that report direct nutrient mass discharge in groundwater to streams and rivers (Jarvie et al, 2008; Rivett et al, 2011; Milosevic et al, 2012). Thus, this study may also have implications for understanding nutrient fluxes to urban streams in general. Some investigation and discussion of the controlling factors of these nutrient discharges will also be made.

1.3 Approach

The research objective was achieved using a field-based study of a small stream reach of Dyment's Creek, an urban stream in Barrie, Ontario that flows directly into Lake Simcoe. Detailed monitoring of a small, 28 m reach (Site A) and additional measurements over a larger reach (Site B) were done from July 2010 to May 2012. Calculation of the mass discharge was restricted to base flow periods, as rain events involved complex changes in flow patterns, which were beyond the scope of this work. The mass discharge calculations are based on measurements made at depths of 5 to 10 cm. Thus, they represent the discharge to the stream interface, but may not fully represent

the mass crossing the interface as there was no direct data on the fate of the nutrients at the interface and what proportion actually entered the stream. The scientific approach included:

1. Development of a conceptual model for groundwater flow of Site A, using collected sediment samples and hydraulic head data.

2. Quantification of groundwater discharge at Site A using heat as a natural tracer, with supporting measurements provided by Darcy velocity calculations and seepage meters.

3. Determination of the nutrient concentrations in stream and groundwater, and the associated water chemistry conditions and potential co-contaminants.

4. Quantification of groundwater nutrient discharges to Site A, if and when they occur, using interpolation of the water flux and concentration data.

5. Extrapolation of the above findings to Site B, combining measured nutrient concentrations and groundwater gradients for this larger reach with water flux data from Site A, along with a discussion of the broader-scale implications of this study to i) Dyment's Creek, ii) the Lake Simcoe Watershed and iii) urban streams in general.

2. Background Literature

2.1. Urban Streams and Groundwater

Streams in urban areas have several unique characteristics. Due to increased imperviousness in the watershed, causing increased runoff, urban streams generally have "flashier" storm hydrographs and have an increased peak flow during high flow events (Paul and Meyer, 2001; Walsh et al, 2005). As the watershed becomes more urban, there is often a morphological change to the stream, a change in sediment supply and texture, and ecosystem changes (Paul and Meyer, 2001; Hatt et al, 2004; Walsh et al, 2005). Higher contaminant levels are observed, including increased nutrient concentrations and a decrease in nutrient uptake. Other common characteristics of urban streams include increased temperature, increased turbidity and increased scour (Walsh et al, 2005). Different effects happen at different levels of urbanization. In some locations there has been a threshold value of urban density before which streams were found to be in good condition, and there is a point after which further urbanization will not degrade a stream any further (Walsh et al, 2005). These effects, common among urban streams, have been termed "Urban Stream Syndrome" (Meyer et al, 2005).

A potentially overlooked aspect of urban stream syndrome is contaminant and nutrient loading with groundwater discharge (Roy and Bickerton, 2012). Urban areas feature a large number of potential sources of groundwater contaminants. Sewers, septic tanks, underground storage tanks, runoff, coal tar sites, gasoline spills, and road de-icing are among the sources of urban groundwater contaminants (Howard and Livingstone,

2000; Vazquez-Sune et al, 2005). A number of studies have been done on contaminant plumes discharging to surface water in urban areas, on scales from small reaches of streams (Dickman and Rygiel, 1998; Conant et al, 2004; Abe et al, 2009; Hamonts et al, 2009; Gardener and Royer, 2010; Mayer et al, 2010; Roy and Bickerton, 2010; Schmidt et al, 2011; Roy and Bickerton, 2012) to city scales (Howard et al, 1996, Williams et al, 1999; Howard and Livingstone, 2000; Shepherd et al, 2006; Ellis and Rivett, 2007; Kelly et al, 2010; Qian et al, 2011; Rivett et al, 2011). A list of studies on contaminants discharging with groundwater to surface water bodies is shown in **Table 2.1**.

Table 2.1 Studies on contaminated groundwater discharge to surface water.

Nutrients	Shaw and Prepas, 1989, Shaw et al, 1990, Reay et al, 1992, Kelly et al, 1993, Ptacek, 1998, Carlyle and Hill, 2001, McCobb et al, 2003, Banaszuk and Wysocka-Czybasek, 2005, Banaszuk et al, 2005, Pretty et al, 2006, Jarvie et al, 2008, Kannel et al, 2008, Schilling and Jacobson, 2008, Palmer-Felgate et al, 2008, Claret and Boulton, 2009, Palmer-Felgate et al, 2010, Smolders et al, 2010, Flores-Lopez et al, 2011, Null et al, 2011, Qian et al, 2011, Stelzer et al, 2011
VOCs	Vroblesky et al, 1996, Kim and Hemond, 1998, Lorah and Olsen, 1999, Lyford et al, 1999, Fryar et al, 2000, Conant et al, 2004, Chapman et al, 2007, Ellis and Rivett, 2007, LaSage et al, 2008, Abe et al, 2009, Hamonts et al, 2009, Schmidt et al, 2011
Metals	Dickman and Rygiel, 1998, Nagorski and Moore, 1999, Coynel et al, 2007, Mayes et al, 2008, Baresel and Destouni, 2009, Rivett et al, 2011
Chloride	Williams et al, 1999, Soulsby et al, 2007, Kelly et al, 2008, Meriano et al, 2009, Gardner and Royer, 2010, Harte and Trowbridge, 2010, Kelly et al, 2010,
Uranium	Winde and van der Walt, 2004, Fritz and Arntzen, 2007
Multiple Contaminants	Howard et al, 1996, Lendvay et al, 1998, Howard and Livingstone, 2000, Shepherd et al, 2006, Lorah et al, 2009, Mayer et al, 2010, Roy and Bickerton, 2010, Roy and Bickerton, 2012

Pollutants from the discharging groundwater will affect stream and spring ecosystems. An increase in nutrients in surface waters can cause eutrophication, increase the chance of toxic algal blooms, and impair drinking water quality (Chambers et al, 2001). Landfill leachate entering a stream in St. Catharines, Ontario may have killed off many native invertebrates, which were then replaced by pollutant-tolerant species (Dickman and Rygiel, 1998). In Toronto, there was a strong correlation between the macroinvertebrate taxa found in groundwater springs and chloride contamination (Williams et al, 1999), and in Angus, Ontario, levels of VOCs in the streambed were above levels for ecological health (Conant et al, 2004). In a screening study of streambed contaminants beneath eight streams across Canada, the least contaminated stream still had at least one contaminant above guidelines in 42% of the samples (Roy and Bickerton, 2012).

Urbanization may also cause changes to the amount of groundwater discharging to streams, and has an inconsistent influence on baseflow (Walsh et al, 2005). Recharge to the local aquifer is reduced as the increase of impervious surfaces causes less infiltration in the watershed (Vazquez-Sune et al, 2005). However, this may be counteracted by leaking sewage systems and water supply pipes, and increased irrigation (Paul and Meyer, 2001). Groundwater may also interact with underground structures, such as basements and subways (Vazquez-Sune et al, 2005). All of these factors are difficult to quantify and make the creation of accurate water balance models difficult for urban areas.

2.2 Groundwater Interactions with Streams

While traditionally (prior to the 1990s) considered separate, groundwater and stream water should be considered a single resource (Winter et al, 1998). If the water table by the stream is higher than the stream surface the groundwater will discharge into the stream, and if the water table by the stream is lower than the stream surface, the surface water will seep into the groundwater. The streams under these conditions are termed gaining stream and losing stream, respectively. It is also possible for groundwater to enter one side of the stream and flow out the other – this is often termed a flow-through stream, or enter from the sides and leak out the bottom.

Orghidan (1955) found a distinct biotope under and adjacent to the streambed, which was related to the mixing of groundwater and stream water. He called this near-stream subsurface region the "hyporheic zone". Subsequently, many different definitions of the hyporheic zone have been proposed or used, including an attempt by Triska et al (1989) to quantify it by considering the hyporheic zone as the subsurface zone with at least 10% advected stream water. A common definition applied by hydrologists is that of Harvey and Bencala (1993), who considered the hyporheic zone as "a subsurface flow path along which water 'recently' from the stream will mix with subsurface water 'soon' to return to the stream". Perhaps the most exhaustive is the following proposed by Krause et al (2010):

> *A temporally and spatially dynamic saturated transition zone between surface water and groundwater that derives its specific physical (e.g. water temperature)*

and biogeochemical (e.g. steep chemical gradients) characteristics from mixing of surface- and groundwater to provide a dynamic habitat and potential refugia for obligate and facultative species.

Hyporheic exchange is controlled by hydrologic conditions such as stream stage and groundwater levels, and geomorphological factors such as topography and stream meanders (Brunke and Gosner, 1997; Lautz et al, 2010). For example, a fluctuating stream stage will change the amount of groundwater-surface water mixing and increase particle residence times (Maier and Howard, 2012). The amount of hyporheic exchange and the extent of the hyporheic zone will vary temporally and spatially along the stream (Cardenas et al, 2004; Anibas et al, 2011). As a boundary between oxidized surface water and often reduced groundwater, the hyporheic zone may have steep and complex chemical gradients (Krause et al, 2010).

Groundwater discharge and hyporheic exchange can have substantial effects on the stream's aquatic ecosystems. For example, during disturbances of the above stream such as high flow or freezing events, the hyporheic zone will act as a refuge for benthic organisms (Robertson and Wood, 2010). Some hyporheic organisms have been detected as deep as 4.2 m below the stream (Stanford and Gaufin, 1974). The amount and direction of groundwater-stream exchange has been shown to influence stream benthic productivity (Hunt et al., 2006). Hyporheic exchange and groundwater discharge may also influence fish spawning sites and provide thermal refuge (Burkholder et al, 2008).

Thus, understanding the flux of groundwater to or from the stream is necessary to help manage stream ecosystems (Woessner, 2000).

2.3. Measuring Groundwater Flux and Discharge

2.3.1 Non-thermal Methods for Measuring Groundwater Flux

One common physical method to measure groundwater flux to a stream is to measure the hydraulic gradient between the subsurface and the stream, and then solve Darcy's Equation, provided a reasonable estimate of hydraulic conductivity can be made. The hydraulic gradient can be determined from the water level in piezometers at different depths below or adjacent to the stream, and the water level of the stream, or by use of a potentiomanometer, which measures both simultaneously. Hydraulic conductivity measurement techniques include slug tests and empirical estimates based on grain size analysis (Kalbus et al, 2006).

Groundwater flux can also be measured directly, such as by seepage meters, first developed by Lee (1977). A bottomless cylindrical container (e.g. bucket or halved storage drum) is installed in the streambed, and a plastic bag is attached to collect the water moving across the interface. Seepage meters are prone to error and must be installed carefully (Rosenberry and LaBaugh, 2008). Another non-thermal method of measuring streambed flux is dilution testing using chemical tracers, in which a solute is added at a known rate and the dilution measured downstream is used to determine the input of groundwater (Constantz et al, 2003; Rosenberry and LaBaugh, 2008). Finally, mass balance approaches are often used, in which stream flow is measured at different

locations along the stream and the difference in flow is attributed to exchanges with groundwater (Kalbus et al, 2006). Mass balance approaches only give the net exchange, and do not give any information if specific areas within the reach are recharge or discharge zones.

2.3.2 Heat as a Groundwater Tracer

Heat can be used as a tracer for streambed flux. Deep groundwater (below about 10 m, depending on location) follows the geothermal gradient and remains a fairly constant temperature year round, while stream water temperature varies diurnally and seasonally (Parsons, 1970). In the summer, for example, stream temperatures will be much higher than groundwater temperatures, and cooler areas of the streambed will often be a result of higher groundwater flux. A major advantage of using heat as a tracer is that thermal properties generally vary less in the field than hydraulic properties (Constantz, 2008). Thermal conductivity, for example, often varies by a factor of two (**Table 2.2**) while hydraulic conductivity may vary by orders of magnitude at one location.

The first studies on using heat as a tracer for streambed flux were done in the 1960s. When trying to measure percolation rates in rice paddy fields, Suzuki (1960) developed a method of using streambed temperatures to quantify vertical water flux. His work was based on using the following equation for heat flow, which assumes a purely vertical flow of heat and water:

$$\frac{\partial T}{\partial t} = \frac{\kappa}{c_s \rho_s} \frac{\partial^2 T}{\partial z^2} - q \frac{c_w \rho_w}{c_s \rho_s} \frac{\partial T}{\partial z} \quad (1)$$

where T represents temperature of the soil, z the depth, κ the thermal diffusivity, c_s ρ_s and c_w ρ_w the specific heat of the soil and water, respectively, t is time, and q is the vertical groundwater flux. Assuming a sinusoidal variation of surface temperature, constant groundwater flux and homogeneous thermal properties, Suzuki developed an analytical solution to the equation using the maximum and minimum temperature at two different depths, the difference of occurrence times between the maximum and minimum temperatures at the two different depths:

$$T = T_{AVG} + A\, e^{-az} \sin(2\pi t/P - bz) \quad (2)$$

where T_{AVG} is the average temperature, A is the amplitude of the temperature variation at the streambed surface, P is the period (24 hours of diurnal variations are used), and a and b are constants that include q. The parameters a and b can then be solved, using two different depths, to give an equation for q. Comparison of observed flux values with theoretical values using temperature information showed that the method was most accurate around a recharge flux of 13 cm/s.

Table 2.2: Thermal conductivity values used in heat tracer studies.

Study	Sediment type	Thermal Conductivity (W/m°C)	Method of Determination
Anibas et al, 2009	fine sand with some organics	1.8	literature values
Briggs et al, 2012	till, sand, gravel	1.4	Estimated based on Lapham (1989)
Constantz et al, 2002	sand	1.5	based on literature range of 1-2
Constantz et al, 2003	fine sand	1	literature values
Fanelli and Lautz, 2008	gravel, sand, silt	1.67	Estimated based on Lapham (1989)
	clay, silt	0.84	Estimated based on Lapham (1989)
Gordon et al, 2012	cobbly, sandy gravel with some silt	2.26	Estimated based on Lapham (1989)
	organic rich silt, sand, and gravel	1.3	Estimated based on Lapham (1989)
Goto et al, 2005	marine sediment	1	literature values
Hatch et al, 2010	sand	1.58	literature values
Kalbus et al, 2007	sandy gravel	2	literature values
Keery et al, 2007	sand and gravel	1.4	literature values
Lautz et al, 2010	silt, fine sand, some areas with gravel	0.63	Estimated based on Lapham (1989)
Mutiti and Levy, 2010	sand and gravel	2	literature values
Schmidt et al, 2006	gravel	2	literature values
Stonestrom and Blasch, 2003	sand	2.2	literature values
	sandy loam	1.8	literature values
	clay loam	1.4	literature values
Vogt et al, 2010	sandy gravel	1.9	literature values

Stallman (1965) found that Suzuki's (1960) work was incomplete, and used different techniques to find a and b (eq 2), and found that they could be solved from field data using the following equations:

$$-az = \log\left(\frac{T_{zm} - T_{AVG}}{A}\right) \quad (3)$$

$$b = 2\pi\Delta\phi/Pz \quad (4)$$

where T_{zm} is the maximum or minimum temperature at depth z, P is the period of the temperature variation, and $\Delta\phi$ is the time delay between the arrival of the maximum or minimum temperature between two different points. The flux can then be solved using equation 5:

$$q = \frac{k(b^2 - a^2)}{c_w \rho_w a} \quad (5)$$

It was shown that diurnal variations could be used to measure percolation rates above about 2 cm/day using this method.

A different way of solving equation 1 was proposed by Bredehoeft and Papadopulous (1965). Steady state conditions and homogenous thermal properties are assumed, and temperatures at different locations are taken. Using these conditions, the solution to 1 is:

$$(T_z - T_0)/(T_L - T_0) = [e^{(\beta z/L)} - 1]/[e^{\beta} - 1] \quad (6)$$

Where T_0 is the temperature closest to the streambed surface, T_L is the temperature measurement at depth L, T_z is the temperature at depth z, and β is a parameter that includes thermal properties, the length L, and the flux q. β can be determined from type curves, giving q. This method is accurate for flux values of 0.1 cm/day and above.

2.3.3 Modern Analytical Solutions

2.3.3.1 Temperature Time Series Methods

There has been recent work building on the research of Suzuki (1960) and Stallman (1965) using the difference in response of sediment temperatures at various depths to diurnal fluctuations to develop new analytical solutions to fluid flow. Laboratory studies have shown a clear decrease in amplitude and a lag in thermal response with decreasing flux and increasing depth (Silliman et al, 1995). This is illustrated in **Figure 2.1**, for streambed temperature at depths of 5, 10, and 20cm.

Continuing work from Stallman (1965), a solution to equation 1 with sinusoidal temperature variations at the surface can be shown as (Goto et al, 2005)

$$T(z,t) = A\exp\left(\frac{vz}{2\kappa} - \frac{z}{2\kappa}\sqrt{\frac{\alpha+v^2}{2}}\right)\cos\left(\frac{vz}{2\kappa} - \frac{z}{2\kappa}\sqrt{\frac{\alpha-v^2}{2}}\right) \quad (7)$$

where $\alpha = \sqrt{v^4 + (8\pi\kappa/P)^2}$ and $v = \frac{\rho_w c_w}{\rho_s c_s} q$. Using equation (7), Hatch et al (2006) solved for the ratio of the amplitude of the temperature variation at two different depths (A_r) and the time lag between the different depths ($\Delta\phi$). This means data for the streambed surface is not necessarily required. **Figure 2.2** shows ΔA and $\Delta\phi$ for a change in depth of measurement.

The equations for the amplitude ratio and the change in the time lag can then be solved for q (Hatch et al, 2006):

$$\frac{\rho_w c_w}{\rho_s c_s} q = \frac{2\kappa}{\Delta z} \ln A_r + \sqrt{\frac{\alpha + v^2}{2}} \quad (8)$$

$$\frac{\rho_w c_w}{\rho_s c_s} q = \sqrt{\alpha - \left(\frac{\Delta \phi 4\pi\kappa}{P \Delta z}\right)^2} \quad (9)$$

As q is on both sides of the equations (embedded in α and v), the equations need to be solved iteratively. Like earlier methods, these equations are dependent on the assumptions that thermal diffusivity and heat capacity are invariant throughout the medium.

Both equations 8 and 9 can be used to solve for flux, though there are strengths and limitations to each. Using the amplitude ratio is best for flux rates between -5 and 3 m/d, with downward flow being negative. The time lag is sensitive to fluxes from -10 to 10 m/d, but cannot determine the direction of flux. It is recommended that the data be filtered so diurnal variations can be more easily seen. Annual variations can be used instead of diurnal variations, which may make it easier to see lower seepage rates.

When tested with synthetic data, using the amplitude ratio was more accurate than using time lag and errors were generally about 2-3% of the flow rate (Hatch et al, 2006). The maximum useful depth for temperature measurements, where a clear diurnal signal can be seen, varies with seepage rates and direction, so temperatures at multiple depths (as opposed to just the two needed) should be taken to ensure two useful signals are acquired.

A similar solution using time series analysis was developed by Keery et al (2007):

$$q = \left(\left(\frac{c_s \rho_s \Delta z}{\Delta \phi c_w \rho_w}\right)^2 - \left(\frac{4\pi \Delta \phi \kappa}{P \Delta z c_w \rho_w}\right)^2\right)^{0.5} \quad (10)$$

Dynamic Harmonic Regression (DHR) is recommended as opposed to band-pass filtering to isolate the diurnal signals, as it is more accurate. DHR has been applied in many recent studies (Lautz et al, 2010; Vogt et al, 2010; Briggs et al, 2012; Gordon et al, 2012). Strengths and limitations of the equations developed by Keery et al (2007) are similar to the Hatch et al (2006) method.

These time series thermal methods have been used successfully to determine i) the spatial and temporal variation of fluxes in streambeds in England (Keery et al, 2007), ii) how groundwater flux varies around small dams (Fanelli and Lautz, 2008; Briggs et al, 2012), iii) the difference in flux beneath geomorphic features in a river (Lautz et al, 2010), iv) the spatial and temporal changes in hydraulic conductivity and how it relates to channel discharge, streambed scour, and deposition (Hatch et al, 2010), v) how various analytical methods compare with each other (Rau et al, 2010). Advantages of the time series method include the ease of data collection and insensitivity to streambed scour, as only the distance between the two sensors needs to be known (Hatch et al, 2006). Hydraulic measurements, such as hydraulic gradient and hydraulic conductivity, are not needed. Months of daily temperature records can be taken fairly easily (Lautz et al, 2010). Unlike steady state analytical methods, temporal changes in groundwater flux can be resolved (Rau et al, 2010). Like other thermal methods, thermal properties need to be

accurately estimated, although these properties vary less in sediments than hydraulic properties such as hydraulic conductivity (Constantz, 2008). Note that in a recent study, velocity estimates using amplitude attenuation were found to be different than those obtained using time lag (Rau et al, 2010), though this may be due to different limitations of the two methods.

2.3.3.2 Steady-state Solutions

The steady state method developed by Bredehoeft and Papadopulous (1965) was used by Schmidt et al (2006) to determine flux, though an objective function was used instead of type curves. This method incorporates the assumption that there is no temperature change, such as diurnal variation, with time. While the distribution and fluxes obtained with this method were reasonable, there was some difference between the data and fluxes calculated using hydraulic properties. The largest differences between the two flux measurements occurred at a depth of 0.1 m, the shallowest depth used for temperature measurement in the study. This is likely because diurnal variations have the strongest influences at shallow depths. This model compared well to transient numerical simulation models for the summer and the winter, but underestimated flux in the fall and overestimated it in the spring (Anibas et al, 2009). Larger water bodies are deemed more suited to this method due to lower hydraulic and thermal fluctuations.

Assuming a constant temperature at depth and a changing temperature at the top of the sediments, a different solution was proposed by Silliman et al (1995). A series of solutions can be shown as:

$$T_2^k = T_0(z) + \sum_{i=1}^{k} \Delta T_2^{i,i-1}(z,\tau) \quad (11)$$

With the above boundary conditions, $\Delta T_2^{i,i-1}(z,\tau)$ has a form similar to the Ogata-Banks solution for solute transport:

$$\Delta T_2^{i,i-1}(z,\tau) = \frac{\Delta T_1^{i,i-1}}{2}\left[erfc\left(\frac{z-C\tau}{2\sqrt{D\tau}}\right) + exp\left(\frac{Cz}{D}\right) erfc\left(\frac{z+C\tau}{2\sqrt{D\tau}}\right)\right] \quad (12)$$

With $\tau = t\text{-}t_i$, ΔT_1 is the difference in temperature at the sediment-water interface at two different times, ΔT_2 is the difference in temperature in the sediment at two different times, T_0 is the initial temperature condition, and C and D are coefficients that include thermal properties and vertical groundwater flux (Rau et al, 2010; adapted from Silliman et al, 1995). The flux can then be found by curve fitting. This method assumes constant vertical flux, and the lower limit for this method is around 0.0072 m/d (Silliman et al, 1995). This method was used to estimate the magnitude of water being lost from a creek to an underlying aquifer (Silliman et al, 1995). This method was found to be a quick and easy way to obtain velocity estimates when the vertical flux is not expected to change with time (Rau et al, 2010).

The following steady-state solution to equation 1 to find the temperature as a function of depth was derived by Turcotte and Schubert (1982, p. 400-401), and can be rearranged to solve for q:

$$q = -\frac{\kappa}{\rho_w c_w z}\ln\left(\frac{T(z)-T_r}{T_0-T_r}\right) \quad (13)$$

T(z) is the temperature at depth z, T_r is the temperature at a depth where dT/dz approaches 0, and T_0 is the temperature at z = 0. This model assumes steady state vertical flow. This equation was initially developed to describe temperature at various depths of groundwater near hydrothermal springs. It was used to find the amount of water flowing through hot springs as well as the permeability of the sediments by estimating a value for q (Turcotte and Schubert, 1982). Equation 13 was then used by Schmidt et al (2007) on temperature data presented by Conant (2004) to compare flux estimates derived by a numerical and an empirical model. As the temperature varied diurnally, average temperature values were used. The dataset has both summer and winter temperatures, but only winter data were used as the streambed temperatures were deemed to be closer to a steady state condition (Schmidt et al, 2007). The flux values were generally lower than those obtained by numerical and empirical models, especially the locations with high groundwater flux. The main advantage of this method is the ease at which a reasonable estimate of flux can be obtained, as flux calculation can be done on a spreadsheet program. Schmidt et al (2007) recommended that the Turcotte and Schubert (1982) model be used when there is a large temperature contrast between groundwater and surface water, when surface water temperatures do not vary spatially, and for locations of groundwater discharge as opposed to recharge. This method was also used by Milosovic et al (2012) to determine seepage rates into a stream near a landfill.

2.3.4. Numerical Modelling

Quantification of groundwater-surface water flux can be done using numerical models. Forward modelling, where simulated temperature is compared with observed temperature or optimization and parameter estimation are done (Constantz, 2008). One of the more common models used is the USGS-designed VS2DH finite difference model, developed by Healy and Ronan (1996). This model solves the following energy transport equation:

$$\frac{\partial}{\partial t}\left[\theta c_w \rho_w + (1-n) c_s \rho_s\right] T = \nabla \kappa(\theta) \nabla T + \nabla \theta c_w \rho_w D_H \nabla T - \nabla \theta c_w \rho_w q T + q_s c_w \rho_w T_s \quad (14)$$

Where θ is the volumetric water content, n is porosity, D_H is hydrodynamic dispersion, q_s is the rate of fluid source, T_s is the temperature of fluid source, and q is the water velocity (Healy and Ronan, 1996). Several parameters need to be estimated, such as heat capacity and thermal conductivity. Only an estimate of hydraulic conductivity is needed, as it is often used for model calibration (Stonestrom and Constantz, 2003). The hydraulic conductivity is adjusted until there is a good match between the temperatures simulated by the model and the observed temperatures. For numerical models, observation data such as stream and streambed temperatures need to be known fairly accurately. It is best if there is variation seen in the streambed data, as both the attenuation of the amplitude of temperature variation and the time lag are needed for a unique solution. This model works for both saturated and unsaturated flow conditions, so it can be used to study ephemeral streams (Stonestrom and Constantz, 2003).

When bromide and heat flow using VS2DH were compared, they were found to yield similar results and were deemed comparable tracers for shallow groundwater (Constantz et al, 2003). VS2DH has also been used to measure stream flow in ephemeral channels in the arid US Southwest (Constantz et al, 2002), used successfully with a previous data set (Schmidt et al, 2007), to compare with an analytical model (Anibas et al, 2009), and to assess hydraulic conductivity changes during storm events (Mutiti and Levy, 2010). For more studies that have used VS2DH in the US Southwest, regarding gaining, losing, and ephemeral streams, see Stonestrom and Constantz (2003).

2.3.5. Other Studies Using Heat as a Tracer

It is possible to combine measurements of temperature and hydraulic properties to obtain an empirical relationship between the two. Conant (2004) took several hundred measurements of streambed temperature in both the summer and the winter. A depth of 20 cm was used, as it was deep enough to only have limited diurnal variations while being shallow enough to be easily accessible. Piezometers and slug tests were used at 34 of the locations to find the hydraulic gradient and hydraulic conductivity, allowing Darcy's Law to be used for an estimate of flux. The flux values were then plotted with the streambed temperatures, and a second order polynomial was fitted to the data. This empirical relationship was then used to calculate flux values for the locations where only streambed temperatures were taken. This method was useful as it easily gave flux data for hundreds of locations, allowing the 2D spatial distribution of flux on the meter scale to be

determined for a reach of a river. The empirical relationship used in this study was both time and site specific (Conant, 2004).

Thermal measurements have also been used to qualitatively describe small scale groundwater-surface water interaction. Temperature data were used to identify losing and gaining reaches of a stream (Silliman and Booth, 1993) and determine the spatial variability of groundwater seeps to a marine bay (Dale and Miller, 2007). In both cases this method was found to be quick and effective.

2.3.6 Data Collection

Studies using analytical methods generally measured streambed temperature at multiple depths and used time intervals between 10 and 90 minutes (**Table 2.3**). Although only one or two data points are needed depending on the method, having measurements from multiple depths allows for more accurate values because there are various sensor depths and spacing that maximize signal strength and minimize noise depending on the seepage rate and direction (Hatch et al, 2006). Various different instruments and configurations have been used, such as temperature loggers suspended in PVC (Hatch et al, 2010) and iron pipes (Keery et al, 2007), probes in perforated PVC pipes (Rau et al, 2010), multilevel stainless steel temperature probes (Schmidt et al, 2006; Kalbus et al, 2007), thermistors at the end of rods (Anibas et al, 2009), and temperature loggers installed in wooden dowels (Fanelli and Lautz, 2008; Lautz et al, 2010). Fiber optic high resolution temperature sensors have recently been used, with the cable

wrapped around a PVC core in a steel tube (Vogt et al, 2010; Briggs et al, 2012), allowing temperature measurements at the centimetre-scale.

Table 2.3: Depths at which temperature is measured for analytical models.

Study	Depths measured (cm)	Time between measurements (min)
Schmidt et al, 2006 and Kalbus et al, 2007	10, 15, 20, 30, 50	60
Keery et al, 2007	10, 20, 30, 40, and 12, 24, 36	-
Fanelli and Lautz, 2008	25	10
Anibas et al, 2009 and Anibas et al, 2011: Aa river Lake 77	 10, 25, 50, and 80 to 120 Many depths, up to 460	 15 15
Hatch et al, 2010	10, 25, 45	15
Rau et al, 2010	15, 30, 45, 60	15
Lautz et al, 2010	5, 15, 25	90
Schmidt et al, 2011	10, 30, 50	60
Briggs et al, 2012	Increments of 1.4 until 75	20
Gordon et al, 2012	10, 50	10

Studies using numerical modelling have monitored deeper depths on average than analytical studies, due to the difference in type of data needed for the different approaches. Depths measured for selected studies can be seen in **Table 2.4.** Several studies using numerical modelling in Stonestrom and Constantz (2003) often used depths below one metre. Temperature loggers were often attached to piezometers near the screened intervals (one field site in Constantz et al, 2002; Constantz et al, 2003; Mutiti and Levy, 2010). For empirical studies and qualitative studies, probes were inserted

directly into the sediment (Silliman and Booth, 1993; Conant, 2004) or temperature loggers placed with spacers in a PVC sleeve (Dale and Miller, 2007).

Table 2.4: Depths used for temperature measurements for select research using numerical models.

Study	Depths measured (cm)
Constantz et al, 2002: Santa Clara River Santa Fe River Bear Canyon	 30, 61, 122, 244 300 40, 60, 110, 210, 310
Constantz et al, 2003	50, 70
Anibas et al, 2009 and Anibas et al, 2011: Aa river Lake 77	 10, 25, 50, and 80 to 120 Many depths, up to 460
Mutiti and Levy, 2010	Between 159 and 884

2.3.7. Problems with Using Heat as a Tracer

One of the assumptions inherent in equation 1 is purely vertical flow. In almost every field setting this is violated because there is almost always some horizontal component to the flow. A study of the analytical equations found that horizontal heat flow is negligible if the flow rates are less than 10% of the vertical flow, and that horizontal and vertical heat flow may be comparable if horizontal groundwater flow is >30% of vertical flow (Lu and Ge, 1996). A numerical model has shown that horizontal flow may result in vertical flow calculations being artificially high in areas of low vertical flow (Roshan et al, 2012). In a laboratory study, when the horizontal flux was twice as large as the vertical flux in recharge conditions, the percent error from using the amplitude ratio method from Hatch et al (2006) was greater than 40% (Lautz, 2010).

When the vertical flux was greater than the horizontal flux, the percent error for the amplitude ratio method was less than 20%.

Other assumptions inherent in the time series analytical models that may easily be violated in the field include a purely sinusoidal temperature variation at the surface and a lack of a thermal gradient. In a lab study with constant vertical flux and a non-sinusoidal temperature signal at the surface, estimates using the amplitude ratio, time lag of the maximum temperature, and time lag of the minimum temperature from the Hatch et al (2006) analytical solution showed different values for vertical upward flux on different days (Lautz, 2010). Errors for the amplitude ratio were usually 5-10%, but were higher at lower flows. In general, errors for the time lag method were much higher, and using the maximum and minimum temperature showed different results with non-sinusoidal surface temperatures. Adding a thermal gradient of 5°C per metre caused a slight shift in temperatures at 25 cm depth in low flow recharge conditions (Lautz, 2010). With such a gradient, errors for the amplitude method were usually under 3%, and for the time lag method were slightly higher. A recent study has shown that the presence of a gas phase in the riverbed may alter thermal properties (Cuthbert et al, 2010), which may cause a large degree of uncertainty when using heat as a tracer. Under ideal field conditions, with purely 1D vertical flow, no temperature gradient in the streambed, and purely sinusoidal temperature oscillations, results from the analytical method developed by Hatch et al (2006) were almost identical to those simulated by a model (Lautz, 2010).

2.3.8 Results from Heat-Derived Flux Studies

2.3.8.1 Spatial Variation

Studies using heat-derived streambed fluxes have found great variability in flux spatially along the streambed (Kalbus et al, 2007; Keery et al, 2007; Fanelli and Lautz, 2008; Hatch et al, 2010), vertically through the streambed (Lautz et al, 2012; Vogt et al, 2010; Gordon et al, 2012; Briggs et al, 2012), and temporally (Anibas et al, 2011; Schmidt et al, 2011; Briggs et al, 2012). Spatial differences in streambed flux were often found around geomorphic features in the streambed (Fanelli and Lautz, 2008; Lautz et al, 2010), in agreement with modeling results of Cardenas et al (2004) on how hyporheic zones change around streambed features. Kalbus et al (2007) found that half of the groundwater discharge to a stream was from only 20% of the area. Similar results were found in the Pine River in Angus, Ontario by Conant (2004), where about 25% of the groundwater discharge to the stream was from just 7% of the area. To further illustrate the variability in discharge conditions, Conant (2004) divided the Pine River site into five different types of flow regions: 1) Short circuit discharge, where natural or anthropogenic conduits exist that allow the groundwater to bypass slower flow paths through the streambed, 2) High discharge, where groundwater moves through areas of high hydraulic conductivity such as sand and gravel deposits, 3) Low to Moderate discharge, making up 85% of the Pine River site where the groundwater must move through a low to moderate hydraulic conductivity zones such as silt layers, 4) No discharge, where there is no hydraulic gradient and no water flowing vertically through the streambed (though it may

still be flowing horizontally), and 5) Recharge, where there is downward flow from the river to the streambed (Conant, 2004).

Some models, such as the one developed by Hatch et al (2006), allow the flux to be calculated at different points vertically at one location along the streambed. Studies using this model have shown differences in streambed flux over depth. Recharge rates were commonly higher closer to the streambed, and decreased with depth (Vogt et al, 2010; Gordon et al, 2012; Briggs et al, 2012). A potential reason may be that flow is vertical into the sediments at the streambed, but becomes more horizontal with depth, potentially returning to the streambed downstream (i.e. hyporheic flow; Gordon et al, 2012). No consistent pattern was seen by Lautz et al (2010), though their site had complex stream morphology and heterogeneous subsurface sediments.

2.3.8.2 Temporal Variation in Streambed Flux

Changes in flux over time will be driven by changes in hydraulic gradients (between groundwater and stream) and hydraulic conductivity. A study in Germany found that on longer time scales, there was a link between streambed flux and hydraulic head, though this was not the case for individual events (Schmidt et al, 2011). The link between flux and stream stage (note: not a direct measure of pressure along the sediment surface) is also dependent on local morphology. Briggs et al (2012) found several locations where the flux decreased with a decrease in stream stage, but also some locations where the opposite was true. This was thought to be due to stream flow becoming more turbulent at these locations (Briggs et al, 2012). Seasonal variations in

flux have been reported as well, with winter having significantly higher groundwater discharge rates than summer in one stream (Anibas et al, 2011). This increase in discharge was predominantly from an increase in the previously low-flux locations, as there was only a moderate increase in discharge from the higher flux locations. The general pattern of discharge was similar between the seasons. In Pine River, Ontario, groundwater discharge was higher during the summer, and a similar spatial pattern was seen in both seasons (Conant, 2004).

Change in streambed flux measurements over time have been combined with hydraulic head measurements to study the change in hydraulic conductivity of sediments over time using Darcy's equation. In a generally gaining river in California, the hydraulic conductivity varied over time, by an order of magnitude or greater (Hatch et al, 2010). In most locations, the hydraulic conductivity showed a positive correlation with stream discharge. Higher stream flow was thought to scour the fine grained sediments off the top of the streambed, increasing hydraulic conductivity. An exception to this was a location where groundwater was found to be discharging into the creek, where the conductivity remained fairly constant (Hatch et al, 2010). Lab results have shown that the relation between change in streambed flux and change in hydraulic conductivity is dependent on both the sediment properties and direction of flux. Related work found that hydraulic conductivity of the streambed was positively correlated with the duration of the rising arm of a stream hydrograph during storms, which is also likely due to scour of fine grained sediments (Mutiti and Levy, 2010).

2.4. Measuring Streambed Contaminant Concentrations

2.4.1 Piezometers

The most common method used to determine if groundwater is contributing contaminants to streams is by using piezometers and stream samples. Many studies have used these to measure streambed nutrient concentrations (Shaw et al, 1990; Reay et al, 1992; Ptacek, 1998; Carlyle and Hill, 2001;, McCobb et al, 2003; Banaszuk et al, 2005; Pretty et al, 2006; Kannel et al, 2008; Palmer-Felgate et al, 2008; Schilling and Jacobson, 2008; Claret and Boulton, 2009; Flores-Lopez et al, 2011; Null et al, 2011; Qian et al, 2011; Stelzer et al, 2011). Studies of nutrient movement often involved piezometers at shallow depths (<30 cm) (Pretty et al, 2006; Claret and Boulton, 2008; Flores-Lopez etal, 2011). Combining piezometer data with sediment samples is also common to measure nutrient concentrations. Sediments have been taken to analyze for phosphorus (Carlyle and Hill, 2001; Flores and Lopez et al, 2011) and nitrogen (Stelzer et al, 2011), in order to have a more thorough understanding of nutrient dynamics of shallow interstitial water. Sediment cores have also been taken to measure levels of metals in the streambed (Dickman and Rygiel, 1998), amount of organic carbon in the sediments (Hamonts et al, 2009), and determine the particle size distribution (Pretty et al, 2006).

A very detailed study of a PCE plume travelling from a dry cleaner to a river in Angus, Ontario was done by Conant et al (2004). Forty-one drivepoint piezometers were installed on the shore and 40 piezeometers were installed in the streambed. These

piezometers were used for some water samples, as well as a Waterloo Profiler at 34 different strategic locations, a "mini-profiler", which is a modified soil vapour probe, was used at 5 locations, and 12 multi-level samplers were used. A drive-point sampler was used to take water samplers at 18 different locations at 0.3 m depth, and at half the sites samples were also taken at depths of 0.1, 0.5, 0.7, and 0.9 metres. (Abe et al, 2009).

Chapman et al (2007) used three different transects to study attenuation of a TCE plume from an industrial site travelling to a river. The first transect was near the source, the second halfway between the source and the river, and the third transect was near the river. Multilevel samplers, the Waterloo Profiler, and piezometer nests were used at 57 different locations along the transects (Chapman et al, 2007). This allowed the plume to be studied at great detail in two dimensions as it crossed each transect.

Integral pumping tests are often used to measure mass flux of contaminants through an imaginary plane in an aquifer (Brockelmann et al, 2003). Wells are placed along a plane perpendicular to groundwater flow direction and pumped either sequentially or simultaneously, and the contaminant concentrations at different points in time are measured. Analytical solutions are then used to determine the average contaminant concentration in the plume (Brockelmann et al, 2003). Integral pumping tests were used by Kalbus et al (2007) to determine the mass of contaminants entering a stream by placing the plane parallel to the streambed at a shallow depth.

A quick and relatively inexpensive way to sample shallow groundwater below a stream at a point in time is the mini-profiler system used by Roy and Bickerton (2010).

Screened drive points attached to polyethylene tubing were drilled into the ground at each location to the desired depth, and then water was pumped out and chemical properties such as dissolved oxygen, electrical conductivity, and pH were measured using hand-held probes. When it was clear that the water being pumped was the groundwater and not surface water, samples were taken for chemical analysis. A disadvantage of this type of sampling, with no permanent or semi-permanent installations, is that longer term monitoring is impossible as samples cannot be reliably taken at the same location at a later date.

Large scale studies were completed to measure the impact of contaminated groundwater on the River Tame in the industrial city of Birmingham, UK. Land quality data from consultants, wells and piezometers to sample groundwater, and surface water samples were all used. In total, 14 industrial deep abstraction wells that were regularly pumped by industry, 20 shallow wells, 96 riverbed piezometers, and 128 surface water samples were taken and analyzed for VOCs (Shepherd et al, 2006; Ellis and Rivett, 2007), trace metals (Shepherd et al, 2006; Rivett et al, 2011), and major ions (Shepherd et al, 2006).

2.4.2 Passive Diffusion Samplers

In order to study shallow interstitial water in greater detail, many researchers use passive diffusion samplers, also known as peepers. Peepers, designed by Hesslein (1976), contain chambers placed at different depths covered by a semi-permeable membrane. The chambers are filled with distilled water and then placed into the streambed. Over a period

of time, which varies depending on factors such as the volume of the chambers, the water in the chambers comes into chemical equilibrium with the surrounding water as contaminants diffuse through the membrane. This allows the sampling of water in the streambed at very small intervals. This is difficult to accomplish when using piezometers, as water may be drawn from different depths when pumping. The water sampled using peepers is a true representative sample of concentrations in the pore spaces, and if there is a difference in concentration between water in the large and small pore spaces, water sampled during pumping may be biased by the water in the larger pores. Unlike piezometer or sampling with a mini-profiling system, peepers are not a snapshot of the conditions at a certain point in time but a weighted average over the sampling period. Peepers are often used in studies of nutrient movement from groundwater to surface water, as biogeochemical interactions at the hyporheic zone are very complex, and may have a large influence on nutrient concentrations. Many of these studies combine peepers with piezometers (Reay et al, 1992; Lorah and Olsen 1995; LaSage et al, 2008; Lorah et al, 2009; Stelzer et al, 2011), which allows researchers to collect samples from both small intervals in the shallow streambed and deeper depths that would not be possible to sample with peepers.

Diffusion equilibrium in thin film (DET) gel probes have also been used to measure streambed nutrient concentrations (Jarvie et al, 2008; Palmer-Felgate et al, 2010). Similar to traditional peepers, DET gel probes consist of a polyacrylamide hydrogel held in a small frame placed in the streambed. Solutes then diffuse into the gel, which can then be cut out and sampled (Jarvie et al, 2008). Another type of passive

diffusion sampler is a passive vapour collector, which consists of chambers filled with inert gas and a membrane that only transmits gases and vapours. These were first used by Vroblesky et al (1991) to measure VOCs in discharging groundwater, and have been used in subsequent studies (Vroblesky et al, 1996; Lyford et al, 2009).

2.4.3 Geophysical Methods

Conductivity measurements have been used as a proxy to measure the concentration of a desired solute. If a clear link between the concentration of the solute and the conductivity of the water is established, geophysical techniques can be a quick and relatively inexpensive way to obtain numerous measurements of concentration, as lab analysis is not required. This method only gives approximate concentration values, and there is the possibility of other ions influencing the conductivity values. Conductivity was used by Meriano et al (2009) to measure the impact of road salt derived chloride discharging to a bay in Pickering, Ontario, and by Fritz and Arntzen (2007) to determine uranium concentrations in the hyporheic zone of a stream in Washington.

The use of geophysical tools can also inform the groundwater sampling strategy at a site. For example, Lyford et al (1999) and Conant et al (2004) used ground-penetrating radar (GPR) in conjunction with boreholes to quickly characterize the subsurface sediment around a stream, identifying zones of higher electrical conductivity and preferential flow paths. Resistivity mapping was done by Heeren et al (2011) for a similar purpose. GPR has also been used to identify subsurface sediment layers with high electrical conductivity which may be caused by contaminated groundwater (Lendvay et

al, 1998). A study by Harte and Trowbridge (2010) used resistivity mapping to locate a chloride plume entering a stream, and Roy et al (2009) used resistivity mapping to locate two groundwater septic plumes entering an alpine lake, which were then sampled for nutrients.

2.5. Measuring Streambed Contaminant Discharge and Flux

2.5.1 Mass Balance Approaches to Measure Contaminant Discharge and Flux

Mass balance approaches have been used to estimate the total discharge of contaminants from groundwater to surface water. Howard and Livingstone (2000) conducted an audit for contaminant sources in the Greater Toronto Area, including both point and diffuse sources. Modelling using FLOWPATH was done, using estimated contaminant loads from these sources and water data from 8000 wells, to determine the total contaminant discharge from sub-surface flow into Lake Ontario. Measuring differences in stream contaminant concentrations at different locations has also been used to estimate contributions of subsurface flow to heavy metal concentrations (Coynel et al, 2007; Baresel and Destouni, 2009). In the Ohio River, it was found that ^{99}Tc had a strong correlation with TCE, so differences in ^{99}Tc concentrations in two locations in the stream were used to estimate the discharge of TCE through the streambed between those two locations (LaSage et al, 2008). Researchers in Birmingham, UK, estimated baseflow using both Darcy's equation and incremental increases in flow measured along the river and combined these estimates with contaminant data to obtain an estimate of contaminant

discharge along a 7.5 km reach of the River Tame (Ellis and Rivett, 2007; Rivett et al, 2011).

2.5.2 Combing Heat Tracer Measurements and Contaminant Concentrations

Several studies have used heat tracer methods to study the dynamics of contaminants discharging to surface water, either for determining contaminant flux or to see the influence of changing water flux on discharging contaminants. In a study of a stream in an industrial area of Germany, Kalbus et al (2007) used the analytical solution proposed by Bredehoeft and Papadopulous (1965) and combined it with integral pumping tests to determine the spatial pattern and magnitude of mass fluxes of organic compounds to the stream. The streambed was subdivided into different zones, first by the location of the wells and then by the location of the temperature measurements. The average contaminant concentration was multiplied by the groundwater flux rate to get a mass flux for each zone, and the fluxes of the different zones were then added together to get a result for the entire study area. Milosevic et al (2012) used the analytical approach by Turcotte and Schubert (1982) and Schmidt et al (2007) combined with concentrations of contaminants in samples collected in seepage meters to measure the mass flux of contaminants from a landfill to a nearby stream. Wells were also installed to locate the plume.

Streambed temperatures of Pine River in Angus, ON obtained from Contant (2004) and analyzed by Schmidt et al (2007) were used as part of a study to investigate chlorinated ethane transformation in streambeds (Abe et al, 2009). The groundwater

discharge rates obtained with the temperature data was combined with microbial analysis and streambed water sampling. Similar work was done by Schmidt et al (2011) to study the interaction between groundwater flux, redox conditions, and contaminant concentrations in the streambed. Redox potential sensors were placed with temperature sensors in the streambed, and two transects of nested piezometers were installed. The temperature time series method developed by Hatch et al (2006) was used to obtain water flux measurements from temperature data. Influence of flux on redox conditions was also explored by Fanelli and Lautz (2008) by comparing heat-derived water flux values with nitrate and sulphate concentrations.

2.5.3 Combining Seepage Meter Data with Contaminant Concentrations

Several studies have combined the use of seepage meters and contaminant concentrations to estimate solute flux to a stream. To estimate nutrient fluxes to an estuary in North Carolina, Spruill and Bratton (2008) placed seepage meters within 2 m of mini-piezometers in the streambed, and compared the results with flux values obtained from Darcy's Law. Similar work was completed by Milosevic et al (2012) to estimate nutrient fluxes from a nearby landfill to a stream. Landmeyer et al (2010) used seepage meters and drive-point samplers to determine the influence of groundwater flux rate on oxygenate attenuation in the hyporheic zone along with calculating the total flux of oxygenates to the stream.

2.6. Groundwater Contaminants Discharging to Streams

2.6.1 Nutrients

Groundwater may be an important contributor of phosphorus (most commonly found as phosphate) and nitrogen to surface waters (Dubrovsky et al, 2010). Phosphate is commonly bound to sediment, but it can then desorb into the streambed water (Eby, 2004). Dissolved phosphates are typically measured as soluble reactive phosphorous (SRP) and soluble unreactive phosphorous. Common anthropogenic sources of phosphorus include wastewater (Ptacek, 1998; Palmer-Felgate et al, 2008) and fertilizer (Banaszuk et al, 2005). Phosphorus in groundwater may also originate from organic or inorganic sediment materials (Carlyle and Hill, 2001; Banaszuk et al, 2005; Banaszuk and Wysocka-Czybasek, 2005; Jarvie et al, 2008; Dubrovsky et al, 2010; Palmer-Felgate et al, 2010). Nitrogen is usually found as nitrate, nitrite, and ammonium. Un-ionized ammonia is typically much lower than ammonium concentrations at the pH levels usually seen in surface water and groundwater (Dubrovsky et al, 2010). Ammonium can by produced by mineralization of organic nitrogen in reducing conditions, and nitrate is produced by nitrification of ammonium by autotrophic bacteria (Brady and Weil, 2004). Both are also sourced from synthetic fertilizers.

Nutrients in groundwater discharging to streams must pass through the hyporheic zone in the streambed, where there may be large biogeochemical gradients. Streambed conditions are a very important influence on the concentration and distribution of nutrients in the streambed, and significant spatial heterogeneity has been seen for both

nutrient concentrations and biogeochemical conditions in the streambed on 15 cm scales (Hunt et al, 1997). A study on nutrient dynamics in the streambed of the Boyne River in Ontario found a weak inverse correlation with soluble reactive phosphorus (SRP) and DO, and found that high SRP (>750 μg/L) occurred in locations with low DO, and low SRP occurred in locations with a DO above 3 mg/L (Carlyle and Hill, 2001). Other studies have found similar results (Schilling and Jacobson, 2008; Flores-Lopez et al, 2011), although in some locations there was no link between SRP and DO (Claret and Boulton, 2008). Elevated SRP values are also often found with high DOC (Schilling and Jacobson, 2008; Flores-Lopez et al, 2011) and Fe^{2+} (Carlyle and Hill, 2001). Other studies have shown that SRP is highest in anaerobic, reducing conditions (Banaszuk et al, 2005; Banaszuk and Wysocka-Czybasek, 2005). Reducing conditions may facilitate the release of P from streambed sediments into the groundwater (McCobb et al, 2003; Banaszuk et al, 2005). This may be partially caused by reduction of Fe^{3+} to Fe^{2+}, as it releases P that was bound to the sediments by Fe^{3+} minerals (Carlyle and Hill, 2001). In some locations, there is evidence of an "oxic cap" of well oxygenated sediments in the top few centimetres of the streambed (up to 10 cm) (Jarvie et al, 2008), which may remineralize SRP before it moves into the stream. However, deoxygenation of the overlying water may release a lot of SRP and ammonium to the stream (Jarvie et al, 2008; Palmer-Felgate et al, 2010).

Ammonium is also common in reducing conditions in the streambed, being positively correlated with DOC and negatively correlated with DO (Schilling and Jacobson, 2008). Ammonium is often found in higher concentrations in the hyporheic

zone than either surface water or groundwater (Pretty et al, 2006; Null et al, 2011; Stelzer et al, 2011). Concentrations of nitrate and SRP are commonly inversely correlated (Ptacek, 1998; Carlyle and Hill, 2001; Qian et al, 2011), which may be due to anaerobic denitrification of groundwater nitrate as it moves through the streambed. Nitrate concentrations have been found to sharply decrease where groundwater conditions change from oxic to anoxic (Stelzer et al, 2011).

Seasonal variation has also been seen in hyporheic SRP, ammonium, and nitrate, though it varies by location (Banaszuk and Wysocka-Czybasek, 2005; Pretty et al, 2006; Kannel et al, 2008; Flores-Lopez et al, 2011; Null et al, 2011; Stelzer et al, 2011). Seasonal changes are often due to differences in temperature, amount of precipitation, and source strength / availability (e.g agriculture sources). In a Polish stream, sediments acted as a SRP reservoir in the winter and spring, and then as a source in the summer as low flows in the stream caused a change in redox conditions (Banaszuk and Wysocka-Czybasek, 2005). A study on a river in New York state near agricultural fields found that an increase in manure spreading on the nearby fields led to an increase in SRP and nitrate entering the stream, and increased rainfall also led to an increase in SRP as the rapid movement of water allowed the SRP to travel quickly from local fields through the groundwater (Flores-Lopez et al, 2011). In Nepal, groundwater phosphorus levels were higher after rainfall events (and during the post-monsoon season than the pre-monsoon season) as the higher rainfall increased the infiltration of organic matter to the streambed at the site, lowering the amount of dissolved oxygen (Kannel et al, 2008).

2.6.2 Volatile Organic Compounds

Substantial spatial and temporal variation has been seen in streambed VOC concentrations. This variation is seen on centimetre scale differences, with concentrations varying by a factor of 10 000 over a few metres (Conant et al, 2004). A study in Halifax, NS, sampled groundwater at distances of 8-15m along a stream and found large differences in VOC concentration between adjacent sites, in the case of chlorinated solvents on the order of several thousand µg/L between three sites (Roy and Bickerton, 2010).

VOCs are often transformed as they move through the hyporheic zone, as the mixing surface water creates very different conditions than those found in groundwater. In one industrial area, cDCE, a compound not used by local industry and formed by dechlorination of TCE was found, implying degradation (Ellis and Rivett, 2007), and dechlorination products are often found at other sites (Conant et al, 2004, Hamonts et al, 2009). Whether or not biodegradation occurs in the hyporheic zone seems to be controlled by the physical and chemical composition of the streambed sediments. Conant et al (2004) found that very little biodegradation occurred in the 195 m PCE plume travelled that through the subsurface to the streambed and significant biodegradation occurred in the top 2.5 m of the streambed. Fifty-four percent of the discharge area of the plume was totally transformed at the streambed, with no PCE and only daughter products such as TCE, cDCE, and VC. At one location, the PCE concentration at a depth of 1.2 m was 3639 µg/L while the concentration of degradation products was 557 µm/L, and at a

depth of 1.05 m the concentrations were 125.6 µg/L and 3377 µg/L respectively (Conant et al, 2004). PCE was only seen in three high discharge areas. An overall decrease in VOC concentration may be due to further biodegradation breaking down daughter products and producing only carbon dioxide and water (Conant et al, 2004). A study of an oxygenate spill in Long Island, NY, found that levels decreased in the hyporheic zone (Landmeyer et al, 2010). Biodegradation of these compounds was shown to be controlled by dissolved oxygen levels, which can increase dramatically once groundwater starts mixing with surface water. Physical effects such as dilution and dispersion were also causes of decreased contaminant levels (Landmeyer et al, 2010). In Birmingham, UK, degradation was thought to have occurred as the plume moved through the aquifer, as there was little evidence of it in the riverbed (Ellis and Rivett, 2007). The riverbed sediments had a high hydraulic conductivity, low organic carbon content, and were under aerobic conditions, as opposed to the riverbed in Angus which had a low saturated hydraulic conductivity and anaerobic conditions (Conant et al, 2004). A later study in Angus found that redox conditions and soil organic matter are the major factors determining the extent of dechlorination at the site (Abe et al, 2009). Complete dechlorination of PCE to ethane and ethane only happened in strongly reducing areas. When comparing the impact of changing flux on MCB concentrations in the streambed, it was found that during groundwater discharge conditions MCB concentrations were unaffected by changes in flux and redox conditions, but in groundwater recharge conditions MCB concentrations were lowered possibly due to the downward flow of

surface water increasing the amount of dissolved oxygen and causing degradation of MCB (Schmidt et al, 2011).

Discharge to small surface water bodies as a plume moves from a source to a river can also cause significant attenuation. Chapman et al (2007) found that TCE concentrations fell by about 90% between two transects, and almost disappeared where the plume intersected with the river. There is a pond between the first two transects where there was significant VOC discharge. Concentrations down-gradient of the pond were very low, mostly due to VOC lost to the atmosphere as the plume moved through the pond. There were a couple of minor streams along the plume's path, and overall it was found that half of the plume discharges into these streams and enters the river from there, while the other half was either lost to the atmosphere or through dechlorination. Isotope data showed evidence of some degradation in the aquifer, and cDCE, a daughter product, was found. Parts of the aquifer were favourable for dechlorination reactions, which would transform the contaminants to non VOC compounds (Chapman et al, 2007).

2.6.3 Metals and Chloride

Different chemical conditions in the streambed will also affect concentrations of some heavy metals such as arsenic. Nagorski and Moore (1999) found that arsenic concentrations in the hyporheic zone under a river in Montana were higher than in either the surface water or the groundwater. A larger proportion of the arsenic in the hyporheic zone was Ar(III) compared to the less toxic As(V). The increased arsenic is thought to come from the streambed sediments, which are old mine tailings, due to the reducing

conditions (Nagorski and Moore, 1999). In Birmingham, UK, a large-scale study found the impact of metals on the water quality River Tame from discharging groundwater to be low despite the area's industrial history (Rivett et al, 2011).

Chloride is an especially common contaminant in urban areas (Mullaney et al, 2009). Chloride has been observed moving from groundwater to streams and springs (Kelly et al, 2008; Gardiner and Royer, 2010; Hatre and Trowbridge, 2010) with negative impacts on local fauna (Williams et al, 1999). Road salt is a large contributor of urban chloride contamination in northern cities (Mullaney et al, 2009), and a Toronto study found that about half of the chloride applied as road salt to a major highway travelled through a shallow aquifer to a nearby lagoon (Meriano et al, 2009).

2.6.4 Effect of Groundwater Residence Time on Redox Conditions

The redox conditions in the streambed were controlled by the residence time of the groundwater in the streambed, as sulphate reducing and/or methanogenic conditions were only found when the residence time was more than 10 days (Abe et al, 2009). In Birmingham, UK, the only site that showed some degradation was the one site having finer grained sediments and organic matter (Ellis and Rivett, 2007), and a TCE plume near a river in Maine was only found discharging where there were no fine grained sediments (Lyford et al, 1999). Claret and Boulton (2008) found that sediments with increased hydraulic conductivity generally had shallower gradients in biogeochemistry, where a lower residence time may have indicated less time for nitrification and denitrification to occur, also inhibiting microbial activity because faster moving water

causes a shorter contact time between microbes and nutrients in the groundwater. Abe et al (2009) compared streambed flux to redox conditions and found a link between groundwater residence time and redox conditions. In that study, sulphate reducing and methanogenic conditions only occurred where the groundwater residence time was longer than 10 days. Similar results were seen by Schmidt et al (2011), where there was a clear, linear relation between temperature derived flux values and redox conditions at a depth of 0.1 m. At deeper depths, the redox conditions did not show much variation and were similar to the levels seen in the local groundwater. Such a linear relationship was not observed when only comparing the redox conditions to hydraulic gradients (Schmidt et al, 2011).

2.6.5 Groundwater Contaminant Flux Estimates

Combining water flux data and contaminant data has allowed researchers to calculate mass discharge to streams. Kalbus et al (2007) found the mass discharge of MCB to be about 50 mg/d from the streambed under a 60 m reach of a stream in Germany. Spatial variability of the mass discharge could not be determined because integral pumping tests were used, which give an average contaminant concentration for the study area. Work by Milosovic et al (2012) combining water flux data and concentrations from seepage meters found chloride discharges of about 30 kg/d and ammonium discharges of up to 2 kg/day from 40 m reaches of streams. When compared with the differences in concentration between the beginning and end of the different reaches, the apparent groundwater contaminant contribution was lower than the total

difference. Potential explanations could be an underestimation of groundwater contributions, an overestimation of the contaminant flux in the stream, or other contaminant routes such as surface runoff or seepage from small ponds (Milosevic et al, 2012). McCobb et al (2003) combined groundwater flow models and shallow sediment SRP concentrations and calculated a mass discharge of 0.87 kg/d of SRP from a nearby plume to a pond. The mean SRP flux calculated by McCobb et al (2003) was 142 mg/m^2d.

Using seepage meters and piezometer data, Spruill and Bratton (2008) found that groundwater contributed 95 mg/m^2d of nitrogen (as ammonium) and 18.9 mg/m^2d of phosphorus to a nearby estuary over an area of 1420 km^2, which represents less than 6% of the total input to the estuary for both of the nutrients. Maximum fluxes from individual locations were 85 mg/m^2d for phosphorus and 551 mg/m^2d for nitrogen. These areas of high discharge may have an impact on local flora and fauna. Rivett et al (2011) found flux values of 933 mg/m^2d of phosphate and 0.02 mg/m^2d of nitrate discharging to the River Tame. The study area was a 7.4 km reach of the river, with a streambed area of 0.09 km^2, passing through a heavily industrialized and urbanized area of Birmingham, UK.

Lower SRP flux values of 0.06 to 0.16 mg/m^2d were estimated by Shaw et al (1990) to Narrow Lake, a 1 km^2 lake located in Alberta. This nutrient loading was higher than any other source of nutrients to the lake, and 7 times higher than diffusion from lakebed sediments. A mix of mass balance, Darcy flux calculations, seepage meters, and

lakebed SRP concentrations were used to calculate the flux. These numbers are similar to values seen by Belanger and Mikutel (1985) (mean 0.13 mg/m^{2}d) to a 5 km^2 lake in Florida, using similar methods.

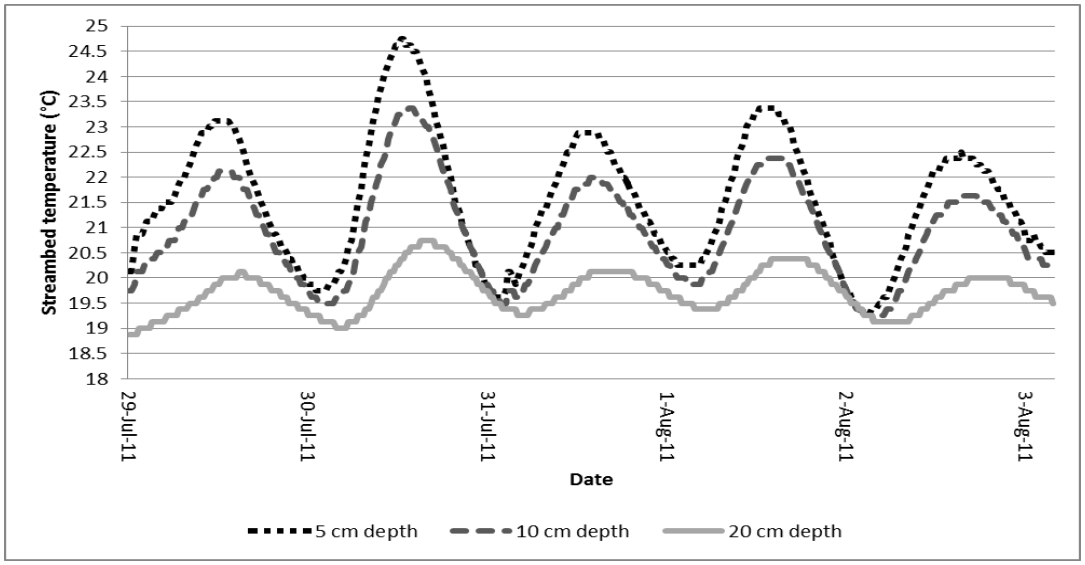

Figure 2.1: Change in the diurnal temperature signal with depth.

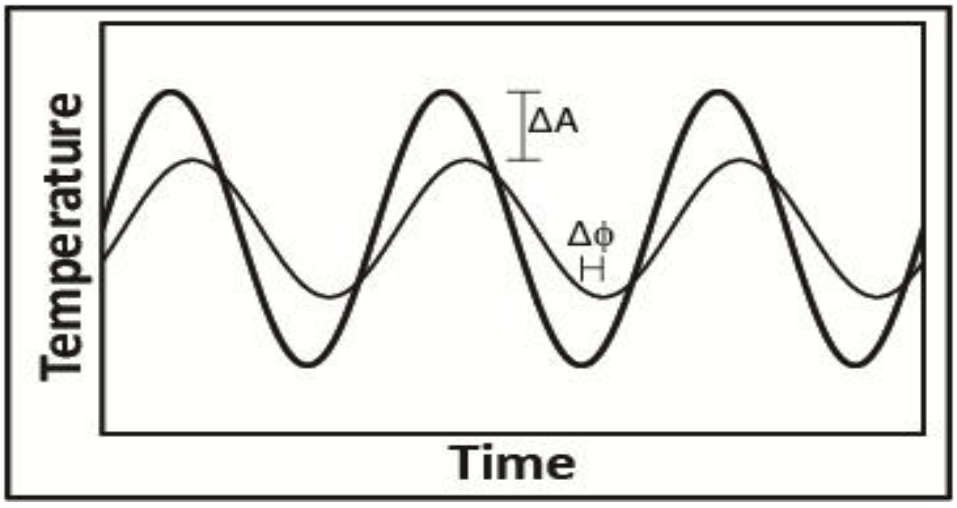

Figure 2.2: Difference between the amplitude (A) and phase (ϕ) of the diurnal temperature signal in the streambed at two different depths.

3. Study Area

This study was performed on Dyment's Creek in Barrie, Ontario, Canada. Barrie has a population of 135 000 and is situated on the shore of Lake Simcoe's Kempenfelt Bay (**Figure 3.1**). Barrie is the largest city in the Lake Simcoe watershed, and is located about 100 km north of Toronto in Simcoe County. Other urban areas in the watershed include Orillia, Newmarket, and Bradford. Dyment's Creek is about 5 km long, with a 5 km^2 watershed. The creek originates in parkland and residential areas near the City of Barrie's current landfill (Sandy Hollow Landfill), and flows north to south. It then curves east and passes through commercial and industrial parks and a major freeway (Highway 400), and moves into residential neighborhoods in the central, older part of the city, passing historic landfills in the vicinity of Brock park, and discharges into Lake Simcoe (**Figure 3.2**).

Previously, a screening study was done along a roughly 1000 m reach of the creek, from Highway 400 to Bradford Street, near where it enters the lake, to determine levels of contaminants in the shallow groundwater that were potentially discharging to Dyment's Creek (Roy and Bickerton, 2012). Contaminants that were found to exceed aquatic guidelines and were therefore a probable risk to aquatic organisms include chloride, nitrate, nitrite, ammonium, metals, and VOCs. The contaminants were widespread, as 30 of the 99 locations studied had at least two contaminant groups (organized into salts, metals, metalloids, petroleum compounds, chlorinated ethenes, other solvent compounds, pesticides, and nitrogen compounds) above aquatic guideline

levels. The only contaminant group that was not found to be a probable risk anywhere in the creek was pesticides, although only select ones were analyzed (Glyphosate, AMPA, 2,4-D, Picloram, and MCPA). Ammonium, nitrate, and nitrite were found to exceed aquatic guidelines, and phosphorus levels were above those considered a risk for hypereutrophic conditions (Roy and Bickerton, 2012). The presence of the sweetener saccharin, which is no longer commonly used in Canada, suggests that old landfills along the creek may be contributing some of these contaminants (Van Stempvoort et al, 2011), although there are many other potential sources. Historic point sources may include dry cleaners, gas stations, sewers, a tannery, and other industry.

Our study focuses on a reach of Dyment's Creek found to have high levels of nutrients by Roy and Bickerton (2012). The width of the stream in the study area ranges from about 2 to 6 m and the depth during base flow conditions ranges from about 5 to 50 cm. The several historic landfills, in use in the early 1960s, are shown in **Figure 3.3**. The creek is tree-lined through most of the study area, and passes under roads in culverts. Roads, residential backyards, storage units, and parks are nearby the creek in the study area. The stream supports a number of fish, amphibians, birds, and invertebrates. Garbage, some of which may be from illegal dumping, can be seen in the stream, along the shore, and buried in the streambed. For this study, the area is divided into two sections, Site A and Site B (**Figure 3.2**). More detailed work was done at Site A, the smaller site.

Site A is located at 44.378180 N, 79.69440 W, is 28 m long, and has a streambed area of 115 m^2. The streambed is generally sandy with some silty areas, and there are several large boulders and fallen tree branches (up to 50 cm diameter) in the streambed. The stream bank on the northern side is lower than on the southern (about 50 cm compared to about 80 cm). The elevation on this side does not increase noticeably until about 10 m away from the creek, where there is a steep 5 m hill. Several apparent groundwater seeps are visible at the base of this hill and right by the creek. There are no road crossings over Site A, and the stream is fairly straight.

Site B is about 450 m long, located just upstream of Site A. As with Site A, the streambed is mostly a mix of sands and silts, with some boulders and tree branches. The topography at the edge of the stream is variable, and at one location for about 100 m there is a concrete wall right by the southern bank of the stream. There are two road crossings along Site B, as well as another just upstream. There is a sharp, almost 90° curve in the stream near the upstream end of the site.

Figure 3.1: Location of Barrie within southern Ontario (Google, 2012).

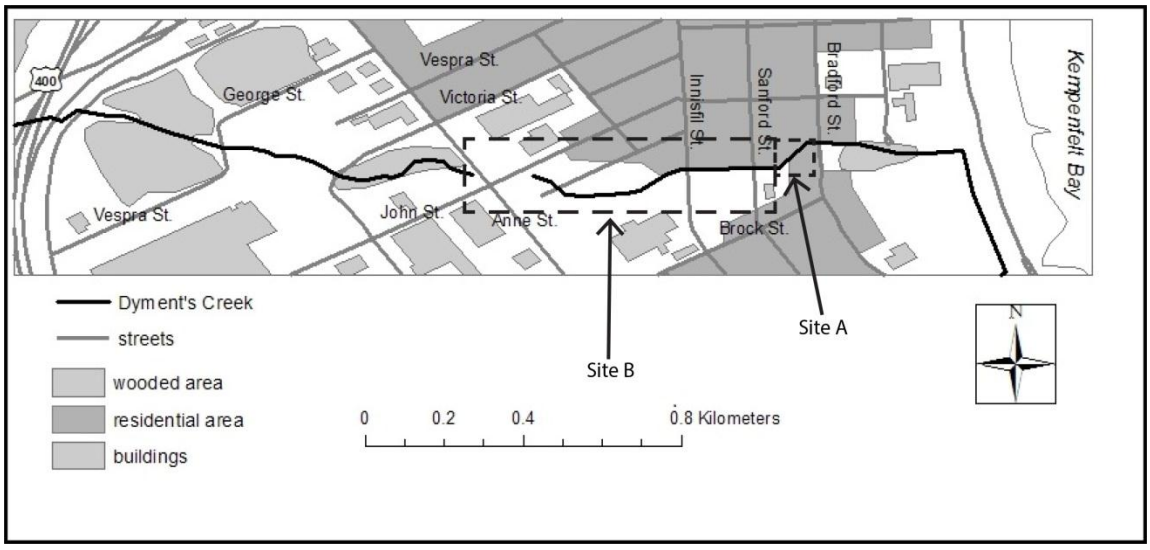

Figure 3.2: Map of portion of Dyment's Creek studied by Roy and Bickerton (2012), from highway 400 to Site A, through old downtown of city of Barrie.

Figure 3.3: Location of former landfills (shaded in orange) along Dyment's Creek (light blue line) in relation to Site A (red box) and B (purple box) (Google, 2012).

4. Methods

4.1. Water Levels

4.1.1 Stream Stage and Discharge

Stream stage was determined at the downstream end of Site A using a pressure transducer (Micro-Divers Model DI601, Schlumberger Limited). Pressure (in units of cm H_2O) and temperature were measured every 15 minutes with an accuracy of +/- 1 cm of water (cm H_2O) and 0.1 °C, and a resolution of 0.2 cm H_2O and 0.01 °C. A Baro-Diver (Slumberger; Accuracy of +/- 0.5 cm H_2O, resolution of 0.1 cm H_2O) was installed at the site to allow for barometric pressure compensation of stream and well pressure readings.

Stream discharge was calculated at a single transect at Site A **(Figure 4.1)** weekly to bimonthly (total 17 times) throughout the study period using the mid-point method (Turnipseed and Sauer, 2010), with readings every 10 cm across the transect. A vertically-averaged stream velocity, determined using a flow meter (Global Water Model FP101; range of 0.1-4.5 m/s, accuracy of 0.03 m/s) was calculated by moving it up and down at a consistent pace, and water depth at a spacing of 10 cm was measured along each transect. Stream stage-discharge curves were then created so the stream discharge could be estimated in between discharge measurement points.

4.1.2 Water Level Wells

Twelve wells, labelled P1-P12, were installed using a direct-push technique near the stream at Site A to measure hydraulic head **(Figure 4.1)**. The wells were made of

PVC and slotted for the bottom 10 cm. Six of the wells, labelled P1-P6, had an ID of 2.1 cm, and six of them, labelled P7-P12, had an ID of 2.7 cm. The wells were installed on May 31, 2011 and pressure transducers were installed on June 28, 2011 (Micro-Divers Model DI601, Schlumberger). On April 13, 2012, two additional wells, labelled DWN and DWS, were installed to depths of 457 cm and 487 cm on each side of the stream (**Figure 4.1**) and pressure transducers (Micro-Divers Model DI601, Schlumberger) were placed into the wells. Bentonite clay was used to seal the edge around each well. The depth of the screened section relative to our datum (the lowest stream stage point measured at the stream stage location) of the wells are shown in **Table 4.1**. Pressure transducers (Micro-Divers Model DI601, Schlumberger) were also placed in two municipal monitoring wells about 100 m upstream of the site on June 15, 2011, with measurements being taken every 15 minutes at depths of 4.86 m and 6.02 m relative to the datum.

In November, 2011, slug tests were performed on P1-P12 to determine the field hydraulic conductivity of the surrounding sediments. For this, pressure transducers (Micro-Divers Model DI601, Schlumberger) were set to measure water levels at every half second. Water was displaced by using a metal slug or by quickly adding water to the wells, and the results were analyzed as described by Hvorslev (1951). For L/R = 8, as was the case with the wells used, the shape factor was determined by Hvorslev and the resulting equation to calculate hydraulic conductivity is:

$$K = \frac{r^2 \ln(\frac{L}{R})}{2LT_0} \quad (15)$$

where r is the radius of the well, L is the length of the well intake, R is the radius of the well intake, and T_0 is the time lag, defined as the time it takes for the water level to rise or fall 37% of the initial change.

Table 4.1: Depth of the middle of the well screen for the wells at site A (**Fig. 4.1**) relative to the Site A datum (i.e. the lowest measured level of the stream stage).

Well	Depth relative to datum (cm)
P1	-65
P2	-31
P3	+34
P4	-55
P5	-57
P6	-32
P7	-34
P8	-41
P9	-71
P10	-43
P11	-38
P12	-34

4.2 Water-Flux Calculations

4.2.1 Heat Tracer Flux Calculations

Vertical groundwater flux was determined at Site A using the temperature time series method developed by Hatch et al (2006) and the analytical equation developed by

Turcotte and Schubert (1982). The Hatch et al (2006) method uses temperature measurements at different depths in the streambed as a tracer to determine flux based on the propagation of the diurnal temperature signal through the streambed. With increasing flow and depth, the amplitude of the temperature signal decreases (Silliman et al, 1995). The Turcotte and Schubert (1982) method requires stream temperature, streambed temperature at one known depth, and deep groundwater temperature at a depth with no annual temperature variation.

4.2.1.1 Temperature Measurements

Thermochron iButtons (model DS1921Z; Thermochron Limited) were used as temperature sensors and data loggers (2048 measurements can be stored). The manufacturer claims a temperature range of -5°C to 26°C, an accuracy of +/- 1°C, and a resolution of 0.125 °C. Other research has shown that iButtons have an accuracy of +/- 0.5°C 95% of the time (Hubbart et al, 2005; Johnson et al, 2005), which was supported by testing in our lab. The iButtons have been used successfully in previous studies for monitoring groundwater-surface water interaction (Fanelli and Lautz, 2008; Lautz et al, 2010).

The iButtons were installed in ¾" ID iron rods to protect them from water and the elements. The rods were 152 cm long with a tapered point, and installed by hand up to 91 cm into the streambed to ensure physical stability. Field and laboratory studies were done by Alexander and MacQuarrie (2005) to determine if heat conduction along installations can have an impact on streambed temperature measurements. Three different

types of pipe material were tested: steel, steel with foam insulation, and PVC; the researchers found that the change in temperature due to conduction along the material was less than the thermal resolution of the probes used in the study (0.156 °C) (Alexander and MacQuarrie, 2005). Similarly, Keery et al (2007) tested both wooden and iron probe installations, and found the temperature profiles to be nearly identical. There is also the potential that the material may cause a time lag with changing temperatures. This could impact time series methods, though the amplitude ratio is much less sensitive. Steel pipes were found to be much less susceptible than PVC pipes, and a diameter of one inch or less for both materials was found to have negligible lag (Cardenas, 2010).

Seventeen temperature rods, labelled TR-A to TR-Q, were installed at Site A (**Figure 4.1**)**.** Stacked wooden dowels (5/8”) were used to place the iButtons at the desired depths. **Figure 4.2** shows the experimental setup. For most of the study period (i.e. June 29, 2011 to May 10, 2012), the iButtons were installed at depths of 5, 10 and 20 cm (as shown in **Figure 4.2**), although for June 1, 2011 to June 29, 2011 they were installed at depths of 5, 15, and 20 cm. Temperature measurements were taken every 20 minutes from June 1, 2011 to September 25, 2011 and every 40 minutes from September 25, 2011 to May 10, 2012. The iButtons were collected and returned to their positions without removing the iron rod to ensure consistency of the sampling locations and prevent preferential flow paths from being created. As it took several hours to download the data, the temperature data is not continuous from June 2011 to May 2012; rather they are broken up into nine different study periods (**Table 4.2**).

Table 4.2: Temperature Rod study periods.

Study Period	Time frame
1	June 1 to June 28, 2011
2	June 29 to July 14, 2011
3	July 14 to August 11, 2011
4	August 11 to August 31, 2011
5	August 31to September 25, 2011
6	September 25 to November 19, 2011
7	November 21, 2011 to January 17, 2012
8	January 17 to March 7, 2012
9	March 14 to May 10, 2012

4.2.1.2 Sediment Thermal Properties

Heat tracer methods to calculate groundwater discharge require the thermal properties of both water and streambed sediments. Streambed sediment samples were taken at Site A using a hand-operated corer for particle-size analysis, bulk density calculation, and to determine thermal properties. Sediment volume ranged from 120 – 200 cm^3. Samples were taken at all the temperature rod locations except for TR-E and TR-P, and at the mini-piezometer (see section **4.3.1**) locations of PS-1-2, PS-2-1, and PS-3-1. A deep (150 cm) sediment core was also taken near P9 by a hand-auger on November 1, 2011. The sediment samples were brought to the lab and oven-dried at 105

°C for at least 24 hours, and then sieved using the method described by Sheldrick and Wang (1993). Sieve sizes of 2 mm, 1.4 mm, 1 mm, 0.7 mm, 0.5 mm, 0.355 mm, 0.180 mm, 0.09 mm, and 0.045 mm were used. Porosity was then calculated using the following formula, assuming a particle density of 2.56 g/cm^3 (Brady and Weil, 2004):

$$n = 1 - (\frac{\rho_B}{\rho_D}) \quad (16)$$

Thermal properties of the sediment were then calculated using the guidelines of Lapham (1989). Volumetric heat capacity of the solids was calculated using the equation from de Vries (1963):

$$c_T x_T = c_S x_s + c_w s_w \quad (17)$$

where c_T, c_s, and c_w are the volumetric heat capacities of the bulk sediment, the solids, and the water, respectively, and x_T, x_s, and x_w are the volume fractions of the bulk sediment, solids, and water, respectively; and assuming a volumetric heat capacity of water of 4.184 J/cm^3°C.

4.2.1.3 Calculation of water flux

Calculations of water flux using the Hatch et al (2006) method were done using the MATLAB program VFLUX, designed by Gordon et al (2012). For the input, VFLUX requires the temperature data for two separate depths of measurement, the time of each temperature point, the distance between depths, and the thermal properties of the sediment. VFLUX produces flux values for every two hours, although in this study daily

averages were used as they may be more accurate (Gordon et al, 2012). VFLUX goes through six major steps to calculate flux (Gordon et al, 2012):

(1) First, the data is resampled to ensure an equal time interval between each temperature measurement at the different depths. For each of our study periods, the sampling rate was the same for every depth (either 20 minutes or 40 minutes), so resampling was not required.

(2) The data is resampled to 12 samples per fundamental cycle, which in our case is a diurnal signal, and is filtered to reduce edge effects.

(3) The diurnal signal is isolated from the trend, noise, and harmonics using the Dynamic Harmonic Regression (DHR) developed by Young et al (1999) and available in the Captain's Toolbox (Young et al, 2004).

(4) Amplitude and phase information is extracted from the fundamental signal.

(5) The desired sensor pairs are chosen. For our study, flux was calculated between the sensors at 5 cm and 10 cm, 5 cm and 20 cm, and 10 cm and 20 cm.

(6) Flux is calculated using equations (8) and (9) developed by Hatch et al (2006).

The temperature rods were also used to calculate flux using the Turcotte and Schubert (1982) method. The stream temperature was obtained using the stream stage pressure transducer and the pressure transducer installed in the deepest monitoring well was used for the deep groundwater temperature. As there was still some seasonal variation in the municipal well, annual averages were used.

4.2.1.4 Streambed Temperature Snapshots

In order to have a more detailed snapshot of streambed flux, the distribution of streambed temperatures at Site A was measured in a similar manner to that of Conant et al (2004b). These were taken on August 2011 (426 points) and January 2012 (400 points) for use with the Turcotte and Schubert (1982) method, similar to previous work by Schimdt et al (2007). Temperatures were measured by inserting a handheld thermometer (Tracable Model 90205—27, Cole-Parmer) 12 cm into the streambed. The temperature reading on the thermometer was allowed to stabilize before a reading was made. Readings were taken along 25-30 transects perpendicular to the stream, spaced 1 m apart. Along each transect, readings were taken every 5-25 cm, the finer spacing applied in areas with steeper temperature gradients. Larger distances resulted if there was an obstruction (i.e. a very large rock). The mean difference between points was 20 cm. Stream temperatures were measured at every two transects, and the average stream temperature for each day was used to calculate flux. The pressure transducer installed in the deepest monitoring well was used for the deep groundwater temperature.

4.2.2 Seepage Meters and Darcy Flux

Two seepage meters (Lee, 1977) were installed in the streambed at Site A **(Figure 4.1**). The bottom half of a HDPE bucket (area of 0.06 m^2) was used and placed upside down into the sediment. A tube was placed through the bottom of the bucket and connected to a 10 L plastic bag. A T-junction valve was connected to the tube and acted as an on/off switch, with one end leading to the stream and the other to the bag. The

valves were open to the stream for a week before the first measurement so the seepage meters could equilibrate. A hole was drilled into the bottom of the bucket to allow any air caught during installation to escape. This was left open for a week and then sealed with a rubber stopper. The bags were pre-filled with about 500 mL of water to minimize bag resistance (Rosenberry et al, 2008). The volume of water collected by the seepage meter bags was measured weekly or biweekly from late July 2012 to November 17, 2012 by emptying the bag into a graduated cylinder. If the bags appeared to be nearly full when being measured, they were emptied except for about 500 mL to minimize bag resistance.

Flux values were also calculated using Darcy's Law at the five water level wells located closest to the stream (P6, P7, P9, P10, P11, **Figure 4.1**). The assumption of straight line flow for the Darcy's Law calculation is likely not correct at this location, but this calculation will still give a rough estimate. The slug test values were used for hydraulic conductivity, and hydraulic gradient was measured as the difference between the well water level and the stream stage over the straight line distance between the well screen and the closest stream bank.

4.3. Contaminant Monitoring

4.3.1 Mini-Piezometer Sampling

Fourteen mini-piezometers were installed along the banks of the stream to monitor groundwater nutrient and other contaminant concentrations. These consisted of stainless steel pipes (½ inch ID) with a perforated tip covered with nytex screening. These were placed on the north (PN) and south (PS) sides of the stream in roughly 4

transects (e.g. PN1, PN2, PN3, PN4) about 5-7 m apart, with eight mini-piezometers at a depth of roughly 10 cm below the streambed (e.g. PN1-1) and six at a depth of roughly 40 cm below the streambed (e.g. PN1-2; not installed at PN3 and PS3). The shallow and deep mini-piezometers were installed within 15 cm of each other, except for PS1-1 and PS1-2. The locations of the mini-piezometers are shown in **Figure 4.1.**

Mini-piezometers PN1-1, PN1-2, PN2-1, PN2-2, PS1-1, PS1-2, PS2-1, and PS2-2 were installed on June 9, 2011 and sampled up to 11 times until March 12, 2012, and PN-3-1, PN-4-1, PN-4-2, PS-3-1, PS-4-1, and PS-4-2 were installed on July 14, 2011 and sampled up to 8 times until March 21, 2012. Time between sampling ranged from one week to two months. Stream samples were also taken at these times, near the downstream end of Site A and just upstream of Site B.

Groundwater from piezometers and stream water samples were taken for analysis of soluble reactive phosphorus (SRP), ammonium, volatile organic compounds (VOCs), anions, metals, alkalinity, water isotopes, sweeteners, and pesticides. Groundwater was sampled with a peristaltic pump connected to the mini-piezometers using a peristaltic Master Flex tubing and ¼" polyethylene tubing (**Figure 4.3**). Contaminant sampling commenced once field parameters stabilized: temperature, pH, and electric conductivity, and dissolved oxygen, measured with handheld meters (YSI Professional Plus,and YSI ProDO probe, respectively, Hoskins Scientific). Stream samples were collected by drawing stream water up through a syringe. Samples were filtered and preserved as necessary in the field, as described in **Table 4.3.**

Table 4.3: Preservation protocol for water samples.

Sample	Volume	Filtration	Preservation
SRP	50 ml	0.2 µm	None
VOCs	40 ml	None	pH <2 with $NaHSO_4$, no head space
Ammonium	30 ml	0.2 µm	pH 5-6 with 10% HCl
Anions	30 ml	0.2 µm	None
Metals	125 ml	0.2 µm	pH <2 with HNO_3
Alkalinity	125 ml	None	None
Water Isotopes	30 ml	None	None
Sweeteners and Pesticides	30 ml	0.2 µm	None

4.3.2 Peeper Sampling

Passive diffusion samplers (peepers; Karsten Liber, Toxicology Centre, University of Saskatchewan) were installed in the streambed at 16 locations at Site A, corresponding to the locations of mini-piezometers PS2-1 and PS3 and the majority of the temperature rods (**Figure 4.1**), except by TR-N, TR-P and TR-Q. It was not possible to install peepers in these locations due to the coarse streambed materials. The peepers were constructed from acrylic and were rectangular, with dimensions of 32 cm (height) x 6.5 cm (width) x 1.3 cm (depth) with a pointed tip allowing for easy installation **(Figure 4.4)**. Each had 5 chambers, spaced 2.5 cm apart, with dimensions of 2.5 cm (height) x 5.1 cm (width) x 0.8 cm depth, with a volume of 10.2 mL per chamber.

In the lab, peeper chambers were filled with degassed Milli-Q water and covered with 0.2 µm Supor dialysis membranes (Pall Life Sciences). The peepers were stored in a bucket of degassed Milli-Q water during transport to the field. Each peeper was installed

with the top chamber just at the sediment surface, with the other chambers at depths of 2.5-5 cm, 7.5-10 cm, 12.5-15 cm, and 17.5 to 20 cm. For simplicity each chamber will be referred to by its deepest depth (e.g. 2.5-5 cm as 5 cm chamber). Peepers were allowed at least 3 weeks to equilibrate.

Peepers were deployed for three different time periods: November 1, 2011 to November 22, 2011, December 21, 2011 to January 11, 2012, and January 26, 2012 to March 15, 2012. The peepers were sampled for SRP, ammonium, and VOCs. During sampling, peepers were taken out of the sediment and placed on a table, and sampled chamber by chamber. Five mL from each chamber were used for SRP, and because the peepers had 0.2 μm membranes, no filtration was needed. Two mL from the chamber were then used for VOC sampling, quickly placed in a 43 mL glass vial pre-filled with 40 mL Milli-Q water and preservative, and then topped up with Milli-Q water to ensure there was no headspace. For ammonium sampling, 2 mL were taken and then put in a 5 mL bottle pre-filled with 2.5 mL Milli-Q water to minimize headspace. Ammonium samples were frozen by the end of the field day. Field blanks were also taken at the beginning and end of sampling days.

4.3.3 Site B Contaminant Discharge

For a more general understanding of the nutrient and contaminant concentrations discharging from shallow groundwater to Dyment's Creek, the screening approach of Roy and Bickerton (2010) was applied to both sides of the stream for the larger study reach, Site B. Samples were taken in the streambed along each bank at both sides at 46

locations, about 10 m apart, over three days in July 2010. There were no major storm events in this time. Two stream samples were also taken, at the upstream and downstream ends of the reach.

A mini-profiler system **(Figure 4.5)** was used to take these samples. A hollow rod with a stainless steel perforated drive point connected to ¼" polyethylene tubing was driven with a hammer-drill in the ground at each location. The tubing was connected to a peristaltic Master Flex pump. While the rod was being drilled into the ground, stream water was being pumped through the tubing and out the drive point to minimize clogging. Groundwater was collected from a depth of 20 cm to 145 cm (median depth was 45 cm) , Water was first pumped out into a cylinder, where temperature, electrical conductivity, pH, and dissolved oxygen were measured to ensure the water being sampled was not stream water moving along shallow hyporheic flow paths. The sampling procedure was as described in section **4.3.1**.

A hydraulic potentiomanometer (Winter et al, 1988), which measures the hydraulic head difference between the shallow groundwater and the stream, was used at 16 locations along Site B (October 18, 2011) to determine the local hydraulic gradients.

4.3.4 Sample Analysis

Both SRP and ammonium were analyzed using spectrophotometry. A Thermo Scientific Evolution 160 spectrophotometer was used to measure SRP using a mixed reagent containing ammonium molybdenate and antimony potassium tartate. The absorbance was measured at 885 nm. Ammonium was analyzed using a Beckman

Coulter DU 720 General Purpose spectrophotometer. The absorbance was measured at 640 nm using a phenolhypochlorite reagent. Standards of 0, 0.05, 0.1, 0.25, 0.5, and 1 mg/L were run with the samples, and dilutions were used for concentrations found above 1 mg/L.

Volatile Organic Compounds were analyzed with a purge and trap gas chromatography and mass spectrometer system using a Teledyne Tekmar Aquatek 70 autosampler, a Teledyne Tekmar 3100 Sample Concentrator purge and trap, an Agilent G1530A gas chromatographer, and a HP/Agilent 5973 mass selective detector.

Anions were analyzed with a Dionex 2500 ICS Ion liquid chromatographer system, major cations (Al, Ca, Fe, K, Mg, and Na) were analyzed using a Horiba Jobin Yvon Ultra 2 inductively coupled plasma (ICP) system, and trace metal samples were sent to the National Laboratory for Environmental Testing in Burlington, Ontario, and analyzed using Inductively Coupled Plasma-Sector Field Mass Spectrometry (NLET Method #2003). Alkalinity was analyzed using HACH digital titration method 8203 with 1.6 N H_2SO_4. Sweeteners and pesticides were analyzed using a Dionex 2500 ICS Ion liquid chromatographer system combined with an Applied Biosystems AB Sciex Q Trap 5500 triple quad mass spectrometer with an electrospray ionization source in negative mode (IC/ESI/MS/MS) as described by Van Stempvoort et al (2011).

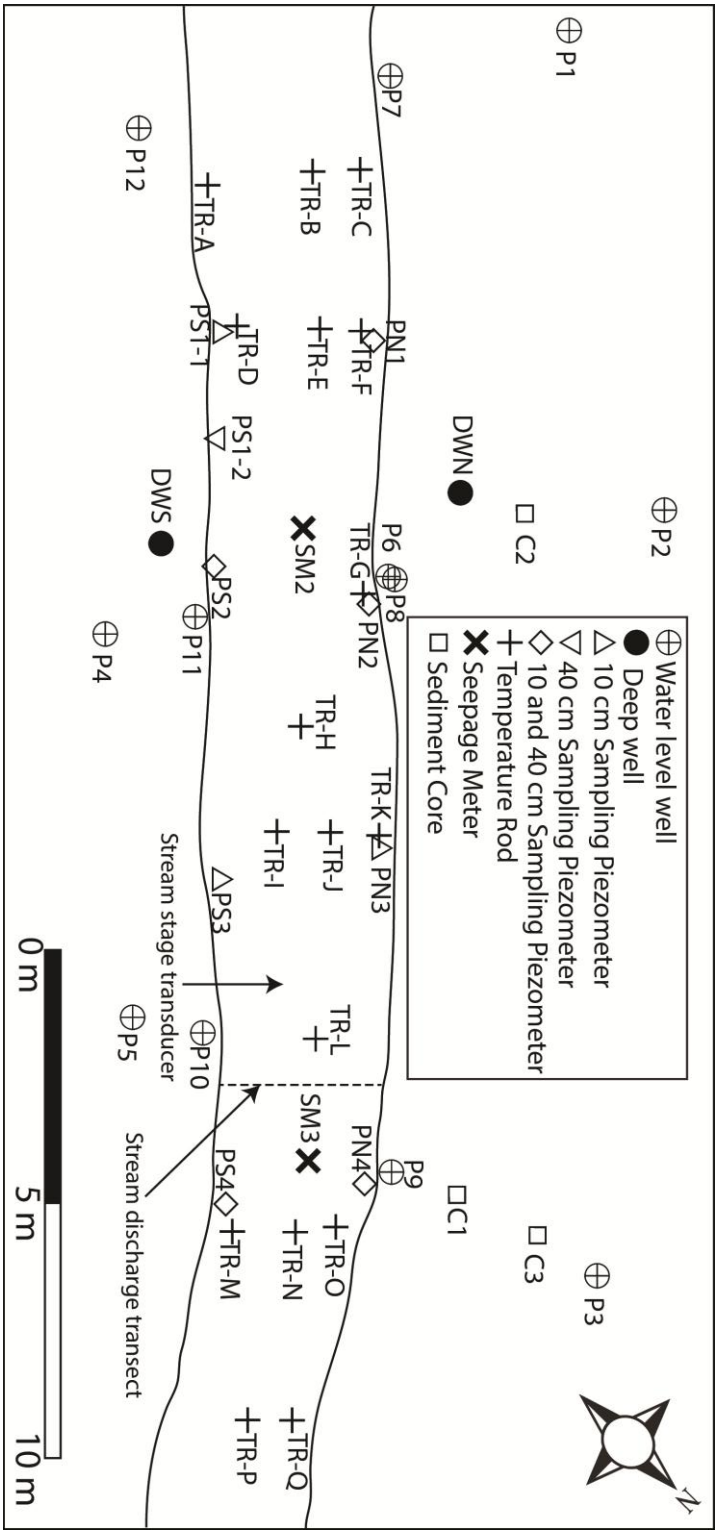

Figure 4.1: Location of installations at Site A.

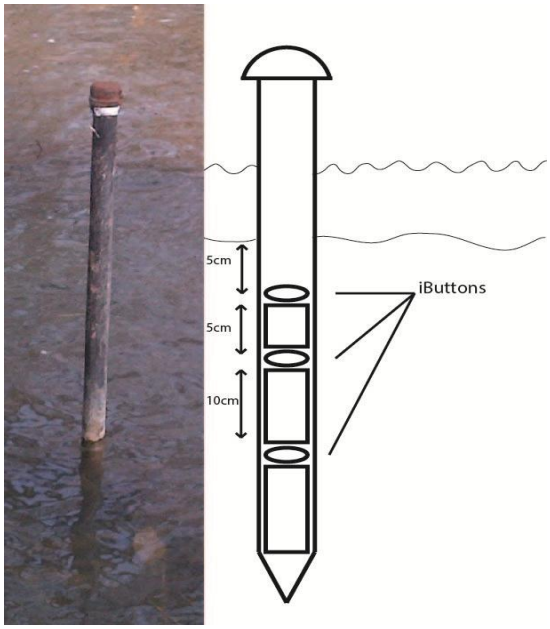

Figure 4.2: Temperature rods with iButtons placed on wooden dowels for spacing.

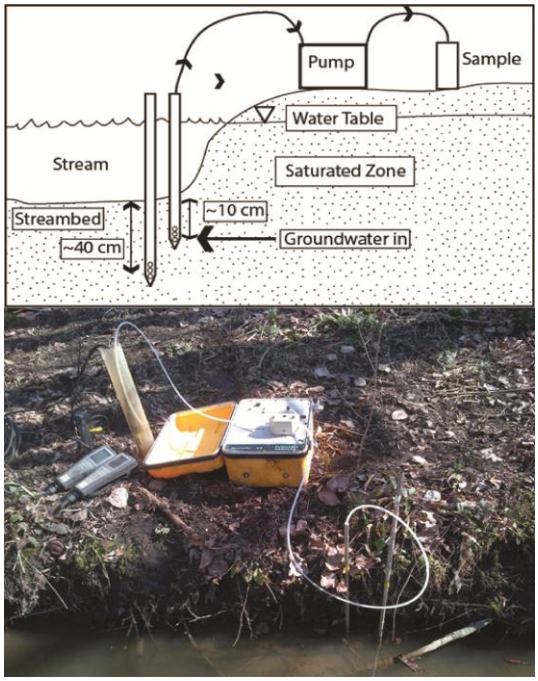

Figure 4.3: Mini-piezometer sampling.

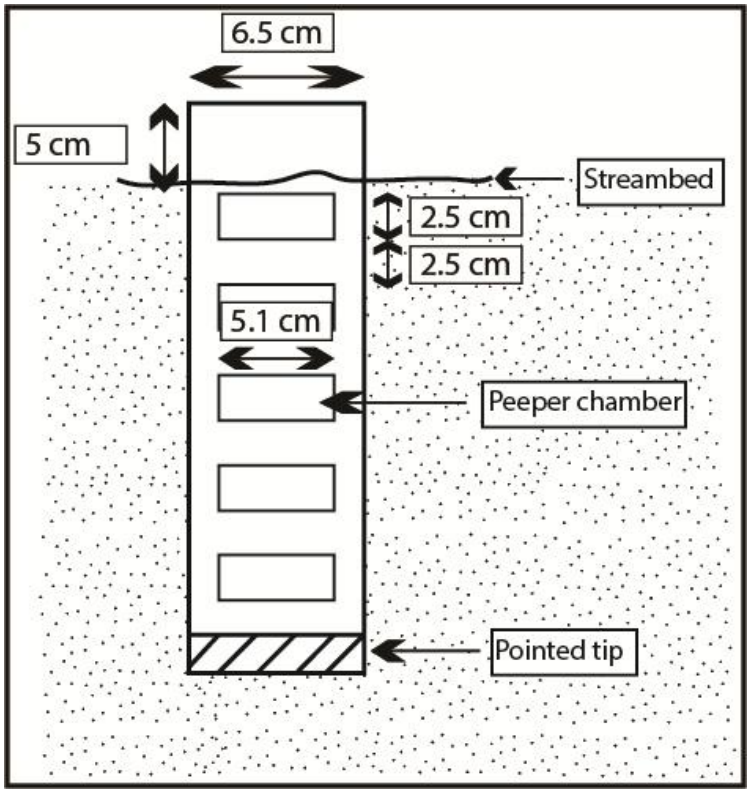

Figure 4.4: Peeper installation

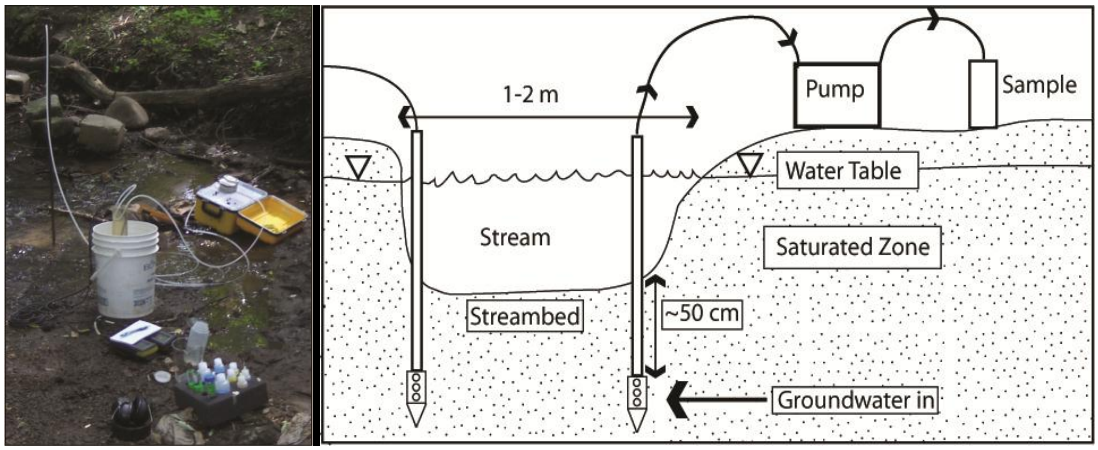

Figure 4.5: Mini-profiler system.

5. Results and Discussion

5.1 Site A Characterization

5.1.1 Sediment Samples

Hydraulic conductivity for the streambed sediments and one stream bank core (C1) was estimated from the particle size distribution of the collected sediment samples using the method developed by Hazen (1911). Sediment composition was similar across the streambed, with all locations but TR-I and TR-J being composed of at least 90% sand (USDA particle size classification). The range of streambed hydraulic conductivity values was $9*10^{-4}$ m/s to $2*10^{-5}$ m/s. The deep core on the stream bank (C1) was finer grained than the streambed sediments and had a lower hydraulic conductivity value of $2*10^{-7}$ m/s.

The average bulk density calculated for the streambed sediments was 1.56 g/cm^3, with a standard deviation of 0.12 g/cm^3. Assuming a sediment particle density of 2.56 g/cm^3, porosity was calculated to be 0.39. Thermal properties of the streambed sediments were determined using the relation with bulk density determined by Lapham (1989). The "coarse grained" curve, for sediments that were at least 50% sand or coarser, was used because the stream bottom sediments at all but two locations were >90% sand. The thermal conductivity calculated was 1.8 W/m°C and the calculated volumetric heat capacity of the sediment was 0.6 cal/cm^3°C, or 2.7 J/cm^3°C. Thermal conductivity was within the range used in previous studies on using heat as a tracer (0.63 to 2.26; **Table 5.2)** and is especially similar to those that also had coarse grained sediment (i.e. values at the higher end of the range for all sediments).

Table 5.1: Sediment composition and hydraulic conductivity values obtained from the method of Hazen (1911) derived from sediment samples collected along the streambed and stream bank core C1 (See **Figure 4.1**).

Location	% Sand (>0.05 mm)	Hazen-derived K (m/s)
TR-A	94	1E-04
TR-B	98	9E-04
TR-C	99	3E-04
TR-D	90	4E-05
TR-F	97	2E-04
TR-G	95	6E-05
TR-H	91	1E-04
TR-I	79	2E-05
TR-J	79	2E-05
TR-K	97	1E-04
TR-L	94	2E-04
TR-M	94	8E-05
TR-N	99	5E-04
TR-O	91	8E-05
TR-Q	97	5E-04
PS-1-2	90	1E-04
PS-2-1	96	1E-04
PS-3-1	97	5E-05
Stream bank core C1	74	2E-07

5.1.2 Slug Tests

The results of the slug tests performed on 14 wells at Site A (**Table 5.2**) show a range of field-saturated hydraulic conductivities (K) from $1*10^{-8}$ m/s to $5*10^{-4}$ m/s, which are values representative of sands and silts (Freeze & Cherry, 1979). All but one of the shallower wells (P1-P2, P4-P12) have higher values than the deeper wells (DWN, DWS), except for P3. Slug tests measure the response time of wells to a quickly changing water level; in anisotropic conditions the water will be preferentially coming from the layer with the highest hydraulic conductivity. As a result, the hydraulic conductivity values may be overestimates, as vertical K values are likely lower given that streambed sediments are commonly layered. The well screen used, with slots along the circumference of the well but not along the bottom, also promotes horizontal flow. The slug test values were commonly lower than the calculated streambed hydraulic conductivity values, most of which were on the order of magnitude of 10^{-4} m/s.

5.1.3 Site A Near-Stream Geology

Cross-sections along two transects at Site A showing sediment core data and hydraulic conductivity values are presented in **Figure 5.1**. Sediment and hydraulic conductivity data not along the transects show a similar level of heterogeneity. Shallow sediments (top 1-2 m) appear to be composed of either sand or peaty (organic) fine-grained sediment layers. The observed hydraulic conductivity values are consistent with the range of sediments (sands and silts) seen in the cores. At locations where they are taken together the sandy layers show conductivity values of 10^{-4} and 10^{-5} m/s, with the

organic silt layer showing conductivity values of 10^{-6} to 10^{-8} m/s. While the data is limited, there was no consistent pattern in the sequence or position of layers, suggesting that the shallow aquifer geology at this site is complex and heterogeneous with multiple angled layers that may pinch out in locations.

Table 5.2: Hydraulic conductivity (K) obtained from well slug tests.

Well	Geometric Mean K (m/s)	Number of Measurements	Maximum Value (m/s)	Minimum Value (m/s)
P1	8E-05	3	1E-04	7E-05
P2	9E-06	3	1E-05	7E-06
P3	2E-07	1	n/a	n/a
P4	3E-06	1	n/a	n/a
P5	1E-05	4	2E-05	6E-06
P6	5E-05	1	n/a	n/a
P7	1E-04	3	2E-04	1E-04
P8	5E-05	5	7E-05	4E-05
P9	2E-05	6	2E-05	1E-05
P10	2E-05	4	6E-05	1E-05
P11	3E-04	4	7E-04	5E-05
P12	5E-04	3	5E-04	5E-04
DWN	4E-07	1	n/a	n/a
DWS	1E-08	1	n/a	n/a

5.1.4 Stream Discharge

The stream stage at Site A from July 14, 2011 to May 10, 2012 is shown in **Figure 5.2 A**. The stage datum for this site was chosen as the lowest level of stream stage recorded during the study period, about 5 cm above the streambed at that location. This site had the characteristic "flashy" storm hydrograph pattern, common in urban streams, consisting of a large, quick rise in stream stage followed by a quick decline (Walsh et al,

2005). Baseflow, the relatively steady low flow periods between storm events and outside the period of snow melt inputs, generally remained below 10 cm, and was at its lowest level in late September and early October, 2011. The stage surpassed 10 cm during mid-March 2012, which likely reflects the input of melting snow, given that there was a sharp rise in air temperatures during that time.

Stream discharge measured at Site A ranged from 480 L/min on July 14, 2011 to 18 000 L/min on October 26, 2011. A logarithmic rating (stage-discharge) curve (**Figure 5.3**) showed a good relation within this range, with an R^2 of 0.85. This rating curve cannot be reliably used for discharge values above the maximum measured value of 18 000 L/min, such as during storm events. Using this relation, baseflow was calculated to range from about 620 L/min to 2500 L/min, except for the high flow period in mid-March 2012 where it reached 12 500 L/min.

5.1.5 Well Levels

The daily average water levels, representing hydraulic head at the well screen in wells P1-P12 are shown in **Figure 5.2 B,C**, with the average for the time period shown in plan view in **Figure 5.4**. With the exception of P4, P5, and P12 for 10 days at the beginning of the sampling period and P4 during a storm event, the daily average water levels were always above the stream stage (**Figure 5.2**). Water levels were highest further from the stream, decreasing toward the stream, on both sides. The hydraulic head values of the deep wells installed at Site A, DWN and DWS, were higher than the top of the well, >50 cm above the datum. The two wells installed at different depths at the same

location, P6 and P8, displayed a vertical gradient towards the streambed. The consistent hydraulic gradients toward the stream, both horizontally and vertically, indicate that Dyment's Creek at Site A is a gaining reach from July 25, 2011 to the end of the study period.

The water level at wells P1-P3, all situated furthest away from the stream on the north side, increased slowly over time and P12 showed a gradual increase in water level over the first four months. There was no temporal trend in water levels for wells P4-P11 (**Figure 5.2 B,C**). The wells closest to the stream responded very quickly to storm events, suggesting the monitored groundwater zone is well-connected to the stream. For full stream and well water levels see **Appendix A**.

5.1.6 Site A Conceptual Model for Groundwater Flow

As shown in the previous section the hydraulic head levels in the wells were above the stream stage throughout the study area with a few exceptions, indicating groundwater movement towards the stream. The well screens were not all situated at the same depth, although 9 of them are within 25 cm of each other. Using the straight-line distance from the well screen to the stream, the average hydraulic gradient on the near-stream south shore wells (P10, P11) was 0.1 towards the stream (positive), and the hydraulic gradients on the near-stream north shore wells (P6-P9) ranged from 0.24 to 0.47. These gradients are fairly large, indicating that there may be a low hydraulic conductivity layer between the near shore wells and the stream sediments through which the groundwater must pass to reach the stream (Kraise et al, 2012). This is further

supported by the sampling piezometers producing dark, silty water. Large gradients for wells P1-P3 may also be due to the local topography, as they are just down-gradient of a hill (about 4 m high). The strong hydraulic gradients on both shores suggest that the local groundwater does not "flow through" the stream, but enters from both sides. Hydraulic gradients parallel to stream flow direction were low and not uniform in direction. On the northern shore, there are also large horizontal gradients, as the average gradient between P2 and P6, which are placed at a similar depth (3 cm apart), is 0.13. Positive gradients also exist between the deep wells (DWN, DWS) and the surrounding wells, although the exact values could not be calculated. Groundwater at Site A is likely moving preferentially towards the stream along the higher hydraulic conductivity sand layers, although due to the complex geology of the site, it is not possible to predict exact flow paths.

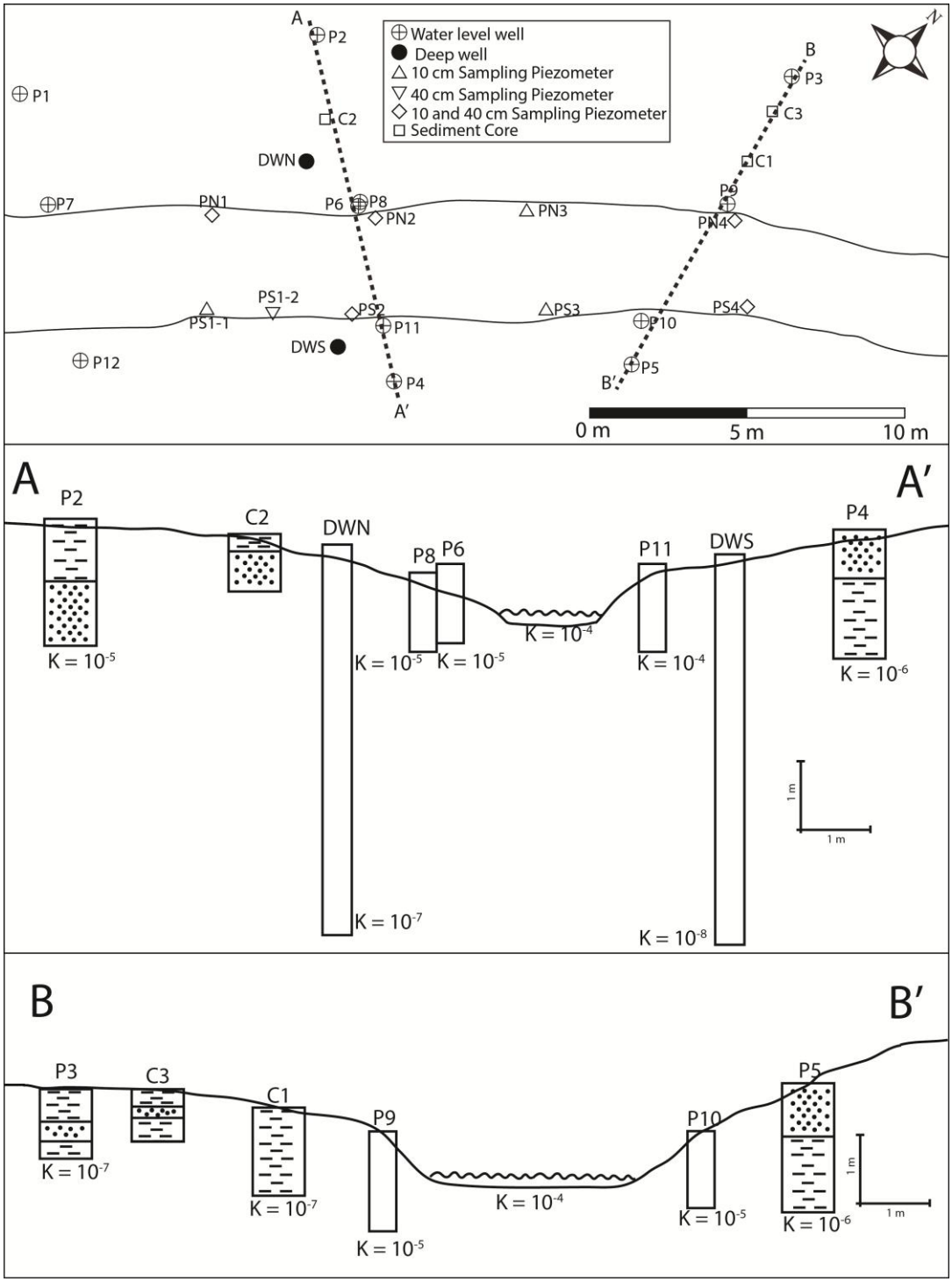

Figure 5.1: Two cross sections with average hydraulic conductivity (K) values (in m/s; see **Table 5.1** and **Table 5.3**), and sediment type. Dots indicate sand layers, while hash marks indicate peaty silt layers. Ground surface estimated between known elevations at wells.

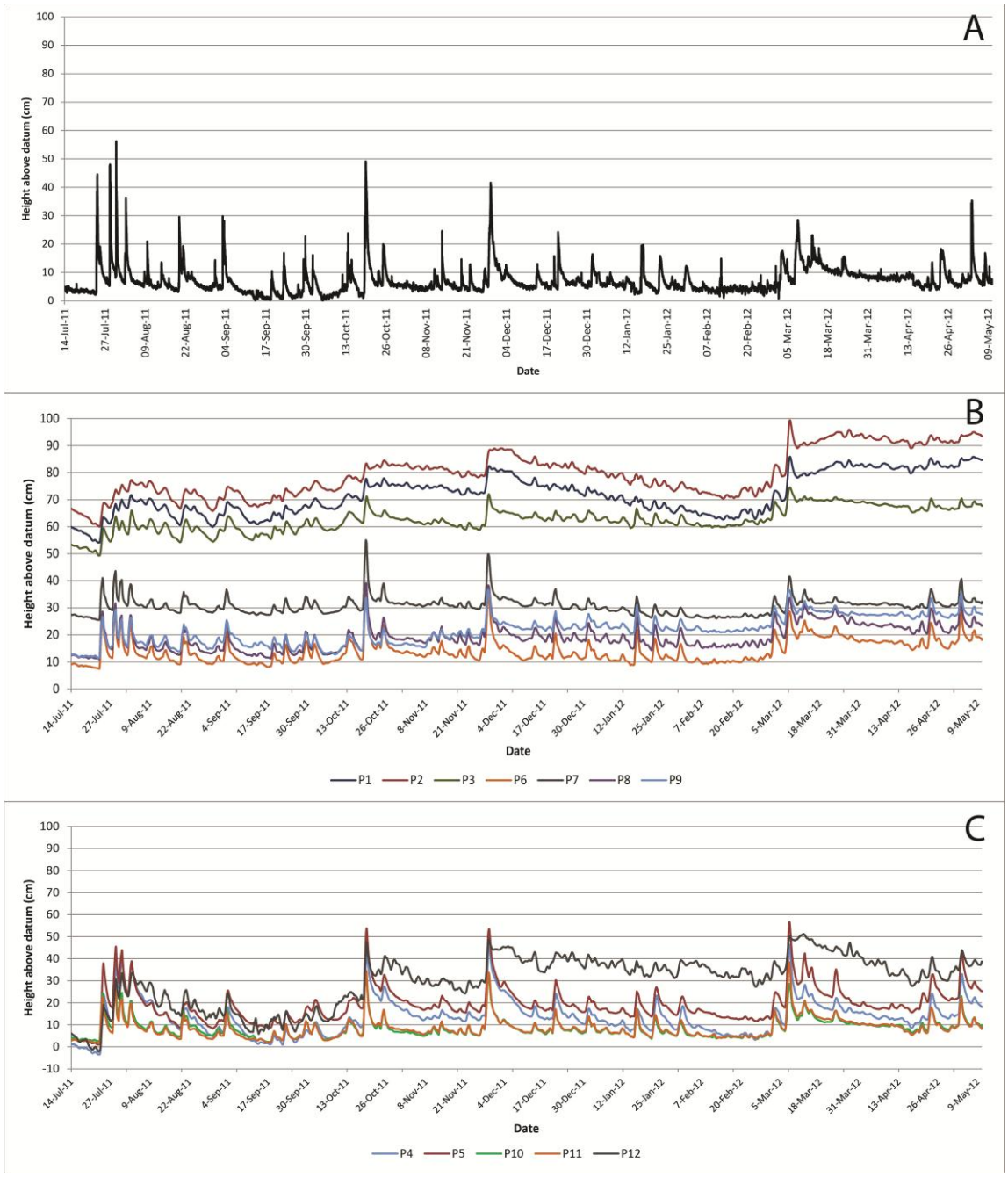

Figure 5.2: A) Stream stage at Site A, **B)** water levels for the wells on the north shore, **C)** water levels for wells on the south shore.

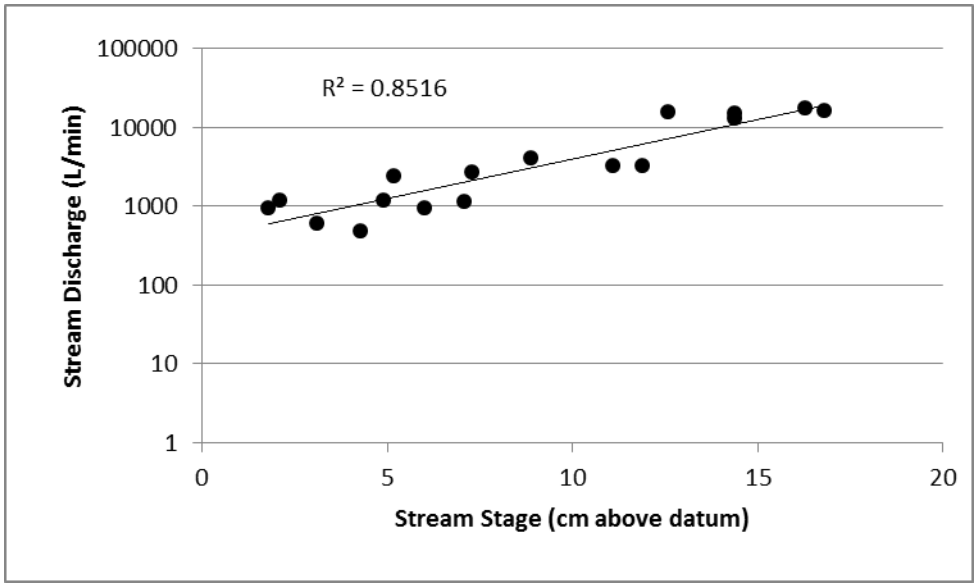

Figure 5.3: Stage-discharge rating curve at Site A. Best-fit line shown.

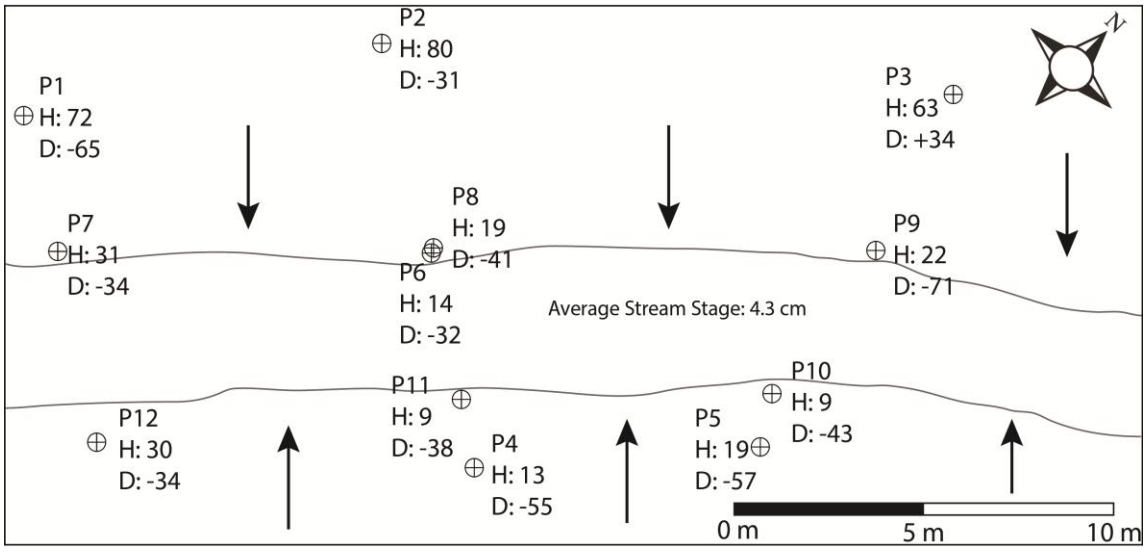

Figure 5.4: Average hydraulic head levels (H, in cm) and well screen depths (D, in cm) relative to the site datum (lowest stream stage) for the wells at Site A. Arrows indicate general groundwater flow directions based on conceptual flow model.

5.2 Groundwater Discharge

5.2.1 Darcy's Law Calculations

Estimates of groundwater flux were calculated by applying Darcy's Law to the hydraulic conductivity calculated using the slug tests (section **5.1.2**) and continuous hydraulic gradient data for the piezometers closest to the stream (P6, P7, P9, P10, P11, **Figure 5.4**). This calculation ignores changes in storage, thus assuming an instantaneous response in flux to the measured head changes, which may not be appropriate for sudden changes associated with rain events. However, base flow conditions, rather than rain events, are the focus of this study. Hydraulic gradient was calculated from the hydraulic head determined by the pressure transducers divided over the straight-line distance from the well screen to the streambed. The assumption of discharging groundwater moving in a straight line diagonally to the streambed is likely incorrect, as groundwater is most likely moving on a curving flow path towards the stream. A longer distance would result in a smaller hydraulic gradient and therefore a lower flux value. Thus, these values are likely overestimated. This flux calculation is also based on an assumption that the hydraulic conductivity measured by the slug tests is representative, and that it is applicable over the entire flow path (i.e. K is homogenous and isotropic in that zone). However, as described in section **5.1.4**, there is potentially a lower K area adjacent to the stream. Also, as discussed in section **5.1.2**, the slug tests used to measure hydraulic conductivity values may have been preferentially measuring the horizontal hydraulic conductivity. Anisotropy ratios of 1:100 have been used in the literature for layered

sediments (Freeze and Cherry, 1979), so it is possible the actual vertical flux values are lower by up to two orders of magnitude. Thus, these calculations are expected to provide an upper range of flux values at these locations, and are useful to determine temporal trends.

The calculated groundwater fluxes are shown in **Figure 5.5,** with mean, maximum, and minimum summarized in **Table 5.3.** Positive values represent flux from the streambed towards the stream. These ranged from a low of 0.12 m/d at P9 to a high of 9.94 m/d at P11. Hydraulic conductivity has a greater influence on these flux values, as the range in K values was an order of magnitude larger than the range in gradients. No geographic trend was evident, which likely reflects the heterogeneity in site geology. The fluxes associated with P6, P9, and P11 showed a small increasing trend over the study period, although this was largely due to snowmelt in mid-March. Fluxes for P7 and P10 did not show temporal trends. These values assume a temporally constant hydraulic conductivity at Site A, which is supported by Hatch et al (2010) for groundwater discharge locations.

Table 5.3: Groundwater discharge calculated using Darcy's Law (values in m/d).

	P6	P7	P9	P10	P11
Mean	1.05	5.70	0.35	0.25	6.59
Max	1.63	6.47	0.50	0.44	9.94
Min	0.57	4.23	0.12	0.13	2.19

5.2.2 Temperature Rods

5.2.2.1 Temperature Data

An example of the streambed temperatures measured by iButtons at the 3 vertical positions (5, 10, and 20 cm; **Figure 4.2**) within the 18 temperature rods (**Figure 4.1**) is provided for TR-L in **Figure 5.6**. The highest temperatures were recorded in late July and early August, and the lowest temperatures in January and February. There is a discontinuity in March due to a gap (one week) in data collection. The large temperature change observed in the groundwater temperatures after this discontinuity is likely due to the rapid increase in air temperature during this time. As expected, the temperatures declined with depth during the summer and increased with depth in the winter. Similar overall patterns were seen in all the temperature rods. The thermal response varied with depth, with the diurnal amplitude being smaller and the phase being shifted later in time for the deeper iButtons. To better illustrate this, a small subset of streambed temperature data (four weeks during July, when daily variation was at its greatest) is shown for TR-I in **Figure 5.7.**

5.2.2.2 VFLUX Results

Mean, median, maximum, and minimum groundwater flux values over the study period are shown for the different temperature rods in **Table 5.4**. Positive values indicate discharge conditions while negative values indicate recharge conditions. The flux values varied from -0.11 m/d to 0.49 m/d, which is within the range of values seen in other studies. The maximum flux values in the literature (for both discharge and recharge)

Table 5.4 Mean, maximum, and minimum groundwater flux calculated using VFLUX from temperatures measured with iButtons at depths of 10 and 10 cm, within the various temperature rods (TR), along with the time periods used for measurements.

Location	Mean flux (m/d)	Median flux (m/d)	Maximum flux (m/d)	Minimum flux (m/d)	Time Period
TR-A	0.14	0.13	0.3	-0.05	June 1, 2011 to September 25, 2011, and March 15, 2012 to May 10, 2012
TR-B	0.32	0.32	0.43	0.14	June 29, 2011 to September 25, 2011, and March 15, 2012 to May 10, 2012
TR-C	0.17	0.17	0.31	-0.09	June 1, 2011 to August 31, 2011
TR-D	0.27	0.28	0.37	0.12	June 1, 2011 to September 25, 2011, and March 15, 2012 to May 10, 2012
TR-E	0.15	0.15	0.29	-0.07	June 1, 2011 to September 25, 2011, and March 15, 2012 to May 10, 2012
TR-F	0.21	0.22	0.35	0.06	June 1, 2011 to September 25, 2011
TR-G	0.34	0.35	0.47	0.19	June 1, 2011 to August 11, 2011
TR-H	0.25	0.24	0.39	0.08	June 1, 2011 to June 12, 2011, July 14, 2011 to September 25, 2011, and March 15, 2012 to May 10, 2012
TR-I	0.21	0.21	0.37	0.06	June 1, 2011 to September 25, 2011, and March 15, 2012 to May 10, 2012
TR-J	0.21	0.24	0.32	0.06	June 1, 2011 to September 25, 2011
TR-K	0.28	0.28	0.43	0.13	June 1, 2011 to September 25, 2011, and March 15, 2012 to May 10, 2012
TR-L	0.18	0.17	0.4	-0.02	June 1, 2011 to September 25, 2011, and March 15, 2012 to May 10, 2012
TR-M	0.22	0.22	0.33	0.01	June 1, 2011 to June 30, 2011, July 14, 2011 to September 25, 2011, and March 15, 2012 to May 10, 2012
TR-N	0.16	0.21	0.34	0.02	June 30, 2011 to August 31, 2011
TR-O	0.21	0.2	0.49	0	June 1, 2011 to September 25, 2011, and March 15, 2012 to May 10, 2012
TR-P	0.12	0.12	0.27	0.03	June 1, 2011 to September 25, 2011, and March 15, 2012 to May 10, 2012
TR-Q	0.06	0.07	0.22	-0.11	June 1, 2011 to September 25, 2011, and March 15, 2012 to May 10, 2012

commonly ranged from 0.2 to 0.6 m/d (Conant, 2004; Schmidt et al, 2007; Fanelli and Lautz, 2008; Schilling and Jacobson, 2008; Schmidt et al, 2008; Lautz et al, 2010) although discharge values up to 1.3 m/d (Anibas et al, 2011) and recharge values approaching 10 m/d have been measured (Vogt et al, 2010; Gordon et al, 2012)

Unfortunately, groundwater flux calculations using the program VFLUX could not be performed for the entire study period because the amplitude of the diurnal temperature variations of the streambed could not always be resolved by the iButtons. Flux could not be determined from mid-September, 2011 to mid-March, 2012; the exact dates differ between the various temperature rods. Additional breaks in data for TR-B, TR-H, TR-M, and TR-N were due to problems with individual iButtons during that time period. Only VFLUX data calculated using the 10 cm and 20 cm depth iButtons will be presented due to a potential issue with the 5 cm data (discussed in section **5.2.5**). These calculations also ignore changes in storage (affecting bulk density – thus, thermal properties) which are not anticipated to affect base flow conditions

Average daily fluxes (TR-A, TR-D, TR-K, and TR-Q) from June 1, 2011 to September 25, 2011 are shown in **Figure 5.8,** and from March 15, 2012 to May 10, 2012 are shown in **Figure 5.9**. These four temperature rods are representative of the range of flux values and variation that were seen in the study area. Plots for the other temperature rods can be found in **Appendix B**. From June to September, 2011, the flux values for TR-A and TR-Q decreased over time (**Figure 5.8**), as well as TR-E, TR-L, TR-O, and TR-P. In the spring of 2012, TR-E, TR-P, and TR-Q, showed a slight increase over time, and

TR-H showed a slight decrease. Short-term variations are likely due to changes in hydraulic gradients caused by storm events, though the effect may be difficult to determine due to the temporal resolution of the method, it will still impact the average values (Gordon et al, 2012). The effect of storm events on groundwater discharge at Site A appears to be complex and is beyond the scope of this paper.

Plots of monthly-averaged groundwater flux are shown in **Figure 5.10**. Kriging was used for the interpolation between the 17 temperature rod points, as this is the most suitable method with data that is both sparse and unevenly spaced (Chang, 2008). Groundwater flux at this site appears to be patchy, but the general pattern appears to hold for the seven sample periods (including summer, early fall, and spring). Similar spatial patterns over time were also seen by Conant (2004). The highest fluxes occurred in the middle of the reach, along the north shore, with consistently lowest values at the down-stream (east) end. Unlike Conant (2004) and Kalbus et al (2007), it does not appear that a large portion of the groundwater discharge is from a small area of "hot spots" in the streambed. Generally, flux decreased through the summer months, especially at the eastern end of the reach. Large spatial variation was seen in the western end.

The total groundwater discharge for this study reach (an area of 115 m^2), as calculated based on the interpolated plots (**Figure 5.10),** varied between a low of 22 000 L/d for September 2011 to a high of 27 000 L/d for June 2011. The discharge calculated using the average flux values for each of the temperature rods over time is 25 000 L/d. Although this data set does not cover flux during the winter, values may be similar given

that the hydraulic gradients towards the stream during base flows were relatively stable seasonally, as is evident in the flux data determined using Darcy's law (**Figure 5.5).**

5.2.2.3 Turcotte and Schubert (1982) Analytical Equation Results

Equation 13 (See section 2.3.3.2) developed by Turcotte and Schubert (1982) was applied to the temperature data for the iButtons at 20 cm depth for three different time periods: July 17 to July 31, 2011, August 10 to August 20, 2011, and August 21 to August 31, 2011. This solution requires stable temperatures at both a deep groundwater location and at the stream. During these time periods the average daily stream temperature was stable. The stream temperature data from the stream stage pressure transducer, located near TR-L, was used. The average temperature from June 28, 2011 to May 10, 2012 for a nearby deep (6 m) municipal well of 11 °C was considered an acceptable approximation for the groundwater temperature at a depth which does not vary seasonally. To calibrate the different temperature loggers (pressure transducer vs. iButton), the temperatures were compared when the iButton temperatures at the 10 and 20 cm depths were the same. At these time periods, there was assumed to be no temperature gradient in the streambed and a similar stream temperature. It was found that the mean difference between the stream temperature measured by the stream pressure transducer and the streambed temperatures measured by the iButtons differed by 0.5 °C during these time periods, with the pressure transducer temperature being lower. This difference was then accounted for in the flux calculation.

The flux results using the Turcotte and Schubert (1982) equation are shown in **Figure 5.11.** Calculated total flux is much less – 12 000 to 13 000 L/d, compared to 22 000 to 24 000 L/d over the same time period for VFLUX. Possible reasons for this difference are discussed in section **5.2.5**.

5.2.3 Temperature Grids

Using the temperature grid data (snapshot of streambed temperatures at a depth of 12 cm measured manually at about 400 locations), the groundwater flux calculated by the analytical equation developed by Turcotte and Schubert (1982) is shown in **Figure 5.12 i**. Kriging was used to interpolate between the data points. While several of the assumptions inherent in the Turcotte and Schubert (1982) equation are not accurate at this location, such as a non-varying stream temperature, the results may be a good approximation (Conant et al, 2004). The stream temperature fluctuated during the sampling days, so for the flux measurements the average stream temperature for that sampling day was used, 18.7 °C for August and 1.4 °C for January. As with the previous section, the average groundwater temperature measured by the deep municipal well of 11°C was used as the groundwater temperature at "infinite" depth. The flux values calculated for August ranged from 0.03 m/d to 0.36 m/d, and the flux values calculated for January ranged from 0 to 0.36 m/d. As flux is based entirely on temperature, the spatial patterns for the flux are the same as for the temperature.

The August and January temperature grids, based on a snapshot of streambed temperatures (about 12 cm depth) measured manually at about 400 locations, are shown

in **Figure 5.12 ii**.. Darker colours indicate temperatures likely associated with increased groundwater flux (i.e. cooler temperatures in August and warmer temperatures in January).

As with the methods using the temperature rods, similar spatial patterns are seen in both time periods, supporting the hypothesis that the spatial variation in groundwater discharge during base flow periods does not change substantially between seasons at Site A. High flux zones occurred at three different locations along the northern shore, with values decreasing towards the south. The total amount of groundwater discharge from the 115 m^2 area is 11 000 L/d for August and 10 000 L/d for January, about 40% of the value calculated with VFLUX, but only slightly lower than those determined by using Turcotte and Schubert (1982) on the temperature rods.

5.2.4 Seepage Meters

The mean, maximum, and minimum flux values obtained from the seepage meters are shown in **Table 5.5.** Flux values are from August 2012 to November 2012. These flux values are 1-2 orders of magnitude lower than determined using the other methods described above. An assessment of the accuracy of the seepage meter measurements follows in section 5.2.5.

Table 5.5: Mean, maximum, and minimum groundwater flux measured by the seepage meters.

	SM-1	SM-2
Mean (m/d)	6.07E-03	7.68E-03
Maximum (m/d)	1.02E-02	1.83E-02
Minimum (m/d)	1.67E-03	2.12E-03
Number of measurements	8	5

5.2.5 Method Comparison

The ranges of flux values calculated by the different methods (Darcy equation, VFLUX, Turcotte and Schubert (1982) equation on both the temperature rods and temperature grids, and seepage meters) are shown in **Figure 5.13.** The flux values from the Darcy equation are the highest, and the flux values from the seepage meters are the lowest, while the temperature-based calculations are most similar. The lowest VFLUX measurements were occasionally negative (see **Figure 5.8 E**), but this could not be shown on **Figure 5.13** due to the log scale.

As mentioned in sections **5.1.4** and **5.2.1**, the flux estimates using Darcy's Law are likely overestimates due to anisotropy in streambed hydraulic conductivity, a potential low conductivity layer under the streambed, and the likely incorrect assumption that groundwater is moving from a straight line diagonally from the wells, which are located on the stream banks, to the stream. An anisotropy ratio around 1:10 would cause the range in Darcy calculated fluxes to move within the range of the temperature derived fluxes. These data are still useful as they provide flux estimates throughout the winter. The seepage meter estimates are likely underestimates due to short circuiting, where an

incomplete seal on the seepage meter allows water to escape under the seepage meter instead of entering the bag. The bottom of the streambed was littered with pebble sized wood debris, plastic, and glass, making a complete seal difficult. Previous studies have also reported lower fluxes using seepage meters compared with other methods, sometimes by up to an order of magnitude (Keery et al, 2007; Milosevic et al, 2012). However, at this site, the seepage meters do provide a direct confirmation of groundwater discharge to the stream, not just toward the streambed.

Potential issues with the temperature derived flux values include the assumptions of homogenous stream thermal properties and vertical flow. The geology under the stream is heterogeneous with multiple high and low hydraulic conductivity layers (Section **5.1**) which may cause both changes in thermal properties with depth and horizontal flow paths along the higher-hydraulic conductivity layers. Thermal properties, such as thermal conductivity, generally do not vary as much as hydraulic conductivity values (Constantz, 2008). Thermal conductivity will generally range by a factor of 2, as opposed to hydraulic conductivity which can range from orders of magnitude at one site. Thus, the range in fluxes associated with the variation in thermal properties is much lower than the range in Darcy estimates due to differences in hydraulic conductivity, which can range by orders of magnitude. While the full effect of horizontal heat flow on these calculations is unknown, it has been found to be negligible if horizontal flow is less than 10% of vertical flow (Lu and Ge, 1996), and in recharge conditions the error from the amplitude method used by VFLUX is less than 20% if the vertical flow is greater than the horizontal flow (Lautz, 2010). It is likely that the temperature derived flux values are

the most representative of conditions at this site because there is less variation expected with their assumptions compared to the assumptions used with the Darcy equation at this site and because of the aforementioned issues with the seepage meters.

Plan view maps are shown in **Figure 5.14** displaying the flux calculated in August by using VFLUX with the temperature rod data, using the Turcotte and Schubert (1982) equation with the temperature rod data, and using the Turcotte and Schubert (1982) equation with the temperature grid data. Both the flux results from the methods using the temperature rods show a similar spatial pattern, although the area of high flux on the northern shore is more pronounced for the Turcotte and Schubert (1982) equation. Unlike the VFLUX data, the highest flux is on the western edge of the northern shore.

The total amount of groundwater discharge from the 115 m^2 area in August is 22 000 L/d calculated from VFLUX, 13 000 L/d calculated from applying the Turcotte and Schubert (1982) equation to the temperature rods, and 11 000 L/d calculated from applying the Turcotte and Schubert (1982) equation to the temperature grid data. Both of the methods that use the Turcotte and Schubert (1982) equation have similar discharge results. This suggests that the spacing of the temperature rods, while sparser than the temperature grids, is fine enough to provide a good approximation of flux at this site.

Sensitivity associated with the Turcotte and Schubert (1982) equation, such as average temperatures chosen and thermal properties, do not account for the difference between the two methods. Lower values calculated from the Turcotte and Schubert (1982) compared to other methods were also seen by Schimdt et al (2007). The higher

flux values calculated by VFLUX are more likely due to differences with the method of calculation as opposed to data point spacing. As noted above, both methods assume strict vertical flow and thermally homogeneous sediment, but VFLUX only requires this between two points in the sediment, while Turcotte and Schubert (1982) require it to an infinite depth. In addition, the VFLUX assumption of sinusoidal diurnal stream temperature variation is also more appropriate than the Turcotte and Schubert (1982) assumption of no temporal variation for this stream. Due to the differences in assumptions, VFLUX is likely the more accurate measure of flux at this location than the Turcotte and Schubert (1982) equation. Though perhaps not as accurate as VFLUX, the Turcotte and Schubert (1982) equation can provide a useful estimate from more limited data sediment temperature data given that only one temperature point is required. Also, for higher density data such as the temperature grids, as installing 400 temperature rods in a 115 m^2 area would not be realistic. This method can also be applied in streams without substantial daily temperature variation, but still have temperature difference between the stream water and groundwater, such as locations with substantial outflows from industry.

One appeal of the temperature grid is that it provides greater spatial coverage than the temperature rods. The flux plot (**Figure 5.12)** shows a generally similar patterns to that of the temperature rods **(Figures 5.10, 5.11)** using VFLUX and Turcotte and Schubert (1982) calculations but has greater details and provides data in areas with sparse or nonexistent temperature rod data, for example, on the southern shore of the stream across from the high flow temperature rod near the middle of the reach.

5.2.6 Issues with 5 cm iButton

For both temperature methods used to quantify flux there appeared to be a difference with depth. For all of the VFLUX data, the flux values calculated between the sensors at depths of 5 and 10 cm were lowest, followed by the flux calculated between the sensors at depths of 5 and 20 cm, and finally the flux calculated at depths of 10 and 20 cm were the highest. For the 3 sensors with a fourth iButton, the calculated fluxes between all the sensors deeper than 5 cm were similar. An opposite trend was seen for the flux values using the Turcotte and Schubert (1982) equation where the values calculated using the 5 cm iButton were larger than those calculated using the 10 and 20 cm iButtons, both of which gave similar values. These results are contradictory, as they show opposite patterns in flux. In addition, the VFLUX values with the iButtons at depths of 5 and 10 cm indicated that for periods of time much of the stream reach became a net recharge zone, despite discharge predicted by the well level data and the VFLUX calculations using the 10 and 20 cm iButtons. If this was the case, water would be converging at around 10 cm depth in the sediment, and would be removed in some unknown way or travel horizontally downstream at this depth at high velocities for a long stretch. Both scenarios are improbable. Given the above two issues, it is apparent that these flux differences with depth are likely not real.

Possible causes for measurement error related to iButtons temperature measurements are discussed here. A change in sediment composition over depth, causing a change in thermal conductivity, does not explain these results, as a higher thermal

conductivity, for example, would result in a higher calculated flow for both methods. Small amounts of entrapped gas were seen in the streambed and this may cause the VFLUX values to appear lower (more upward) than they actually are (Cuthbert et al, 2010), but this would require more entrapped gas in the shallower sediment than the deeper sediment in all of the temperature rod locations, and this was not observed.

These issues could be rectified if the iButton at the 5 cm depth showed values that were artificially closer to the groundwater temperature and with diurnal amplitudes more attenuated than the sediment. While previous research has shown that it is unlikely that heat conducted along the iron rods housing the iButtons will affect the temperature (Alexander and McQuarrie, 2005; Cardenas, 2010), it cannot be ruled out that this may be contributing to the results seen. Another potential problem is that the 5 cm iButton is open to the air space above it, as there is no dowel on top of it, allowing for convection of air within the top portion of the rod (**Figure 4.2**). While the apparent cause is currently unknown, the flux values calculated using the iButtons at 5 cm depths were not included in this study due to these issues.

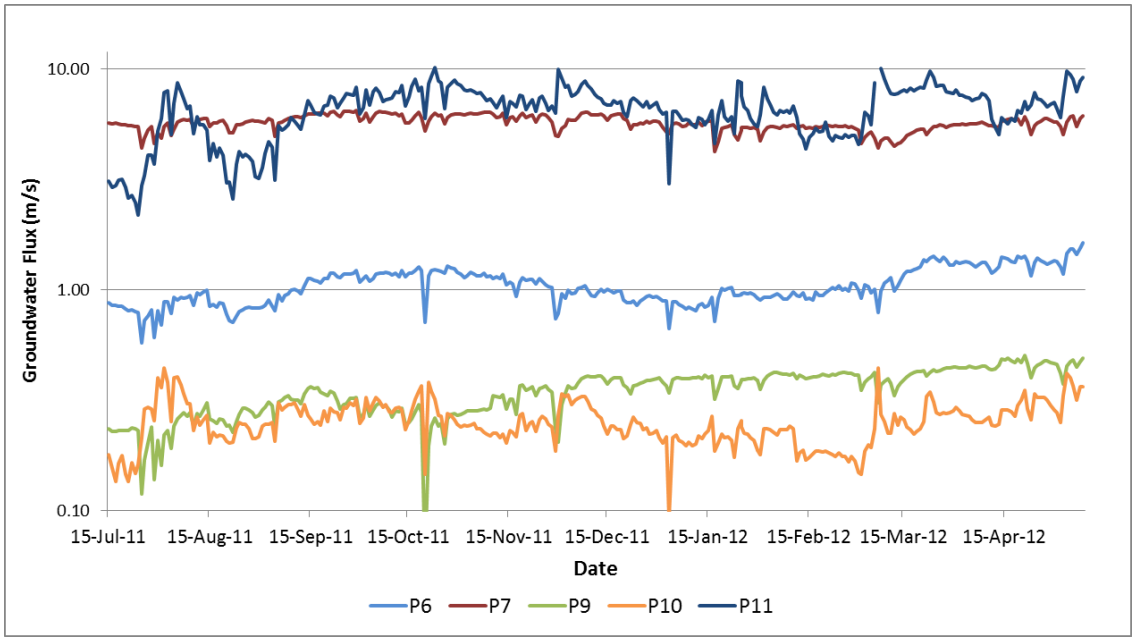

Figure 5.5: Groundwater discharge to Dyment's Creek at Site A calculated using Darcy's Law with data from five near-stream wells (**Figure 4.1**) Note the log scale.

.

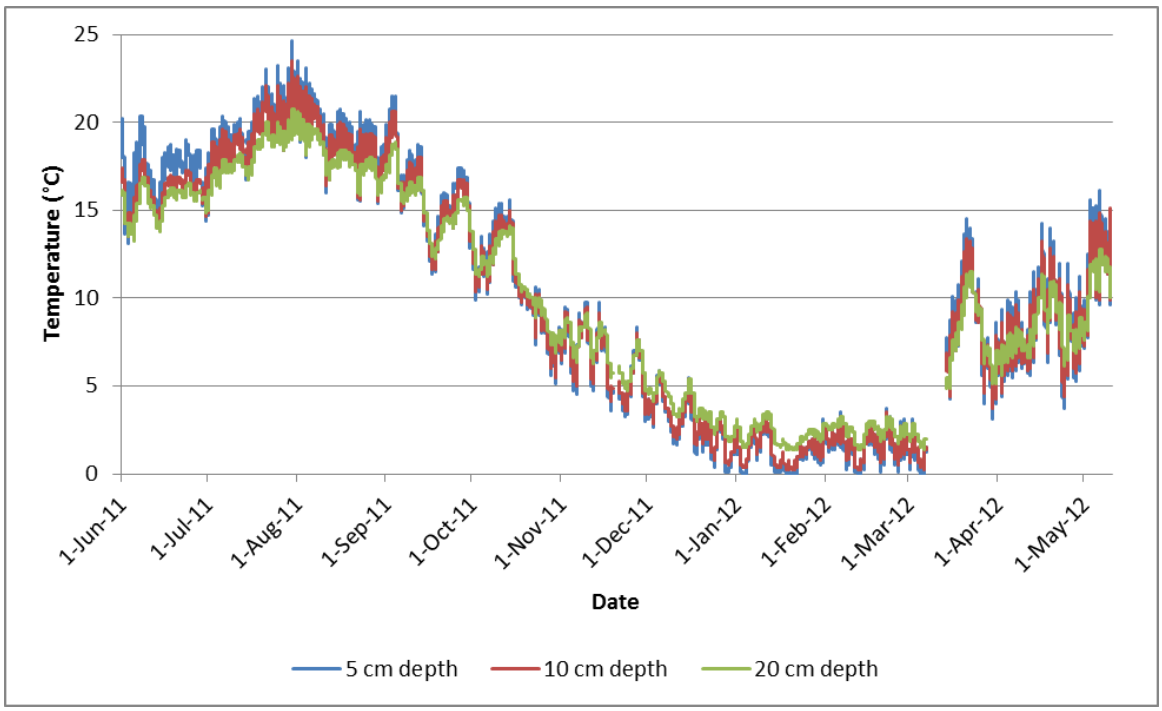

Figure 5.6: Streambed temperature at TR-L for the entire measuring period.

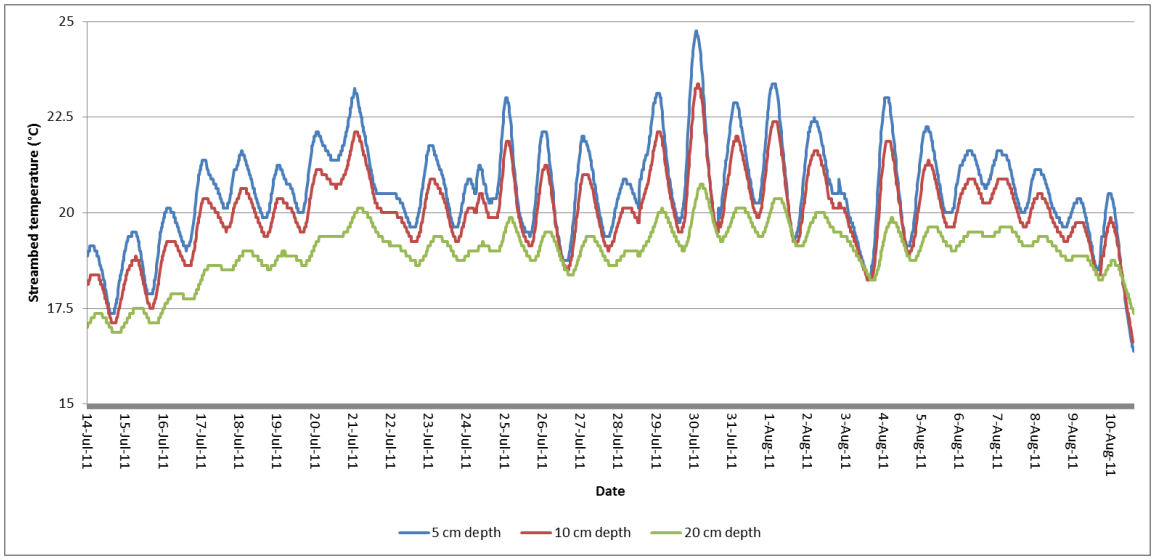

Figure 5.7: Streambed temperature at TR-I for July 14, 2011 to August 11, 2011.

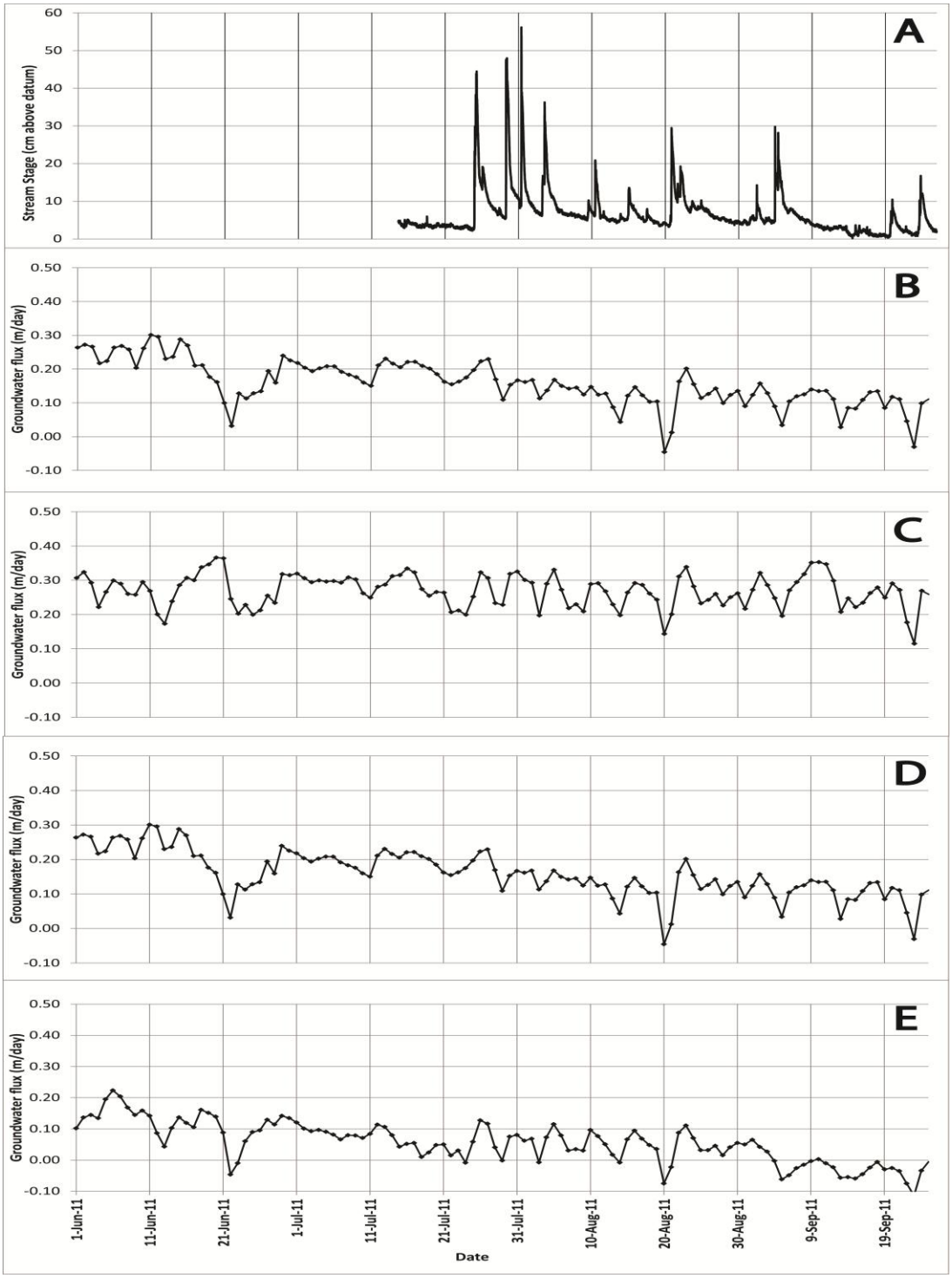

Figure 5.8: A) Stream stage and daily average VFLUX results for **B)** TR-A, **C)** TR-D, **D)** TR-K, and **E)** TR-Q from June 1, 2011 to September 25, 2011.

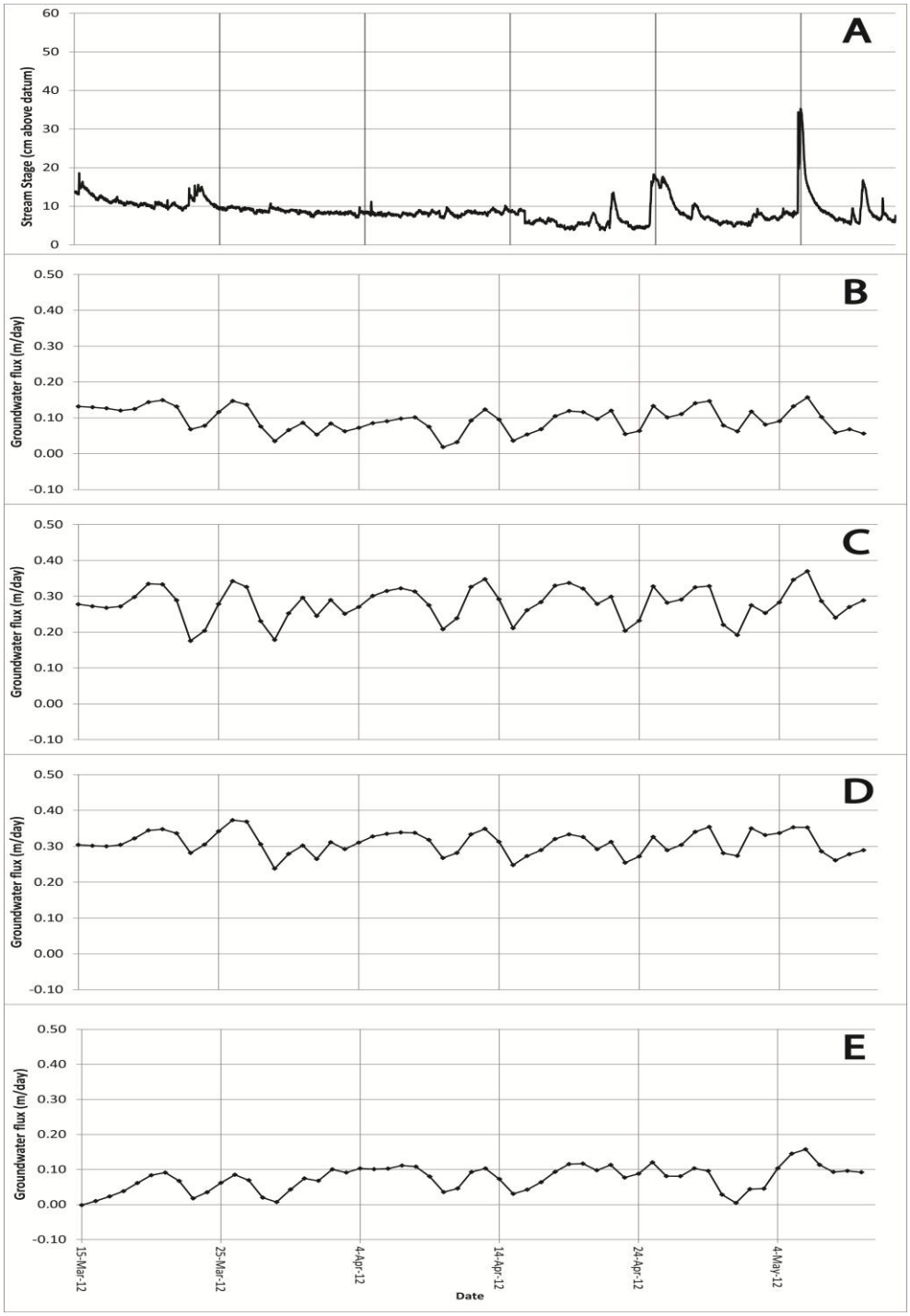

Figure 5.9: A) Stream stage and daily average VFLUX results for **B)** TR-A, **C)** TR-D, **D)** TR-K, and **E)** TR-Q from March 15, 2012 to May 10, 2012.

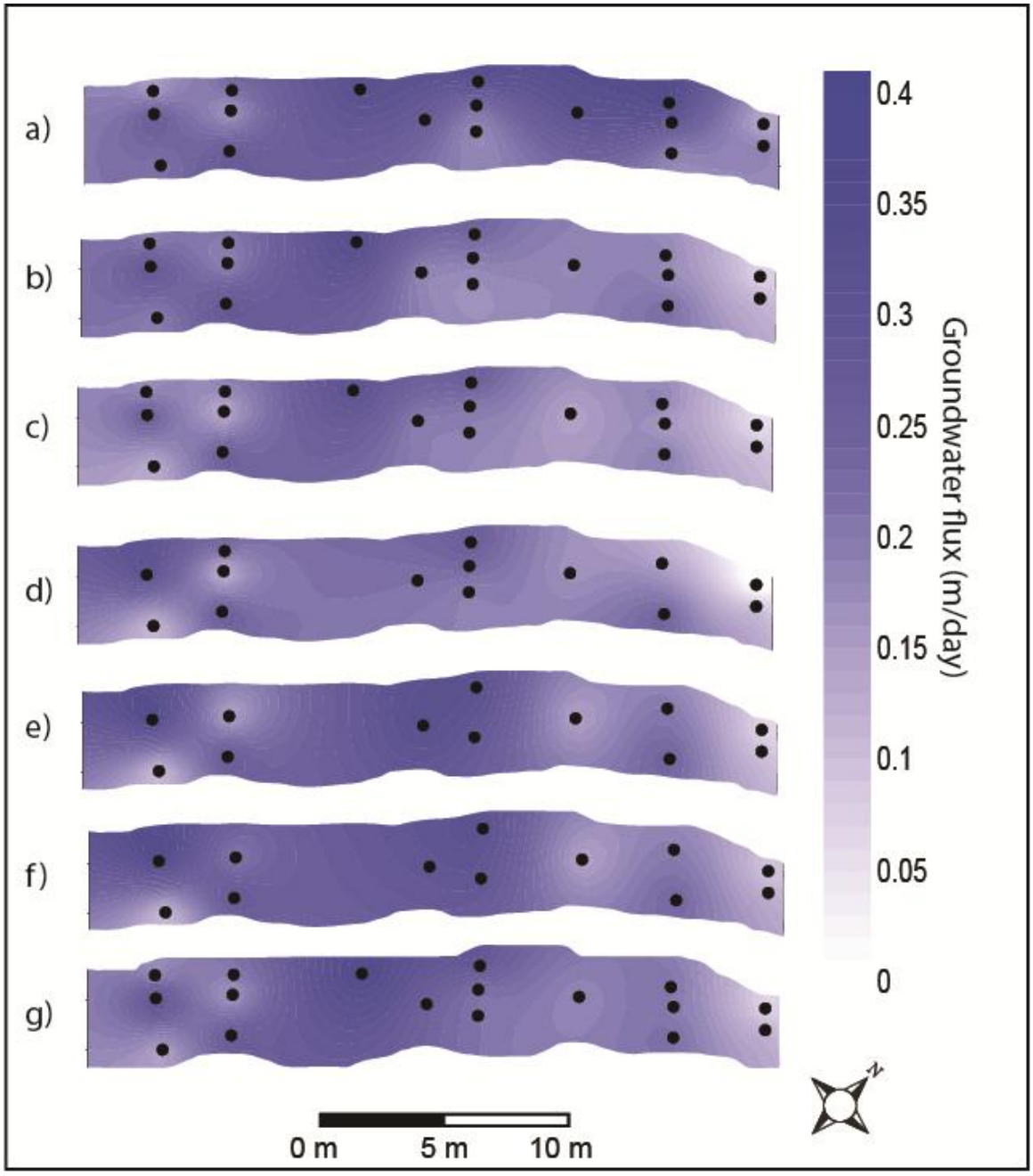

Figure 5.10: Interpolated monthly average groundwater flux for the streambed at Site A, as determined using VFLUX, for **a)** June 2011 **b)** July 2011 **c)** August 2011 **d)** September 2011 **e)** March 15-April 13, 2012 and **f)** April 14-May 10, 2012 and **g)** the interpolated map using the average VFLUX data for the entire study period. Black dots indicate temperature rods used to supply data for that time period.

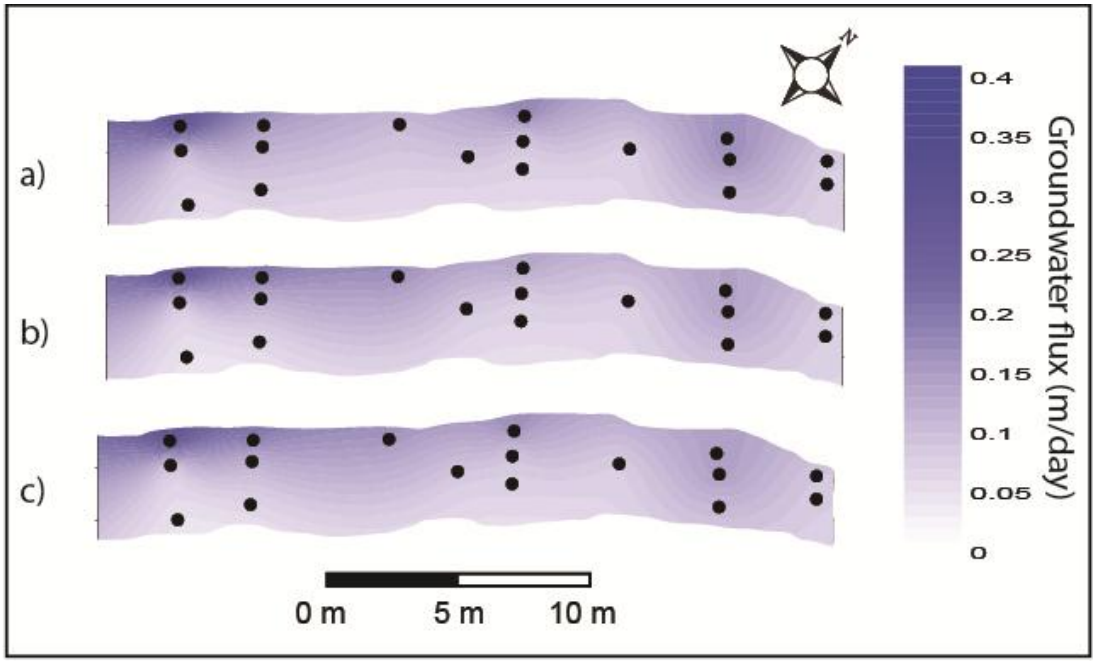

Figure 5.11: Interpolated groundwater flux calculated using the Turcotte and Schubert (1982) equation on the temperature rod data for **a)** July 17 to July 31, 2011 **b)** August 10 to August 20, 2011 **c)** August 21 to August 31, 2011. Black dots indicate data points.

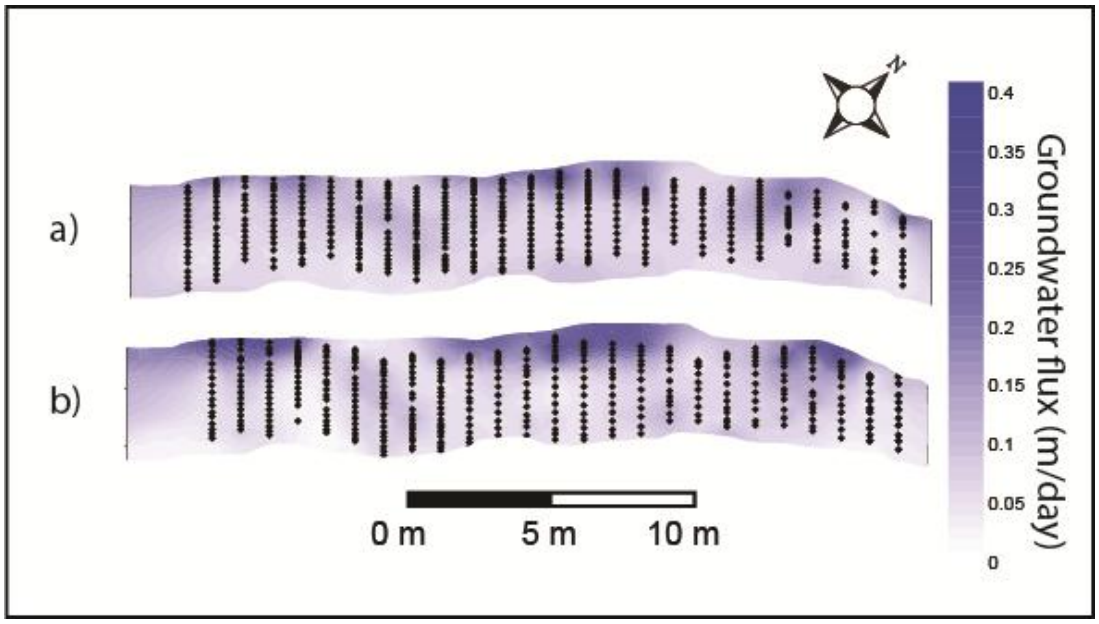

Figure 5.12 i: Interpolated groundwater flux map using the Turcotte and Schubert (1982) equation on the **a)** August 2011 temperature grid and the **b)** January 2012 temperature grid. Black dots indicate data points.

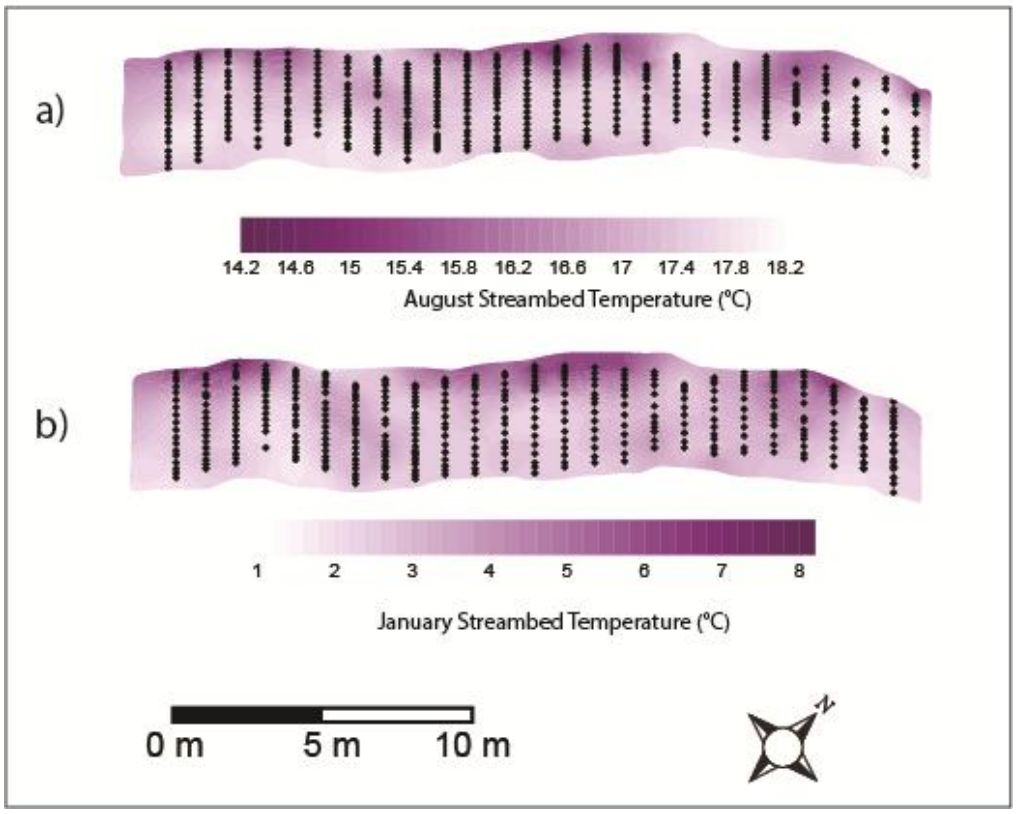

Figure 5.12 ii: Interpolated streambed temperatures at Dyment's Creek used for the flux calculations shown in **Figure 5.12 i.**.temperature grid for a) August 2011 and b) January 2012. Black dots indicate data points.

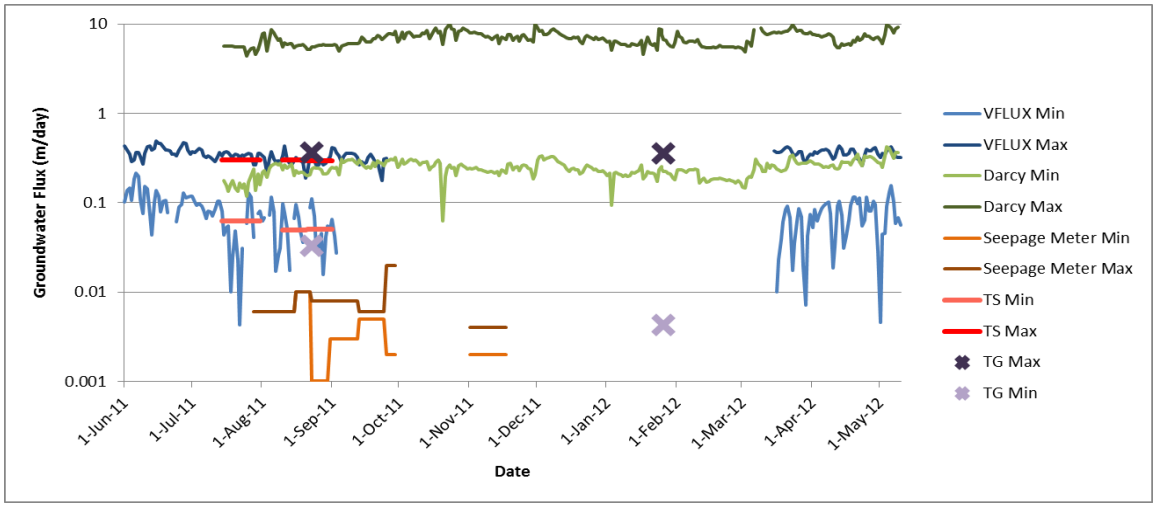

Figure 5.13: Ranges in groundwater flux values calculated using VFLUX, Darcy's Law, the Turcotte and Schubert (1982) equation from both the temperature rod (labelled TS) and temperature grid data sets (labelled TG), and measured by the seepage meters, during the study period. Note the log scale for flux.

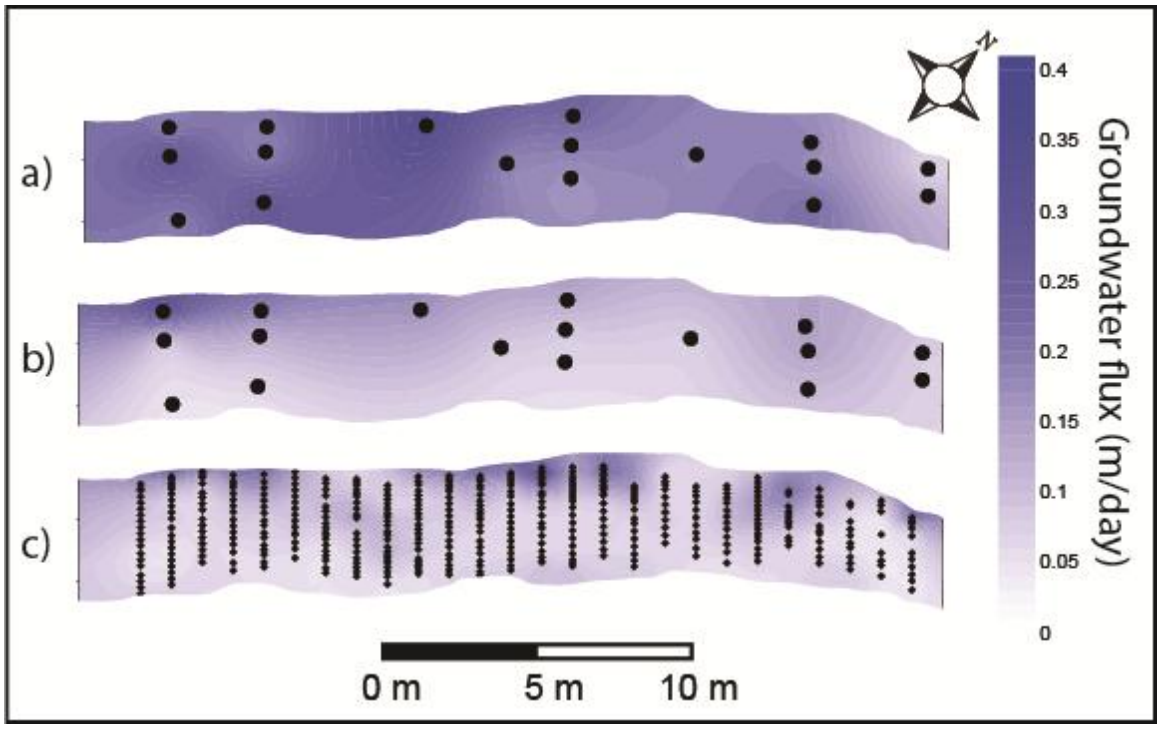

Figure 5.14: Interpolated August 2011 groundwater flux map created using **a)** VFLUX **b)** the Turcotte and Schubert (1982) equation on the temperature rods and **c)** the Turcotte and Schubert (1982) equation on the temperature grid. Black dots indicate data points. Plots shown are the same as **Figure 5.10 c, Figure 5.11 b,** and **Figure 5.12 a**.

5.3 Site A Contaminant Levels

5.3.1 Dyment's Creek Stream Concentrations

The stream SRP concentrations varied throughout the year (**Table 5.6, Figure 5.15**) with a mean of 23 μg/L at Site A and 18 μg/L at Site B. Values at Site A higher than at Site B for 7 of the 10 sampling dates, implying that there is likely a source of SRP between the two locations. There are no strict environmental water quality guidelines for phosphorus in Ontario, but at certain times the levels at Site A approached or exceeded the threshold (35 μg/L) for being considered eutrophic (Canadian Council of Ministers of the Environment, 2004). No consistent seasonal trend was evident, although the data were sparser during the winter months.

Mean stream ammonium concentrations (**Table 5.6, Figure 5.16**) were 0.4 mg/L at Site A and 0.1 mg/L at Site B, and Site A concentrations were always higher than Site B. None of the stream water concentrations exceeded the water quality guidelines for ammonium, which vary depending on the pH and temperature of the water at the time from 0.35 to 15.3 mg/L at the range of water parameter values observed at Dyment's Creek (Canadian Council of Ministers of the Environment, 2010), although on August 17, 2011 the Site A concentration (0.4 mg/L) was 80% of the guideline value (0.5 mg/L). Nitrate concentrations (**Table 5.6, Figure 5.16**) were similar for both locations, with a mean of about 2.8 mg/L. The difference between the two measurement sites was less than 0.5 mg/L for all but one sampling day. The nitrate values observed are far less than the water quality guideline concentration for nitrate of 13 mg/L (Canadian Council of Ministers of the Environment 2012).

Table 5.6: Stream nutrient concentrations at Dyment's Creek.

	Site A SRP (µg/L)	Site B SRP (µg/L)	Site A NH_4^+ (mg/L)	Site B NH_4^+ (mg/L)	Site A NO_3^- (mg/L)	Site B NO_3^- (mg/L)
Mean	23	18	0.44	0.13	2.8	2.7
Standard Deviation	11.01	4	0.05	0.12	0.9	0.5
Max	46	25	0.72	0.25	5.5	3.6
Min	7	14	0.24	0.07	1.8	1.9

5.3.2 Piezometer Concentrations

Piezometer SRP and ammonium concentrations were generally much higher than those observed in the stream **(Table 5.7-5.10)**, so it is likely that under base flow discharge conditions groundwater is contributing these nutrients to the stream**.** Piezometer locations shown in **Figure 4.1**. Mean SRP values ranged from 22 to 787 µg/L, and mean ammonium values ranged from 0.17 to 23.97 mg/L. The maximum observed SRP value (1201 µg/L) is within the range of maximum values of 950 to 1700 µg/L seen in many studies of streambed SRP contamination (Carlyle and Hill, 2001; Banaszuk et al, 2005; Jarvie et al, 2008; Schilling and Jacobson, 2008; Flores-Lopez et al, 2011). Nitrate values at all the piezometers were always lower than the stream values, and the highest mean value was 0.8 mg/L, so groundwater is not likely a significant contributor to stream nitrate concentrations.

Table 5.7: Piezometer SRP concentrations for the northern shore piezometers at Site A.

	PN-1-1	PN-1-2	PN-2-1	PN-2-2	PN-3-1	PN-4-1	PN-4-2
Mean value (µg/L)	606	731	67	46	28	58	22
Max value (µg/L)	1058	1201	110	64	37	126	28
Min value (µg/L)	263	147	25	11	4	21	4

Table 5.8: Piezometer SRP concentrations for the southern shore piezometers at Site A.

	PS-1-1	PS-1-2	PS-2-1	PS-2-2	PS-3-1	PS-4-1	PS-4-2
Mean value (µg/L)	211	609	787	215	704	402	71
Max value (µg/L)	432	886	1017	270	952	731	102
Min value (µg/L)	33	142	585	20	104	178	12

Table 5.9: Piezometer ammonium concentrations for the northern shore piezometers at Site A.

	PN-1-1	PN-1-2	PN-2-1	PN-2-2	PN-3-1	PN-4-1	PN-4-2
Mean value (mg/L)	5.81	3.87	0.79	0.50	0.31	0.22	0.17
Max value (mg/L)	9.00	5.97	1.59	0.75	0.46	0.60	0.30
Min value (mg/L)	1.57	1.18	0.40	0.13	0.11	0.10	0.07

Table 5.10: Piezometer ammonium concentrations for the southern shore piezometers at Site A.

	PS-1-1	PS-1-2	PS-2-1	PS-2-2	PS-3-1	PS-4-1	PS-4-2
Mean value (mg/L)	22.63	19.72	23.97	8.40	8.92	3.89	0.70
Max value (mg/L)	37.50	26.25	34.50	12.25	12.77	8.28	1.04
Min value (mg/L)	7.03	13.90	14.40	4.80	2.01	0.28	0.08

There was considerable temporal variation in SRP concentrations at each location, although there was no consistent trend. Plots of SRP over time are shown for select piezometers in **Figure 5.18**; the four that were chosen are representative of the range of concentration and variation seen. Mean values are shown in **Table 5.11**. Areas with a higher concentration tended to show more variation. With respect to differences in concentrations with depth, the mean shallow piezometer concentrations were always higher than the mean deep piezometer concentrations, with the exception of PN-1 which did not show this pattern. PS-1-1 and PS-1-2 were not included in this depth comparison, as they are located about 2.5 m away from each other, as opposed to <50 cm for the other pairs. Spatial trends are evident, as concentrations on the southern shore and the most-

upstream location (two piezometers located at PN-1) are higher than the concentrations along the rest of the northern shore. Except for the two piezometers located at PN-1, concentrations on the northern shore never exceeded 126 µg/L. Concentrations are consistently high on the southern shore, as only one piezometer has a mean SRP concentration below 200 µg/L. Mean ammonium concentrations were always higher in the shallow piezometers. Similar to the SRP concentrations, temporal variation is seen in ammonium concentrations (**Figure 5.19**) but with no site-wide trend. The highest ammonium concentrations were found along the western portion of the southern shore, at PS-1-1, PS-1-2, and PS-2-1. The lowest concentrations were found along the eastern portion of the northern shore. Full contaminant data can be found in **Appendix C**.

Table 5.11: Mean concentration of redox sensitive species and saccharin for Site A sampling piezometers on the north and south shores.

Compound	Units	Site A Stream	Site B Stream	PN 1-1	PN 1-2	PN 2-1	PN 2-2	PN 3-1	PN 4-1	PN 4-2
SRP	ug/L	24	19	634	766	71	50	31	61	24
NH_4^+	mg/L	0.42	0.13	6.16	4.20	0.84	0.54	0.34	0.22	0.18
SO_4^{2-}	mg/L	24.14	24.69	0.27	0.87	4.12	6.94	6.95	8.75	18.80
NO_3^-	mg/L	2.79	3.04	0.03	0.09	0.17	0.10	0.05	0.04	0.05
Fe^{2+}	mg/L	0.16	0.09	19.90	15.79	0.50	0.79	0.24	0.89	0.46
Mn^{2+}	mg/L	0.15	0.09	0.35		0.15		0.11	0.24	0.11
Saccharin	ng/L	58	42	29	13	32	19	14	0	0

Compound	Units	Site A Stream	Site B Stream	PS 1-1	PS 1-2	PS 2-1	PS 2-2	PS 3-1	PS 4-1	PS 4-2
SRP	ug/L	24	19	217	589	844	283	779	427	77
NH_4^+	mg/L	0.42	0.13	24.19	21.00	25.50	8.90	9.78	4.05	0.75
SO_4^{2-}	mg/L	24.14	24.69	9.79	0.18	0.06	0.03	0.31	11.17	0.16
NO_3^-	mg/L	2.79	3.04	0.84	0.04	0.05	0.04	0.18	0.81	0.05
Fe^{2+}	mg/L	0.16	0.09	22.59	21.08	6.66	4.00	12.03	13.65	1.54
Mn^{2+}	mg/L	0.15	0.09	0.72	1.44	1.67	0.33	1.10	1.04	0.27
Saccharin	ng/L	58	42	169	193	267	143	40	15	2

There is evidence based on the levels of redox sensitive species at Site A (**Table 5.11**) that the groundwater nutrient concentrations are associated with, and may be controlled by, the groundwater redox conditions. A classification scheme for identifying different redox zones, based on the availability of oxygen, is shown in **Table 5.12**, based on similar classifications by Christensen et al (2000), McMahon and Chapelle (2008), and Abe et al (2009) but adjusted to species' concentrations seen at this site as recommended by Christensen et al (2000). Redox classification for the piezometers at this site applied to mean piezometer concentrations of redox sensitive species (**Table 5.11)** is shown in **Table 5.13.** There is a clear geographic pattern for the redox conditions. The piezometers on the northern shore are oxic-suboxic with the exception of PN-1-1 and PN-1-2 (upstream end), which are methanogenic, and the piezometers on the southern shore are either methanogenic or Fe(III) reducing, with the exception of PS-4-2 (deeper down-stream end piezometer) which is oxic-suboxic. As shown in section **5.2**, groundwater flux along the southern shore of the stream is lower than along the northern shore. That the more reducing conditions were seen on the shore with the lower groundwater flux results is not surprising, as a link between low groundwater fluxes and reducing conditions has been observed in the literature (Abe et al, 2009; Schmidt et al, 2011). A lower groundwater flux likely results in a higher groundwater residence time, which allows for more time for reducing processes. Reducing conditions in groundwater may also be caused by high organic matter content (Christensen et al, 2000). The organic peat may be a source of the phosphorus along the streambed at Dyment's Creek, while the landfill contaminants promote reducing conditions. The piezometers classified as

methanogenic have the highest SRP concentrations, while the piezometers classified as oxic-suboxic have the lowest SRP concentrations. Higher SRP in reducing conditions may be due to phosphorus desorbing off sediments (McCobb et al, 2003; Banaszuk et al, 2005). One mechanism is from the reduction of Fe^{3+} to Fe^{2+}, releasing phosphorus that was bound to the sediments by Fe^{3+} (Carlyle and Hill, 2001). This may be occurring at this site, given that SRP piezometer concentrations are correlated well ($R^2 = 0.7$, linear correlation) with Fe^{2+} concentrations (**Figure 5.20**). While the high ammonium concentrations were all located in the reducing locations and usually observed with high SRP concentrations (**Figure 5.21**), there were locations with reducing conditions and high SRP concentration that exhibited low ammonium concentrations. This indicates that redox conditions are not the sole driver of ammonium concentrations at this site.

Earlier work at this site (Roy and Bickerton, 2012) detected many contaminants in this area of the stream associated with old landfills. Van Stempvoort et al, (2011) postulated that the artificial sweetener saccharin may be a useful tracer for older landfills as it has not been widely used in Canada since 1977 (Gougeon et al, 2004). The elevated levels of Saccharin measured from the piezometers on the south shore of Dyment's Creek (**Table 5.12**) may signify that the contaminants in the groundwater on the south shore may be sourced from the nearby landfills, which were in use in the 1960s. These landfills may be a source of the ammonium to the streambed, as ammonium and saccharin piezometer concentrations are positively correlated ($R^2 = 0.77$, **Figure 5.22**). SRP is not as well correlated with saccharin ($R^2 = 0.15$). As no known landfills existed on the southern shore at this location, one possibility is that some of the groundwater was

moving deep under the stream from the northern shore, and discharging near the southern bank, such as seen in Conant et al (2004).

Table 5.12: Criteria for redox zone classification. All concentrations in mg/L.

Redox Condition	NH_4^+	NO_3^-	Mn^{2+}	Fe^{2+}	SO_4^{2-}
Oxic-Suboxic	< 1.5	> 1	< 0.3	< 2	
NO_3^- reducing		> 1	< 0.3	< 2	
Mn(IV) reducing		< 1	> 0.3	< 2	
Fe(III) reducing		< 1	> 0.3	> 2	
Methanogenic		< 1	> 0.3	> 2	< 2

Table 5.13: Redox zone classification of piezometers at Site A.

Location	Shallow Piezometer Redox Classification	Deep Piezometer Redox Classification
PN-1	Methanogenic	Methanogenic
PN-2	Oxic-Suboxic	Oxic-Suboxic
PN-3	Oxic-Suboxic	
PN-4	Oxic-Suboxic	Oxic-Suboxic
PS-1	Fe(III) Reducing	Methanogenic
PS-2	Methanogenic	Methanogenic
PS-3	Methanogenic	
PS-4	Fe(III) Reducing	Oxic-Suboxic

5.3.3 Peeper Concentrations

5.3.3.1 SRP

As discussed in section **2.4.2,** the use of peepers allows for greater depth resolution of groundwater concentrations. In addition, because they were installed in more locations than the piezometers across the streambed (**Figure 4.1**), peepers provided a higher spatial resolution across the streambed. Temporally averaged samples potentially reveal short-term transients not captured by point-in-time sampling, such as a spike in concentrations between piezometer sampling. Concentration of SRP versus depth

plots for five of the peepers and the mean value for the three different sampling periods are shown in **Figure 5.23**, while plots for the other peepers can be found in **Appendix D.** The five that were chosen are representative of the range of concentration and variation observed. The mean concentration in the top chamber (located at the streambed interface) was lower than the others for every time period, likely due to mixing with surface water. Unlike the piezometers, there was no clear trend with depth below the top chamber. Some peepers, such as TR-A, showed a large increase between the first and second chamber. At these locations, it is likely that the top peeper chamber was almost fully exposed to an area of stream water with low SRP concentrations due to streambed scour or improper placement. TR-I showed a sharp increase with depth for all time periods, possibly due to increasing influence of stream water causing increased oxidation. TR-B showed the greatest variation over time, as the pattern with depth was different for every study period. PS-2-1 was fairly typical of peepers showing a high concentration, with no consistent trend with depth. Some of the peepers showing low concentrations, such as TR-K, were consistently low with time and depth. Causes of this may include sediment property heterogeneity, as pore size could affect the redox conditions, horizontal flow paths, such as hyporheic flows, temporal variation in these flow paths, and the peepers may not have been put back in the exact same location in an area with high spatial heterogeneity. This level of variation has been observed in the literature (Jarvie et al, 2008; Palmer-Felgate et al, 2010).

Peeper SRP concentrations also differed considerably from concentrations in nearby piezometers, which has also been observed in previous research (Hunt et al, 1997;

Lorah et al, 2005; Lorah et al, 2009). A possible reason for this is that when sampling by applying a vacuum, such as for piezometers, the larger pore sizes are disproportionately sampled. These large pores may make up only about 10% of the volume, but much more water flows through them (Harvey et al, 1995; Harvey and Nuttle, 1995). In comparison, peepers sample both the larger and smaller pores, the latter of which often have higher concentrations of nutrients (Harvey et al, 1995; Hunt et al, 1997; Lorah et al, 2009). If phosphorus desorbing off sediment in reducing conditions is contributing to SRP concentrations at this site, then the sampling method which samples a greater portion of the smaller pores, with a greater surface to volume ratio and lower natural groundwater flow (i.e. longer groundwater residence time), would be expected to have the higher SRP concentrations. **Figure 5.24** shows SRP concentrations from the 10 cm deep peeper chambers compared to the nearby shallow (depth of 10 cm) piezometer concentrations at each different sampling period (November 2011 peepers compared to Dec 1, 2011 piezometer samples, January 2012 peepers compared to January 31, 2012 piezometer samples, and March 2012 peepers compared to March 21, 2012 piezometer samples). The peeper concentrations are always higher, and two different correlations between the peeper and piezometer concentrations are observed, dependent on the redox condition of the piezometers. For the shallow piezometers considered oxic-suboxic (PN2-1, PN3-1, PN4-1), there is a much larger slope, i.e. higher piezometer concentrations as associated with a much larger increase in peeper concentration. The slope is not as large for the shallow piezometers with more reducing groundwater (PN1-1, PS1-1, PS2-1, PS3-1, PS4-1). For more reducing groundwater, pore size will have much less of an effect on

SRP concentration than for more oxic waters. Water generally moves through smaller pores In the reducing groundwater, much of the oxygen has already been used up, so a smaller pore size (with a longer residence time) would not have as much of a difference on oxygen levels compared to oxic groundwater.

Groundwater discharging to the stream through advection will disproportionally be coming from larger pores, as water is able to move much more quickly through larger pores than smaller pores (Fetter, 1999). The peepers sample through diffusion and therefore do not disproportionately sample the larger pores compared to the piezometers which sample through advection. Due to this, the elevated peeper concentrations were not considered as appropriate as the piezometer data for determining nutrient flux. However, the peepers provide valuable spatial information. Thus, the correlations shown in **Figure 5.24** were used to convert the SRP concentrations seen in the peepers to those that would be expected in the larger pores, so that the peeper data could then be used to determine nutrient flux. For the peepers not located near a piezometer, where there is no redox chemistry data, ammonium concentrations were used to determine whether the concentration should be converted using the oxic-suboxic relation or the reducing relation. An ammonium concentration of 0.5 mg/L or above was considered reducing. There was a clear relation between ammonium levels and the ratio of peeper and piezometer SRP levels (**Figure 5.25**), which supports the use of this method.

For the purposes of calculating nutrient flux (Chapter 5.4), concentrations in the shallow peeper chambers were considered more relevant than deeper chambers as they

would be more representative of concentrations of discharging groundwater. However, the top chambers showed signs of occasional exposure to the stream and thus, the data for chambers at 5 cm depth were used. An interpolated map using kriging of the converted SRP levels for the peeper chambers at a depth of 5 cm for the different sample periods is shown in **Figure 5.26,** along with the map of the mean peeper concentration for the 5 cm chambers and the mean concentration of the 10 cm (shallowest) piezometers. As with the piezometers, higher concentrations were observed along the southern shore near PS-2-1 and PS-3-1, and on the western end of the northern shore near PN-1-1. The major differences seen with the peeper data compared to the piezometer data are a high concentration zone near TR-A (western end of the southern shore) and the area of low concentration along most of the northern shore extending into the centre of the stream. A difference map between the two is shown in **Figure 5.27**. The largest differences were in the centre of the stream, where piezometer concentrations were higher, and at the western end, where peeper concentrations were higher. Comparing average peeper SRP concentration at the temperature rods with the average water flux calculated by VFLUX in section **5.2** show that the highest SRP concentrations are only found in lower flux zones, although low SRP concentrations are found in both high and low flux zones (**Figure 5.28**). As explained in the previous section, this is likely due to the effect of water flux on redox conditions.

5.3.3.2 Ammonium

Ammonium concentrations in the peepers did not vary as much as SRP concentrations. The mean peeper concentration did not vary much with depth or time (**Figure 5.29**), although the peeper chambers at depths of 5 and 10 cm always showed the highest values. With a few exceptions, the only peepers showing a concentration higher than 5 mg/L were found on the south shore (TR-A, TR-D/PS-1, PS-2, PS-3, and TR-M/PS-4). Concentration of SRP versus time plots for five of the peepers and the mean value for the three different sampling periods are shown in **Figure 5.29.** These plots represent the range of concentrations and level of variation seen in all the peepers, which can be found in **Appendix E**. The sharp decrease in ammonium concentrations at the top chamber at TR-A is similar to the decrease in SRP concentrations.

Unlike the SRP concentrations, there was not a noticeable difference in ammonium concentrations between peepers and piezometers at nearby locations (slope of linear regression 1.02, $R^2 = 0.85$). This may signify that the ammonium is not sourced from the sediments in the streambed, so the different redox conditions in the smaller pores may not lead to an increase in ammonium concentrations. This further supports the hypothesis that the ammonium is sourced from nearby landfills. An interpolated map of the ammonium concentration for the peeper chambers at a depth of 5 cm for the different sample periods is shown in **Figure 5.30,** along with the map of the mean peeper concentration for the 5 cm chambers and the mean concentration of the 10 cm sampling piezometers. Kriging was used for interpolation. As with the interpolated SRP

concentration maps, the 5 cm chambers were used. Ammonium peeper concentrations at the 5 cm chamber remained very constant over the sampling period (November 2011 to March 2012). This may be partially due to the sampling method, as peepers show a long term average compared to the piezometers, which show a snapshot in time and exhibited more temporal variation. The peepers also had a shorter sampling period than the piezometers, about five months compared to eight for the piezometers. The highest ammonium concentrations were observed at TR-A and PS-2-1, both located along the southern shore. The difference between the peeper and piezometer concentration maps (**Figure 5.31**) is not the same as with SRP, with two areas where piezometer concentrations were higher along the middle of the stream, and two areas where peeper concentrations were higher along the southern shore.

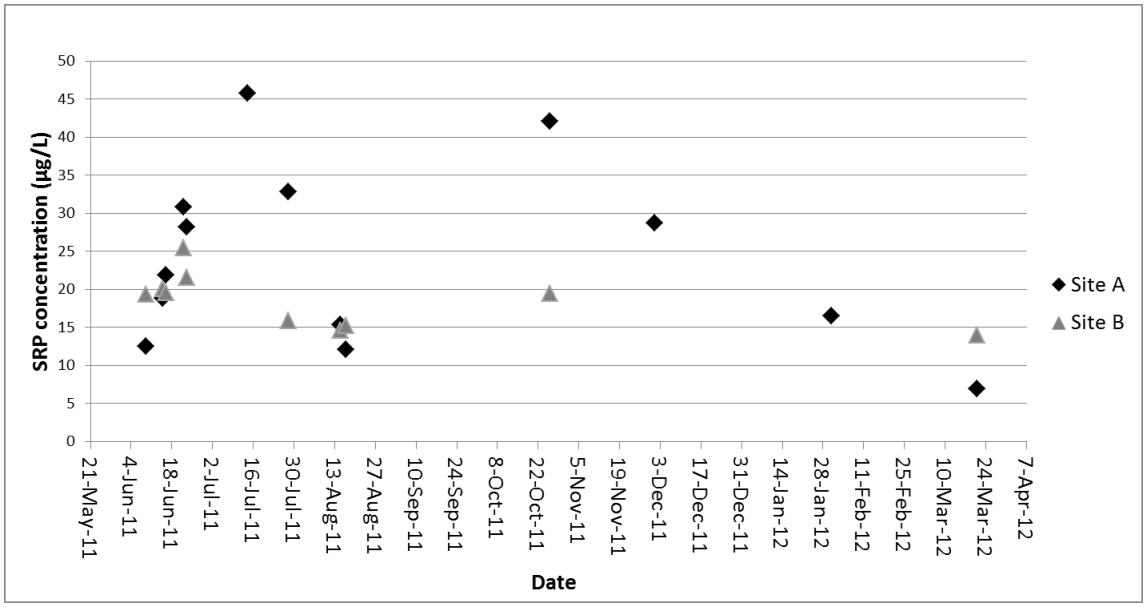

Figure 5.15: Stream SRP concentrations. X-axis interval is biweekly.

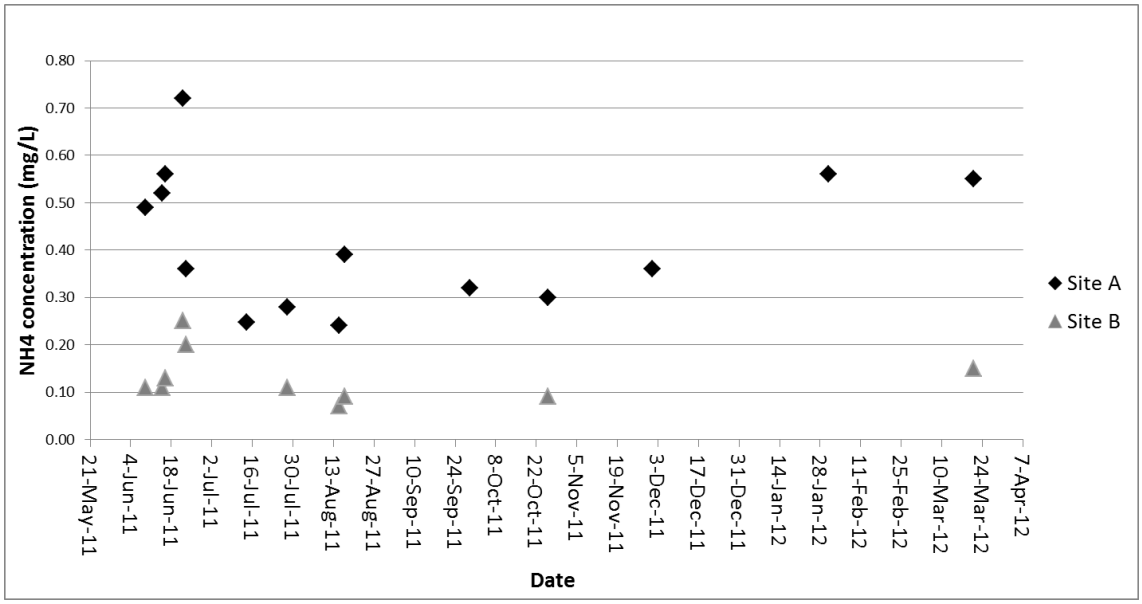

Figure 5.16: Stream ammonium concentrations. X-axis interval is biweekly. X-axis interval is biweekly.

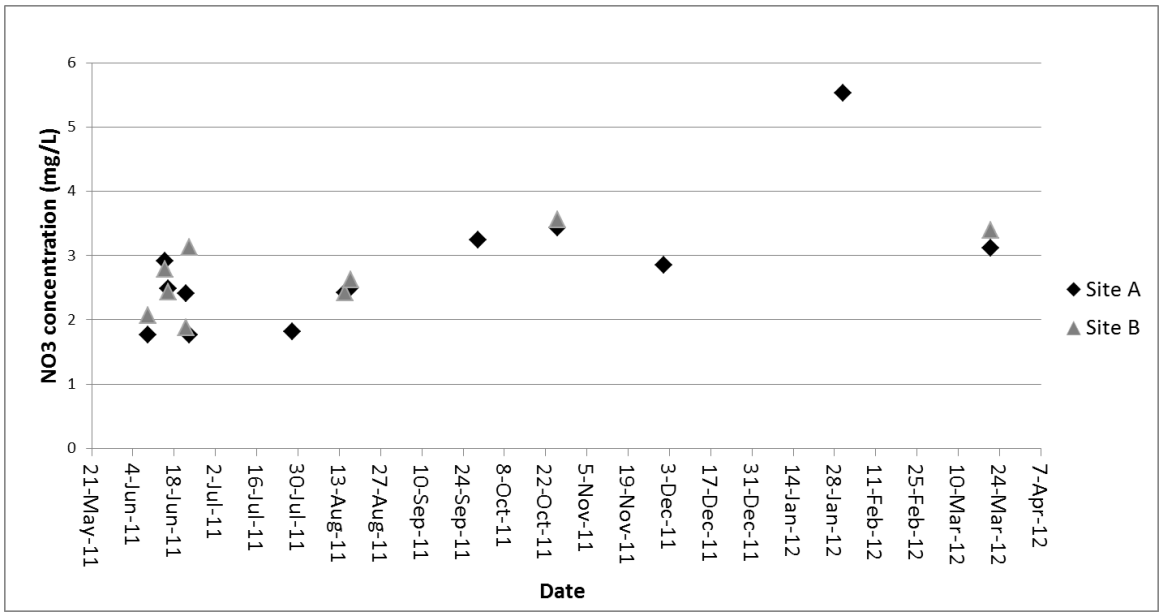

Figure 5.17: Stream nitrate concentrations. X-axis interval is biweekly. X-axis interval is biweekly.

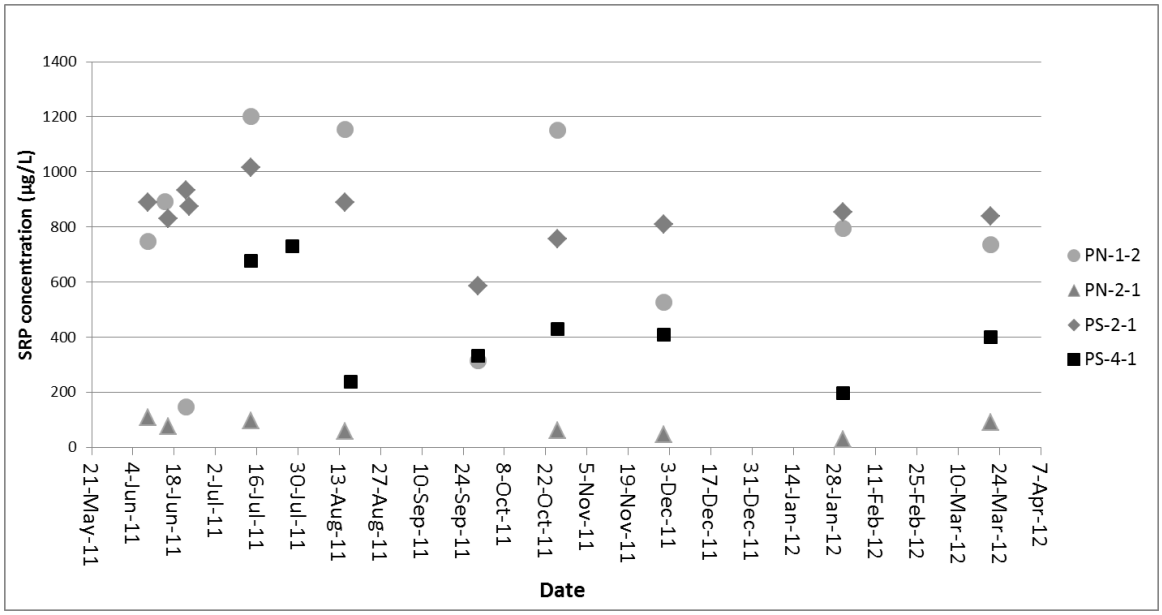

Figure 5.18: Piezometer SRP concentrations for 4 of the 14 piezometers. Complete data is shown in Appendix C. X-axis interval is biweekly.

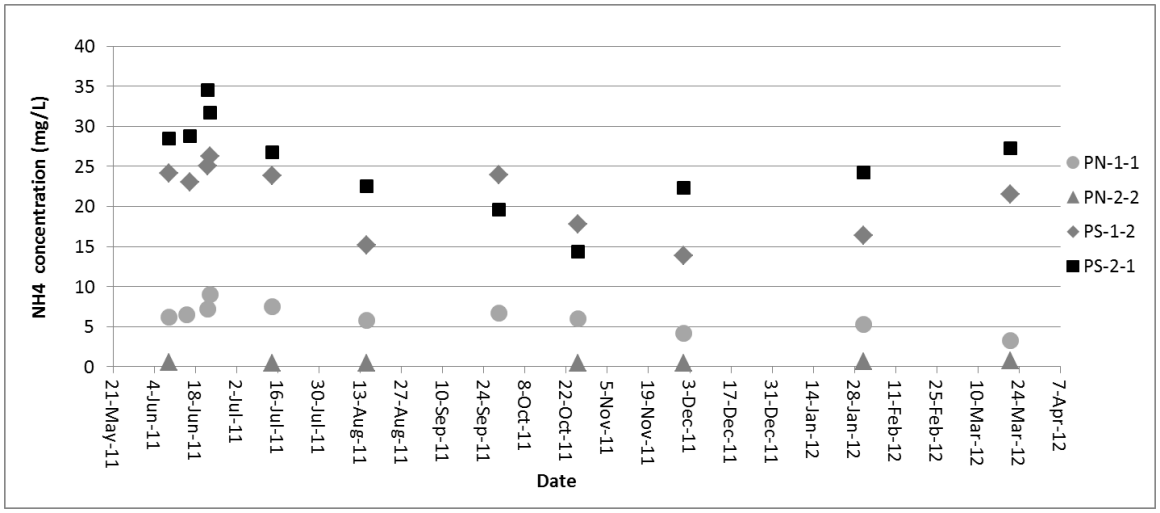

Figure 5.19: Piezometer ammonium concentrations for 4 of the 14 piezometers. Complete data is shown in Appendix C. X-axis interval is biweekly.

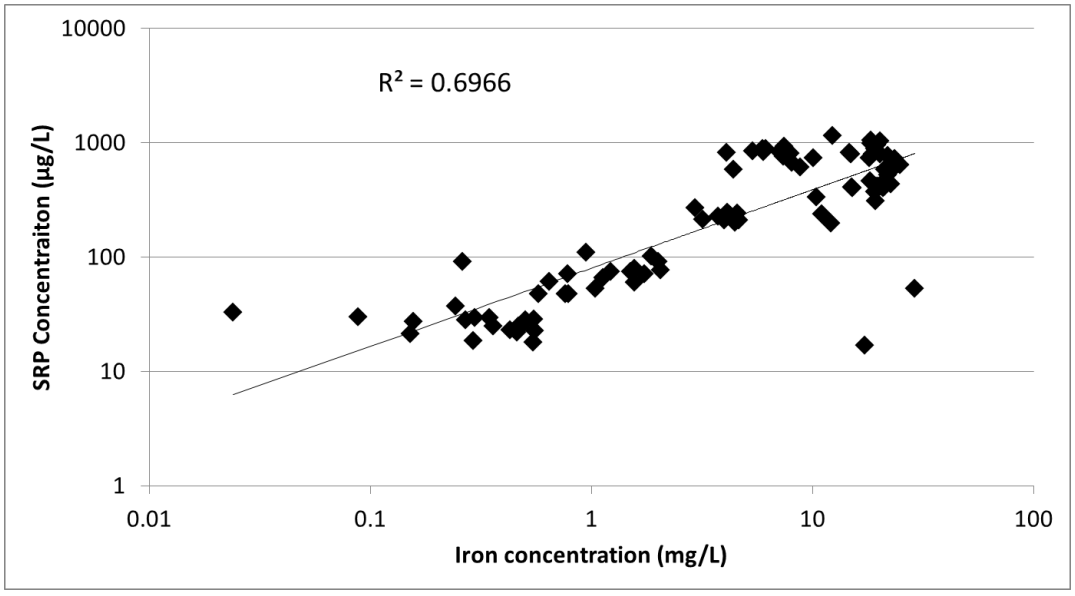

Figure 5.20: SRP versus iron for the piezometers at Site A, with logarithmic correlation fit to the data. Note the log scales.

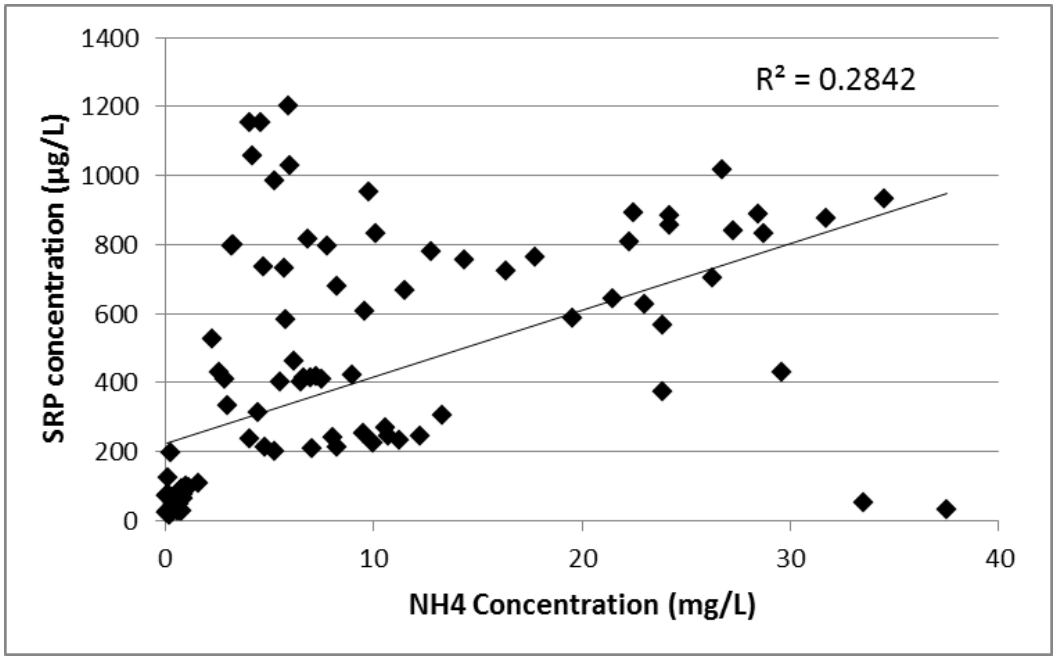

Figure 5.21: SRP versus ammonium for the piezometers at Site A, with linear correlation fit to the data.

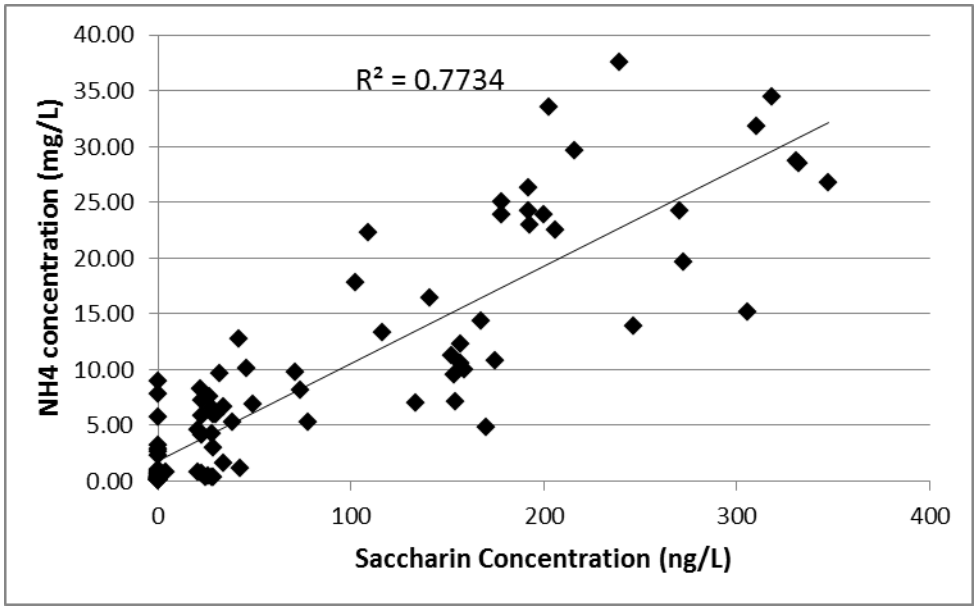

Figure 5.22: Ammonium versus saccharin for the piezometers at Site A, with a linear correlation fit to the data.

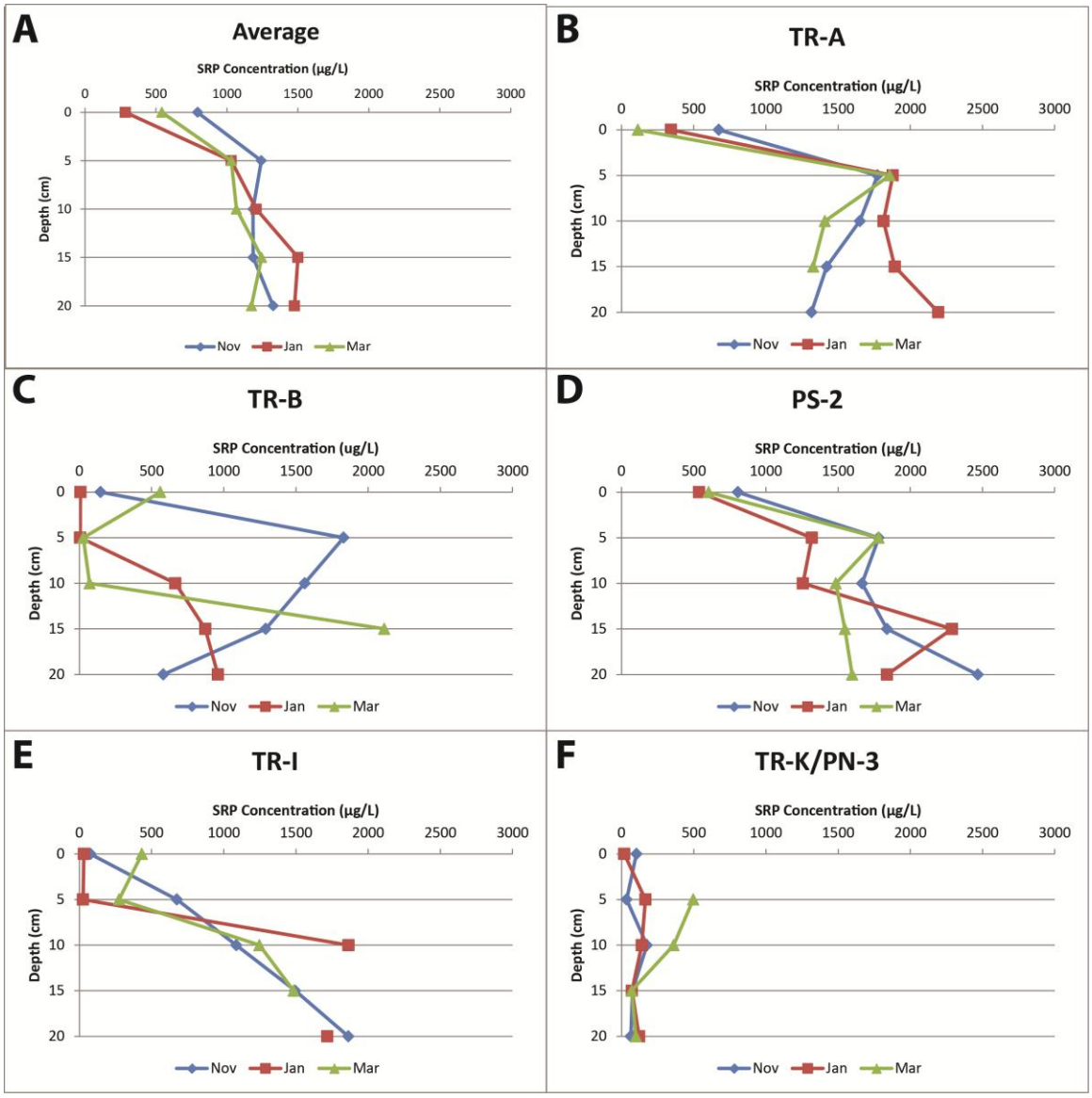

Figure 5.23: Depth profile of SRP concentrations determined with peepers for the 3 sampling periods, November 2011, January 2012, and March 2012, with a) mean for all the peepers, b) TR-A c) TR-B d) PS-2 e) TR-I and f) TR-K/PN-3. Depths are approximate due to slight changes in streambed sedimentation over time. Lines between data points are to help guide the eye. Missing data points are due to ruptured membrane of peeper chamber.

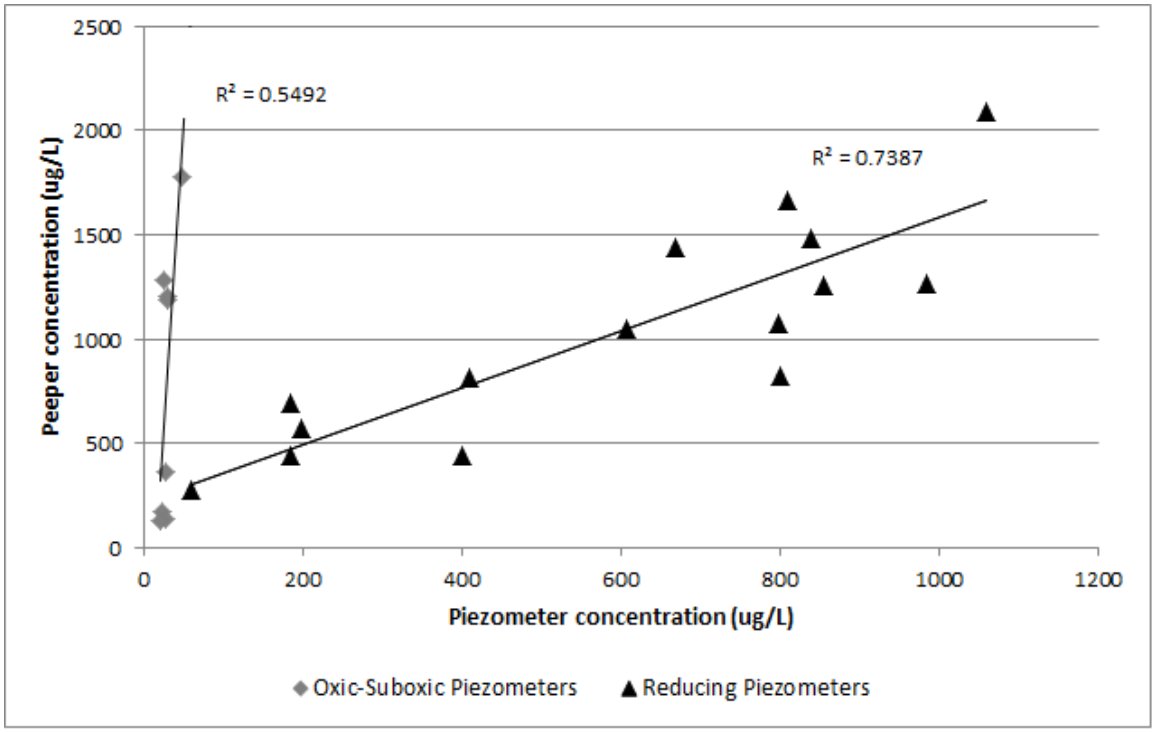

Figure 5.24: Concentration of SRP at a depth of 10 cm for peepers versus piezometers at the same location.

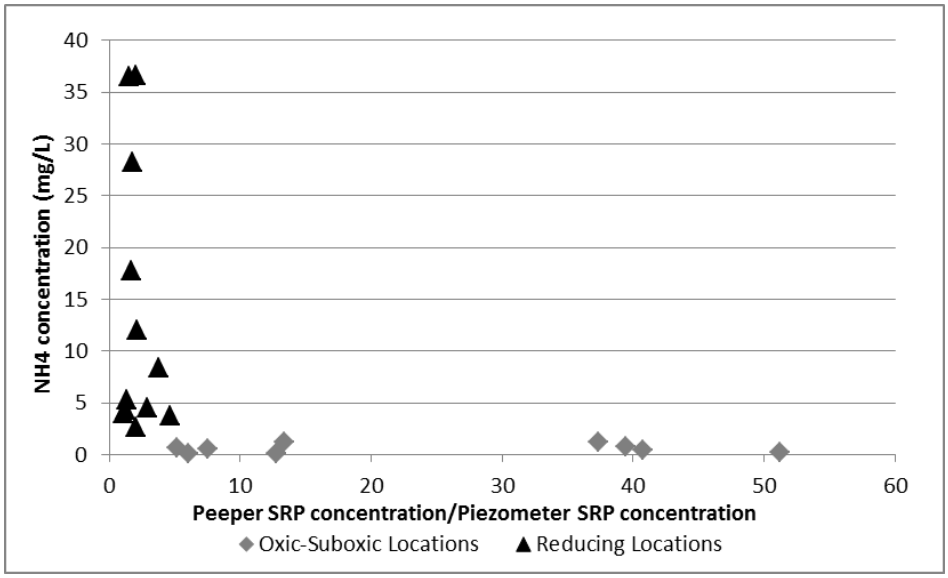

Figure 5.25: Ammonium concentrations versus the ratio of peeper and piezometer concentrations of SRP. Only data from peepers with nearby piezometers, thus supplying redox geochemistry data, are plotted.

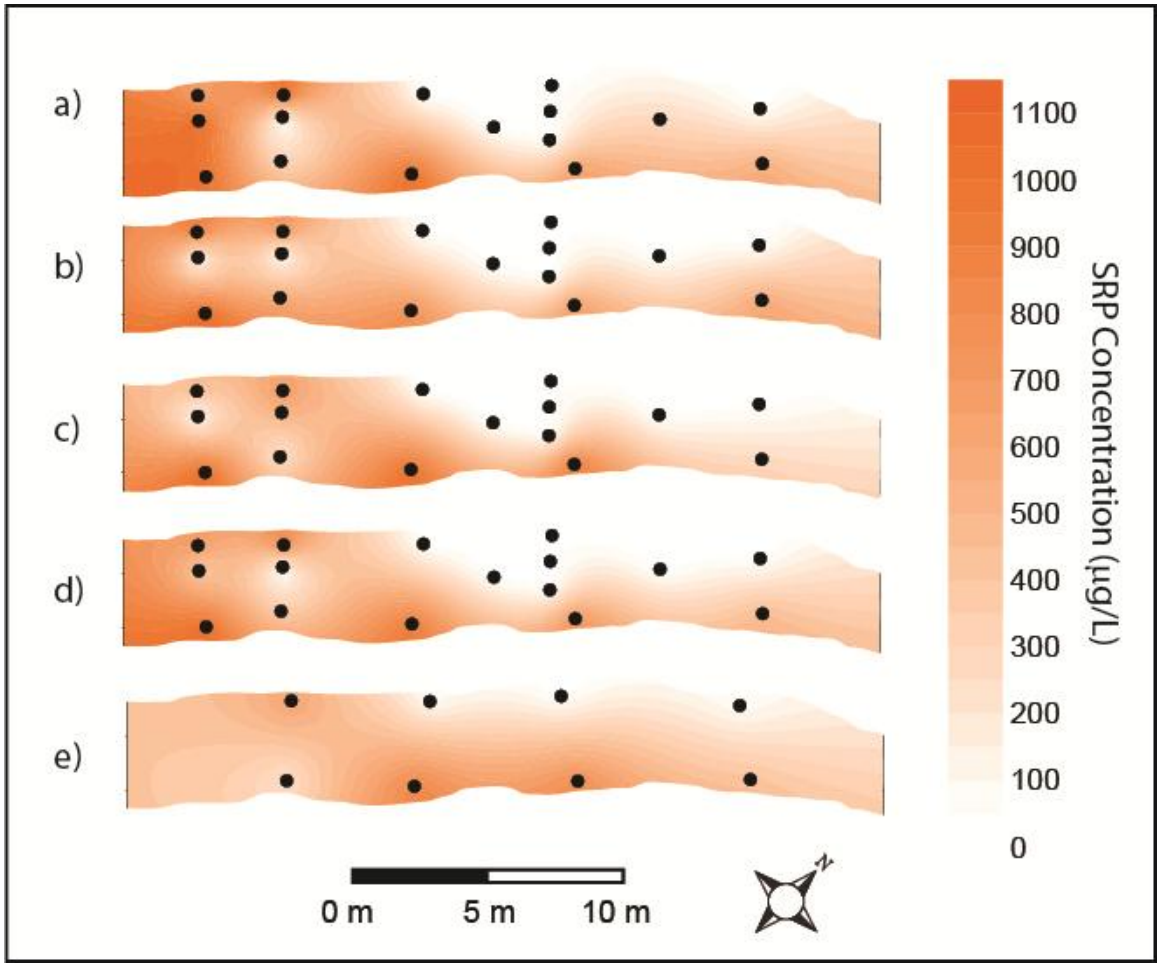

Figure 5.26: Interpolated SRP concentration maps for **a)** November 2011 peeper data **b)** January 2012 peeper data **c)** March 2012 peeper data **d)** Mean peeper data and **e)** Mean piezometer data. Black dots indicate data points (peepers or piezometers).

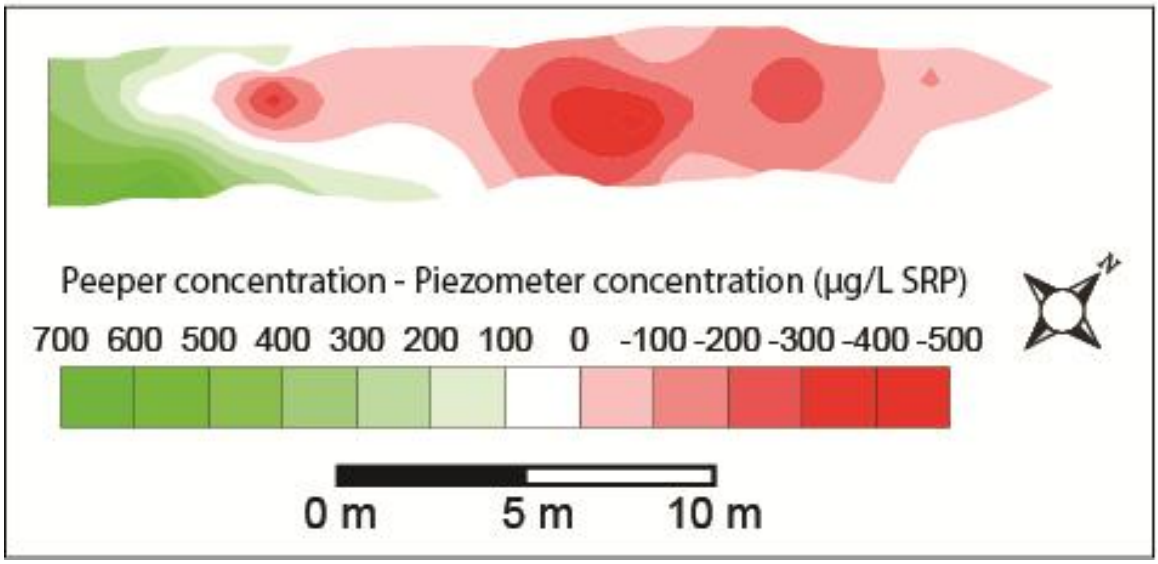

Figure 5.27: Difference between peeper and piezometer concentrations for SRP.

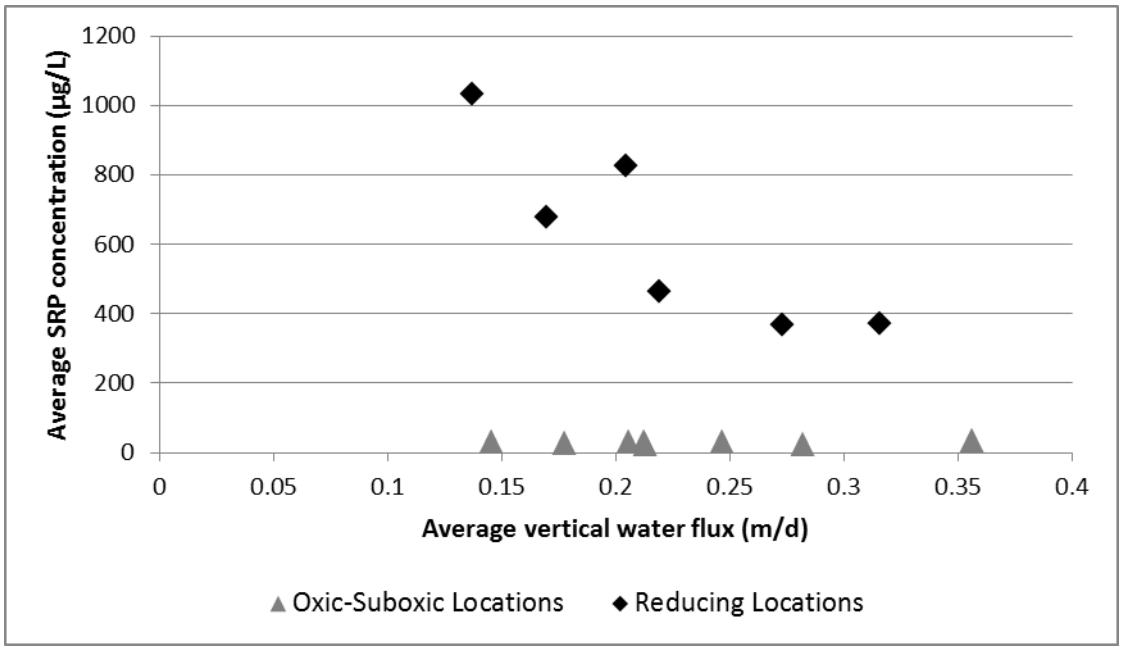

Figure 5.28: Average peeper SRP concentration versus average water flux calculated using VFLUX on the temperature rods.

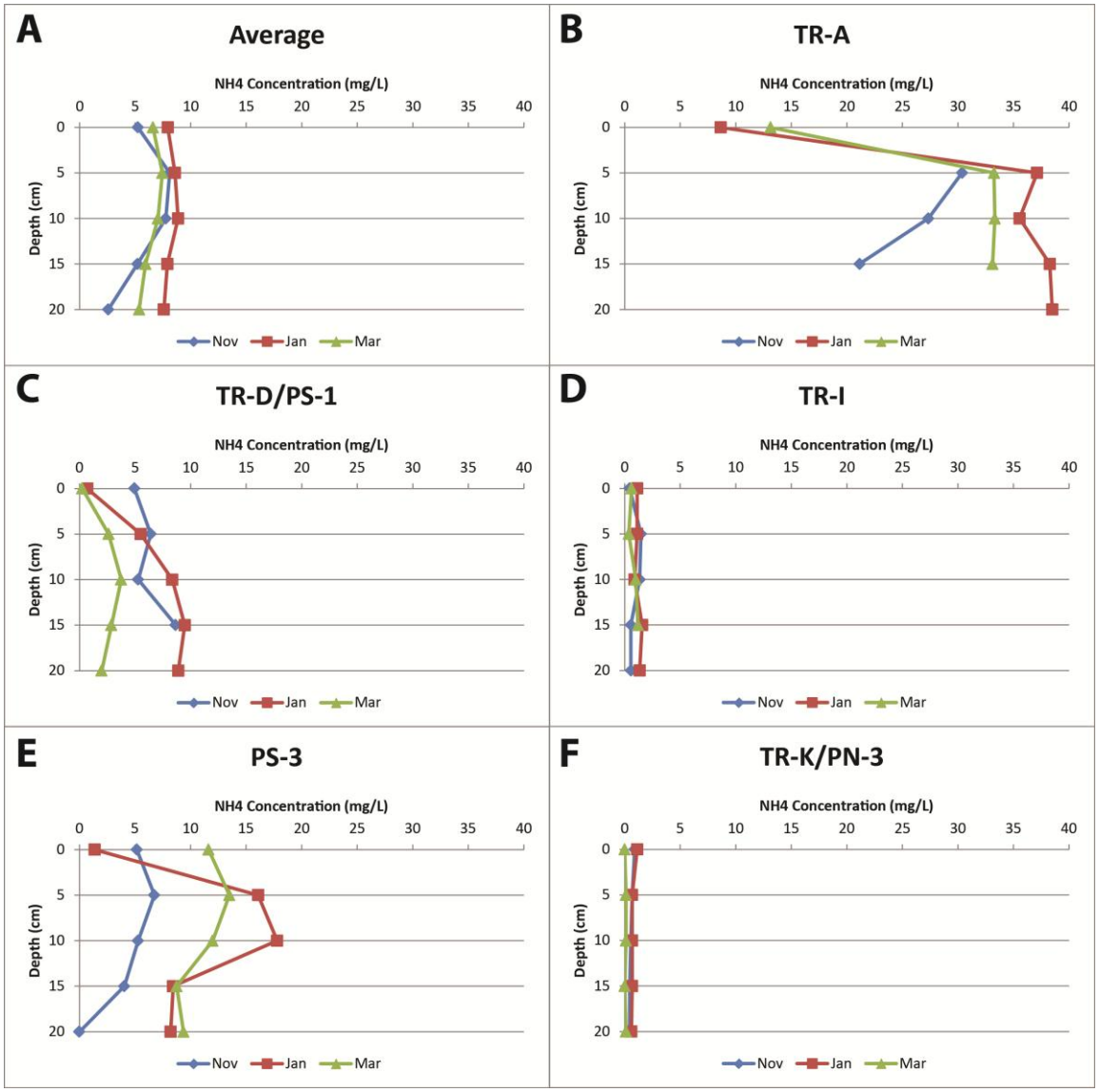

Figure 5.29: Depth profile of ammonium concentrations determined with peepers for the 3 sampling periods, November 2011, January 2012, and March 2012, with a) mean for all the peepers, b) TR-A c) TR-D/PS-1 d) PS-I e) PS-3 and f) TR-K/PN-3. Depths are approximate due to slight changes in streambed sedimentation over time. Lines between data points are to help guide the eye. Missing data points are due to ruptured membrane of peeper chamber.

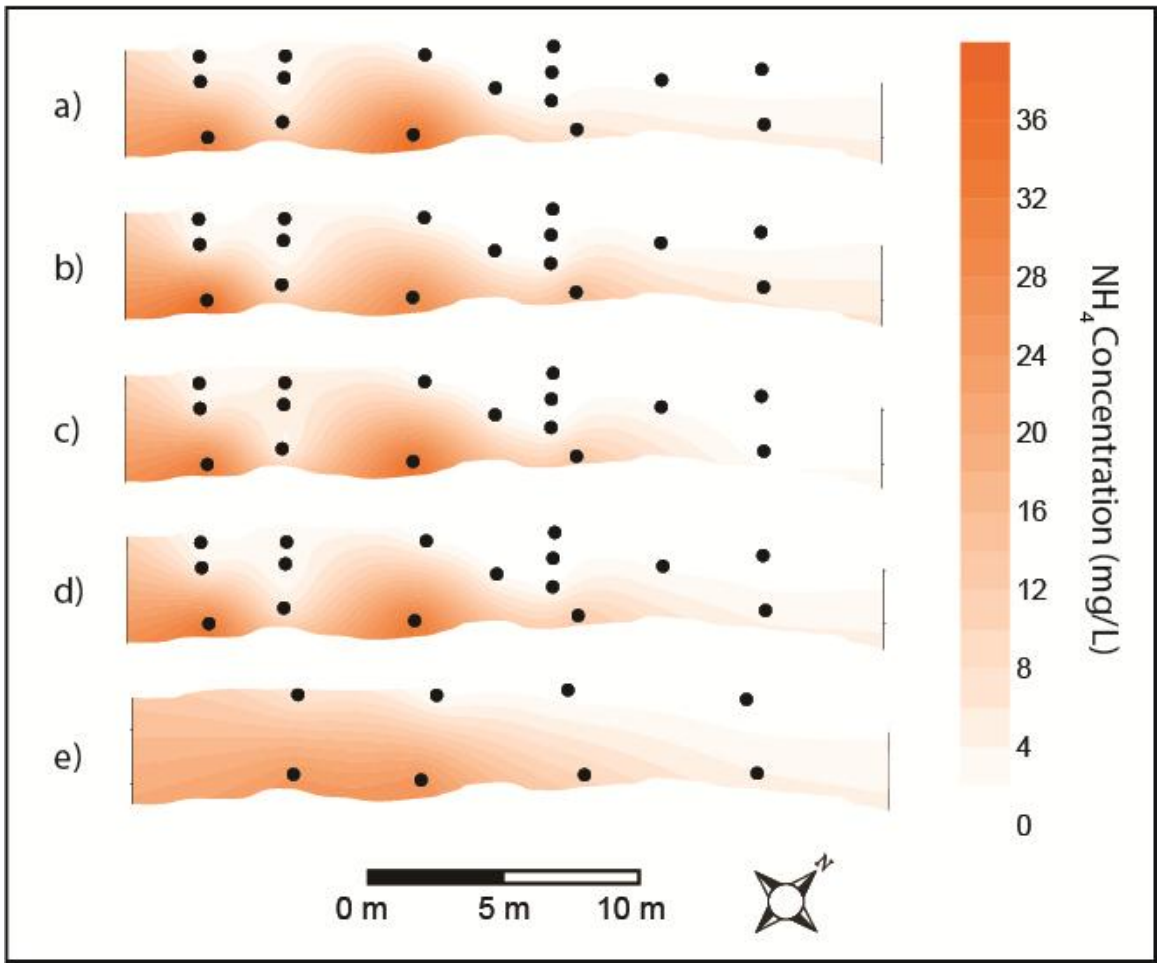

Figure 5.30: Interpolated ammonium concentration maps for **a)** November 2011 peeper data **b)** January 2012 peeper data **c)** March 2012 peeper data **d)** Mean peeper data **e)** Mean piezometer data.

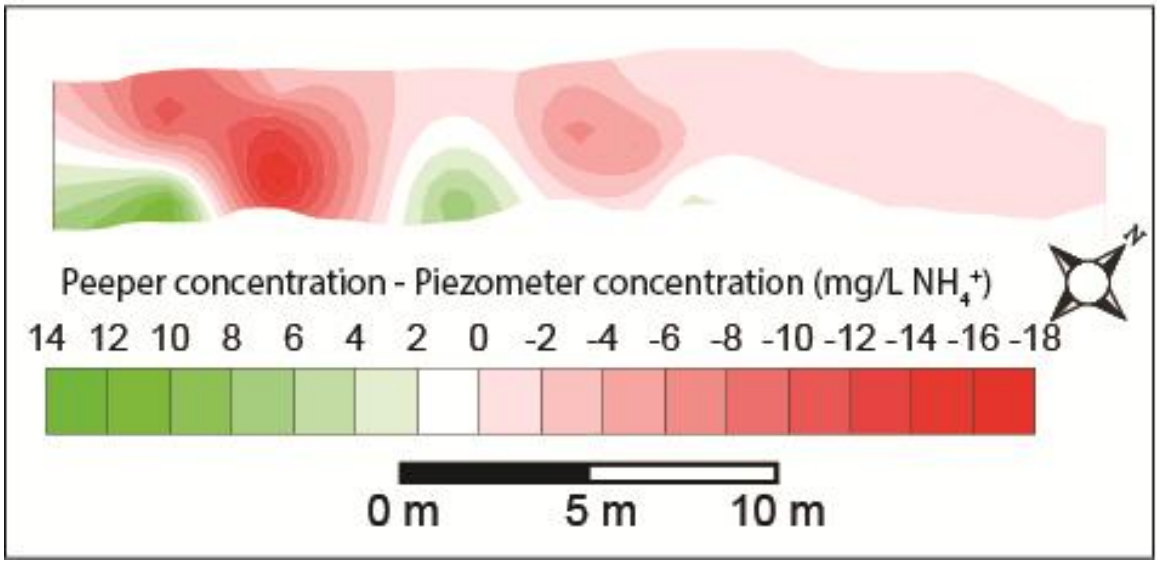

Figure 5.31: Difference between peeper and piezometer concentrations for ammonium.

5.4 Nutrient Mass Fluxes and Discharges

5.4.1 SRP Mass Flux and Discharge

Nutrient fluxes at Site A were determined by multiplying interpolated concentration grids with interpolated water flux grids. To compare results from different methods of measuring water flux and nutrient concentrations, the water flux grids for August calculated using VFLUX, using the Turcotte and Schubert (1982) equation on the temperature rod data, and using the Turcotte and Schubert (1982) equation on the streambed temperature grid were multiplied by the overall average peeper (at 5 cm depth) and piezometer (10 cm depth) concentration grids. Results shown in **Figure 5.32**. While the SRP values for both the peepers and piezometers do show a small variation with time, because there was no overall trend it was reasoned that using an average value would be sufficient given the limited dates for which the peeper data overlapped with water flux data.

All six of the interpolated SRP flux maps for August 2011 showed similar spatial patterns. Zones of high SRP flux were along the southern shore and the western end of the nothern shore. Flux along the middle and eastern end of the northern shore was close to 0 mg/m^2day for all of the combinations. The magnitude of SRP flux from the maps incorporating VFLUX data was highest, due to the higher values of water flux. This is evident in both the flux levels and the total calculated nutrient discharge (**Table 5.14**), with the mass discharge from the data using VFLUX about two times as large. There is

not a large or consistent difference in total discharge between using the peeper contaminant data compared to the piezometer contaminant data.

Method used to calculate water flux	Contaminant concentration data	Total contaminant discharge (g/day)
VFLUX on temperature rods	Peepers	8.1
VFLUX on temperature rods	Piezometers	8.3
Turcotte and Schubert (1982) equation on temperature rods	Peepers	4.6
Turcotte and Schubert (1982) equation on temperature rods	Piezometers	4.5
Turcotte and Schubert (1982) equation on temperature grid	Peepers	3.6
Turcotte and Schubert (1982) equation on temperature grid	Piezometers	3.7

Table 5.14: Total SRP discharge for August 2011 for the different combinations of concentration and water flux data collection methods.

For the SRP flux calculated using VFLUX and the peeper data (**Figure 5.32 a)**, the areas of high SRP flux (>100 mg/m^{2}day) are along the southern shore and at the western end of the northern shore, with the highest SRP flux of 213 mg/m^{2}day at PS-2. Much of the northern shore has an SRP flux of <10 mg/m^{2}day. The total mass discharge of SRP over the 115 m^2 study area calculated with this method is 8.1 g/day. The nutrient flux maps created using the Turcotte and Schubert (1982) equation and the peepers are shown in **Figure 5.32 b** and **c.** Unlike with the SRP flux data calculated using VFLUX**,** the area near the western end of the northern shore has a proportionally higher SRP flux

than the rest of the study area, with a maximum value of 207 mg/m^{2}day for **Figure 5.32 b** and 163 mg/m^{2}day for **Figure 5.32 c**. This is due in large part to the Turcotte and Schubert (1982) method results giving that area a proportionally larger water flux than areas on the south shore. The effects of the lower water flux from the Turcotte and Schubert (1982) method can be seen from the lower magnitude of the SRP flux in **Figure 5.32 b and c** compared to **a.**

At Site A, it appears that the spatial pattern of SRP concentrations is the primary driver, as opposed to water flux values, of the spatial pattern of SRP flux. The areas of high SRP flux are all areas of high SRP concentration, while much of the high water flux zones along the northern shore exhibit low SRP flux. This pattern is understandable at Site A as the range in common SRP values is much larger than the range in the common water flux values calculated by VFLUX. As a result, the spatial distribution of the SRP concentrations is more dominant than the water flux distribution for estimating nutrient flux at Site A. This may vary for other streams, depending on the range of values and heterogenity of the SRP concentrations and the water flux. A gaining stream with groundwater flux that is spatially heterogeneous but with a fairly uniform SRP concentration would show the opposite pattern.

As the VFLUX data was reasoned to be the most accurate water flux data in section 5.2, the most accurate contaminant flux data will likey be using the monthly VFLUX data and the average peeper data. The peeper data was chosen over the piezometer data due to having greater spatial coverage. The mass discharge of SRP over

time is shown in **Figure 5.33**, ranging from a low of 8.1 g/day in August to a high of 9.9 g/day in April. Given limited temporal trends suggested for water flux (section **5.2**) and SRP concentrations (section **5.3**), strong seasonal variation in mass fluxes during base flow conditions was not likely at this site. Future conditions may deviate from those seen here, through natural variation or changes associated with human activity (e.g. digging up the landfills). Fluxes may differ markedly during storm events, as the groundwater flux becomes more variable and complex, but more detailed investigation of this is the focus of future study.

While the above data is the best estimate of flux, there is still some uncertainty. This will be explored by determing the minimum and maximum nutrient flux that can be calculated by combining the nutrient concentration data and temperature-derived water flux data. The result for SRP is shown in **Figure 5.34**. This represents the range of values that could be calculated for this stream reach if one of the data sets was more severely restricted in time (e.g. only a single snapshot data set available). It also provides realistic bounds to the discharge that could be achieved from the ranges observed, if the concentrations and water fluxes are completely uncorrelated temporally. For the maximum SRP flux, the VFLUX results from June 2011 and the peeper data from November 2011 were used, and the total discharge is 11.3 g/day. For the minimum flux, the water flux results from the January 2012 temperature grid and the March 2012 peeper data were used, and the total discharge is 2.7 g/d, which is lower by a factor of four.

This range of calculated groundwater discharge values leads to an average flux range of 23 to 96 mg m^{-2} d^{-1} for the 115 m^2 area, with a best estimate, using the average VFLUX and peeper data, of 75 mg m^{-2} d^{-1}. These values are higher than the SRP flux observed by Shaw et al (1990) (0.1 mg m^{-2} d^{-1}) and Rivett et al (2011) ($9.3*10^{-4}$ mg m^{-2} d^{-1}), although the study areas, a lake and a 7.4 km reach of a river, were larger than the sections of Dyment's Creek studied. Smaller diffusive flux values were also measured by Jarvie et al (2008) (0.8 mg m^{-2} d^{-1}), using gel probles in a stream impacted by agriculture and sweage. A range of values in groundwater phosphate flux of 0 to 85 mg m^{-2} d^{-1}, closer to the values at Dyment's Creek, was found by Spruill and Bratton (2008) entering an estuary. In that study, both groundwater phosphate concentrations (up to 4000 μg/L) and water flux (up to 0.43 m/d) were similar to values observed at Dyment's Creek, and sediments were a possible source of nutrients.

Using the range in baseflow values calculated (620 L/min in fall to 12500 L/min in spring) and the maximum and mimimum calculated SRP discharge, groundwater discharge at Site A could increase stream SRP concentrations by 3 to 12 μg/L during low baseflow conditions and 0.15 to 0.62 μg/L during high baseflow conditions. These values are 13 to 50% of the average Site A stream concentration of 24 μg/L during low baseflow, and 0.6 to 3% during high baseflow. The average stream SRP concentration was used as there was no temporal trend and no correlation between SRP concentration and stream discharge. This is a large change over such a small reach (28 m), even for the lower range of values. This may be due to a number of factors. It is possible that not all of the measured SRP flux was transferred to the stream, as the values measured were from

depths of 5 to 10 cm, not the streambed interface. Some of the SRP may have been removed by biological processes, and some may have been returned to the sediment due to the "oxic cap" effect described by Jarvie et al (2008), where oxic conditions at the streambed interface allow SRP to resorb. Regardless, these results indicate that groundwater in this 28 m reach of the stream is a significant source of phosphorus to the stream and local ecosystems.

5.4.2 NH_4 Flux

Ammonium flux was calculated in a similar fashion to SRP flux. The average peeper and piezometer concentrations multiplied by the different methods to calculate flux used for August 2011 are shown in **Figure 5.35**. For all six combinations of concentration and water flux data, high ammonium flux is seen on the southern shore from the western end of the study area to the centre. The flux data calculated using the average piezometer concentration is a little more smoothed out due to the sparseness of data. The highest ammonium flux at one location is seen on **Figure 5.35 a**, with 7.7 g/m^2day. The total ammonium discharge calculated for the different combinations for the 115 m^2 study area is shown in **Table 5.15.** As with the SRP data, the higher magnitude of water flux calculated with VFLUX results in an ammonium flux about twice as high as when calculated with the Turcotte and Schubert (1982) equation. Unlike with SRP, there is a clear difference between the discharge calculated using peepers compared to piezometers, with the discharge being 26-36% higher when calculated using piezometers.

This is due to a low ammonium zone around TR-D in the peeper data that is not captured in the piezometer data interpolation (**Figure 2.29**).

Table 5.15: Total ammonium discharge for different combinations of concentration and water flux data collection methods.

Method used to calculate water flux	Contaminant concentration data	Total contaminant discharge (g/day)
VFLUX on temperature rods	Peepers	174
VFLUX on temperature rods	Piezometers	218
Turcotte and Schubert (1982) equation on temperature rods	Peepers	80
Turcotte and Schubert (1982) equation on temperature rods	Piezometers	110
Turcotte and Schubert (1982) equation on temperature grid	Peepers	66
Turcotte and Schubert (1982) equation on temperature grid	Piezometers	86

The ammonium flux calculated from the monthly VFLUX water flux data multiplied by the average peeper concentration data was determined to be the most accurate for this study for the same reasons as stated in section 5.4.1. The monthly ammonium discharge is shown in **Figure 5.36,** ranging from a high of 205 g/day in June to a low of 173 g/day in August. As with the SRP concentrations, large seasonal ammonium trends during baseflow are unlikely based on both the temporal water flux (**5.2**) and concentration (**5.3**) data.

As with SRP, the minimum and maximum ammonium discharge that could be calculated by combining ammonium concentration data with the various water flux calculation methods is shown in **Figure 5.37**. The minimum discharge was calculated using the Turcotte and Schubert (2012) equation on the January temperature grid data and the November 2011 peeper data, and resulted in a total discharge of 52 g/day, and the maximum discharge was calculated using the June 2011 VFLUX data and the July 2011 piezometer data with a result of 346 g/day. This range of groundwater discharge values leads to an average flux range of 450 to 3000 mg m^{-2} d^{-1} for the 115 m^2 area, with a best estimate around 1700 mg m^{-2} d^{-1}. This is high compared to fluxes measured by Spruill and Bratton (2008), with a high of 551 mg m^{-2} d^{-1}, although ammonium concentrations at that site were lower than the shallow groundwater at Dyment's Creek.

Using the range in baseflow values calculated (620 L/min in fall to 12500 L/min in spring) and the maximum and mimimum calculated ammonium discharge, groundwater discharge at Site A leads to an increase in stream ammonium concentrations of 0.06 to 0.39 mg/L during low baseflow conditions and 0.003 to 0.02 mg/L during high baseflow conditions. These values are 15 to 96% of the average Site A stream concentration of 0.4 mg/L during low baseflow, and 0.7 to 5% during high baseflow. As with the SRP discharge, the upper boundary of 96% for the low baseflow amount appears unrealistically high, possibly due to the same reasons discussed in section **5.4.1.** The lowest calculated ammonium discharge during baseflow conditions leading to an increase of 0.06 mg/L is high for a 28 m reach of stream, and indicates that groundwater at Site A is a significant source of ammonoum to the stream and local ecosystem.

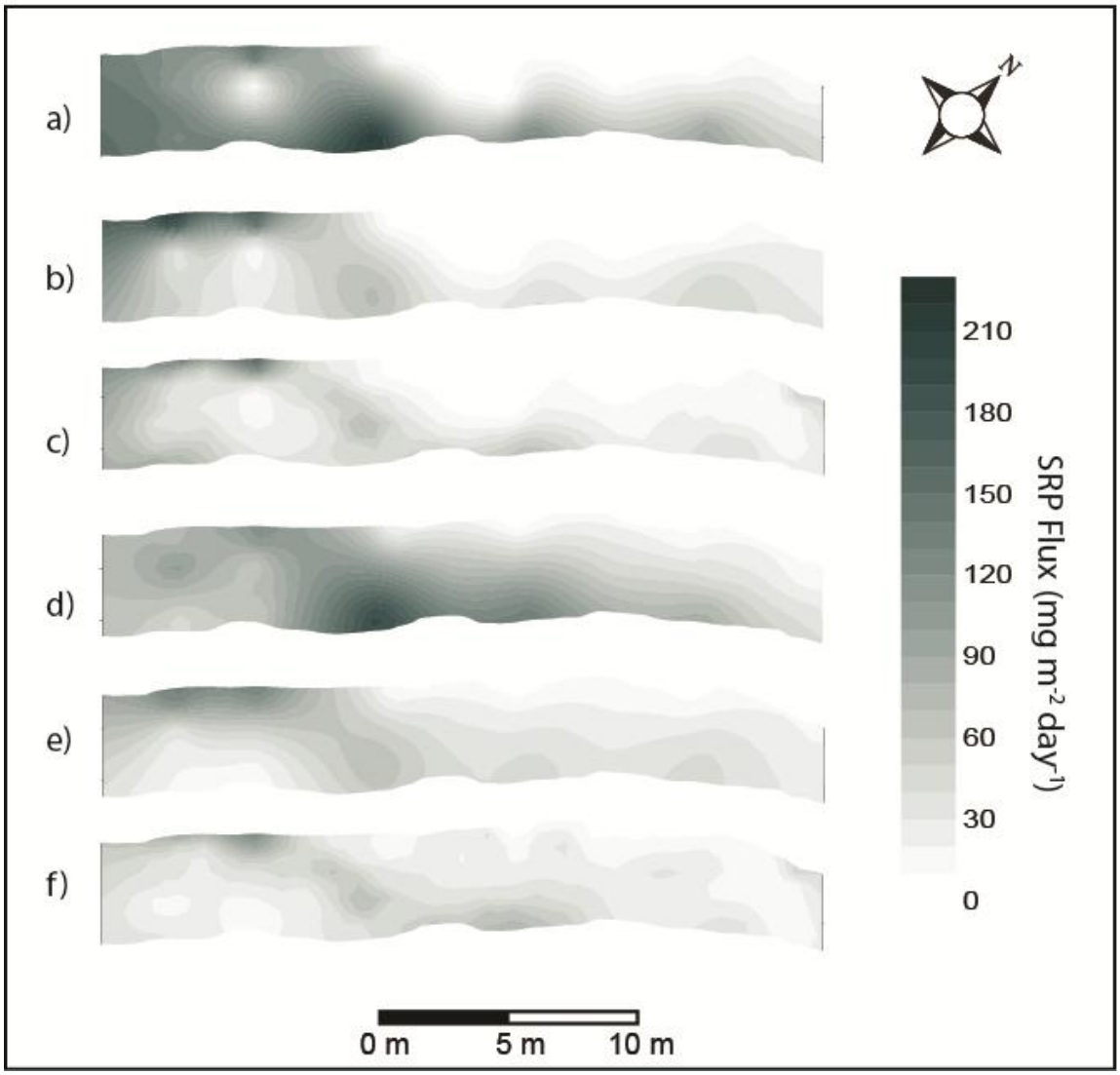

Figure 5.32: Interpolated SRP mass flux maps for August 2011 created by combining the mean peeper data with the August 2011 **a)** VFLUX data **b)** Turcotte and Schubert (1982) temperature rod flux **c)** Turcotte and Schubert (1982) temperature grid flux, and the mean piezometer data with the August 2011 **d)** VFLUX data **e)** Turcotte and Schubert (1982) temperature rod flux **f)** Turcotte and Schubert (1982) temperature grid flux.

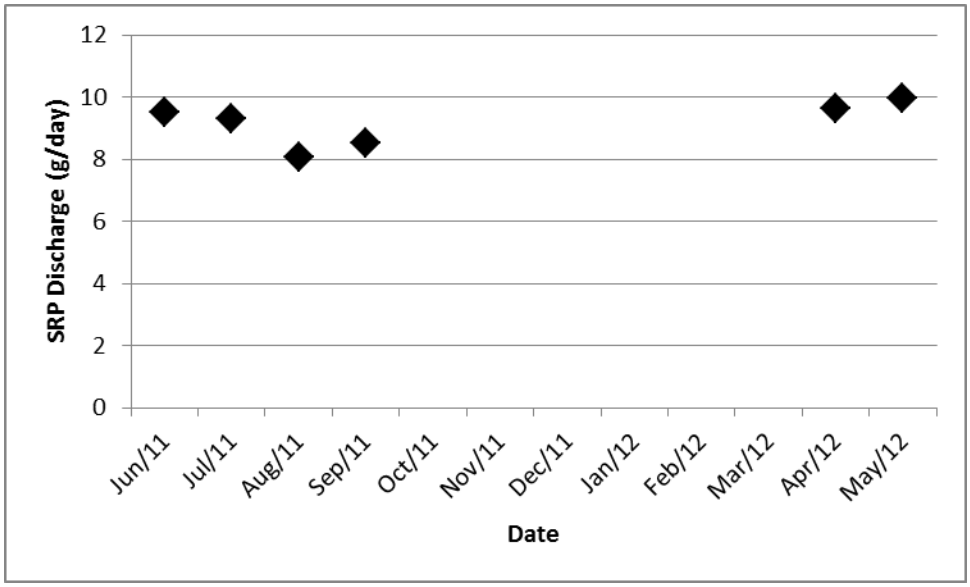

Figure 5.33: SRP flux over the study period, calculated by combining the mean peeper concentration data with the monthly VFLUX groundwater flux data.

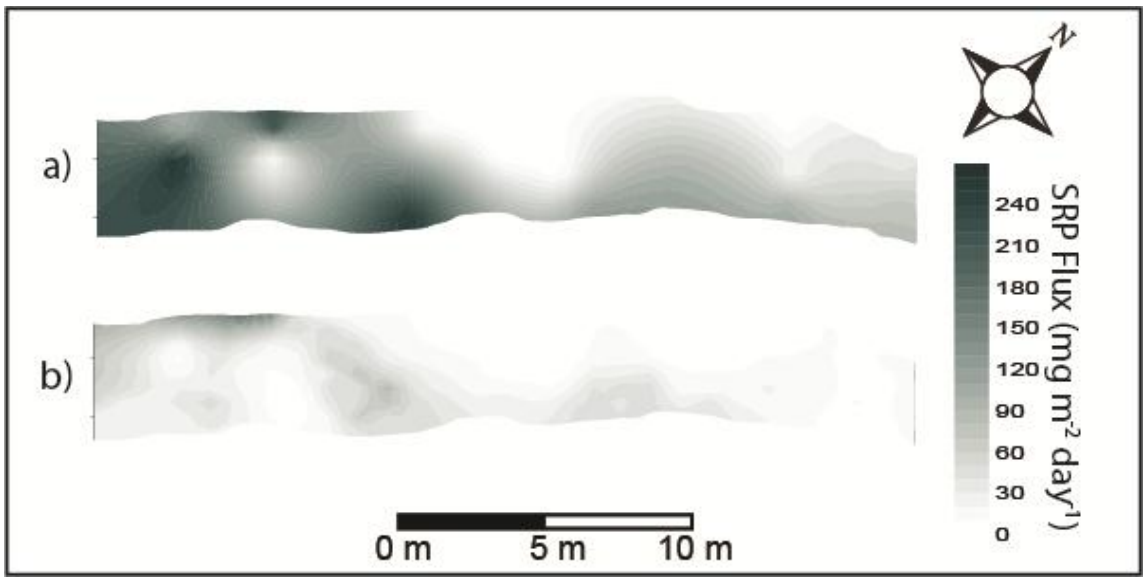

Figure 5.34: Interpolated maps for the **a)** maximum and **b)** minimum calculated SRP mass flux. Maximum flux is calculated using the June 2011 VFLUX data and the November 2011 peeper data, while minimum flux is calculated using the January 2012 temperature grid data and the March 2012 peeper data.

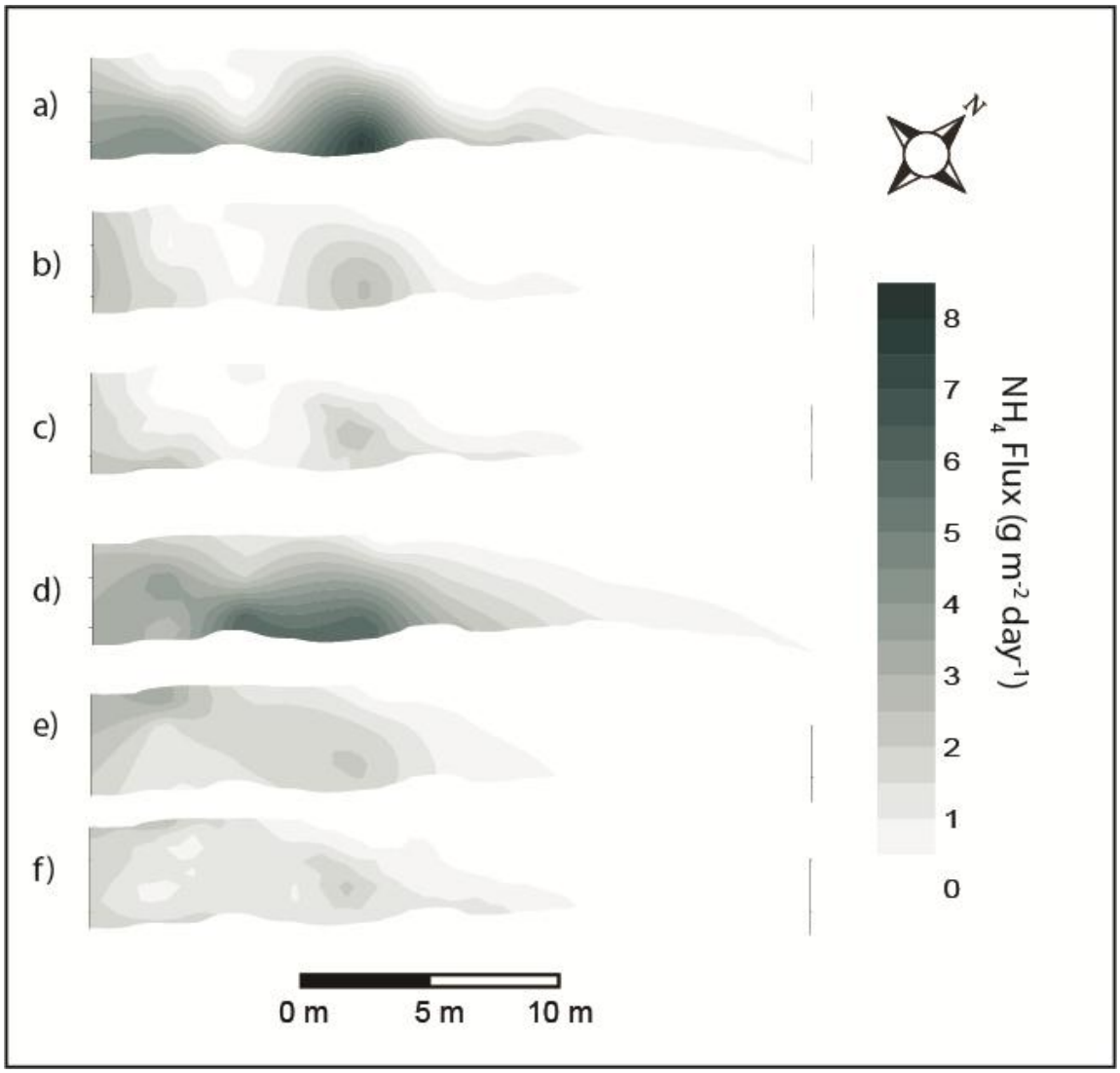

Figure 5.35: Interpolated ammonium mass flux maps for August 2011 created by combining the mean peeper data with the August 2011 **a)** VFLUX data **b)** Turcotte and Schubert (1982) temperature rod flux **c)** Turcotte and Schubert (1982) temperature grid flux, and the mean piezometer data with the August 2011 **d)** VFLUX data **e)** Turcotte and Schubert (1982) temperature rod flux **f)** Turcotte and Schubert (1982) temperature grid flux.

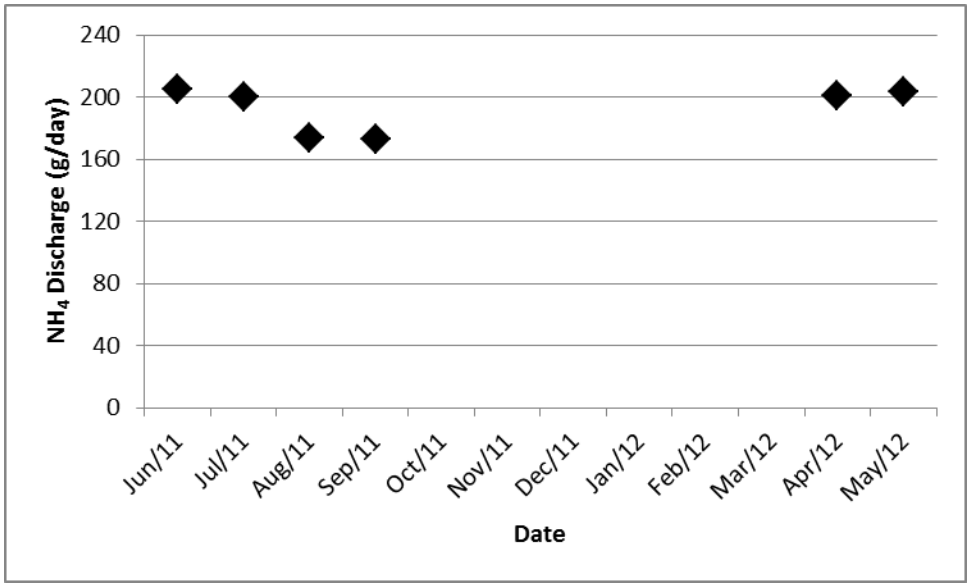

Figure 5.36: Ammonium (NH_4) flux over the study period, calculated by combining the mean peeper concentration data with the monthly VFLUX groundwater flux data.

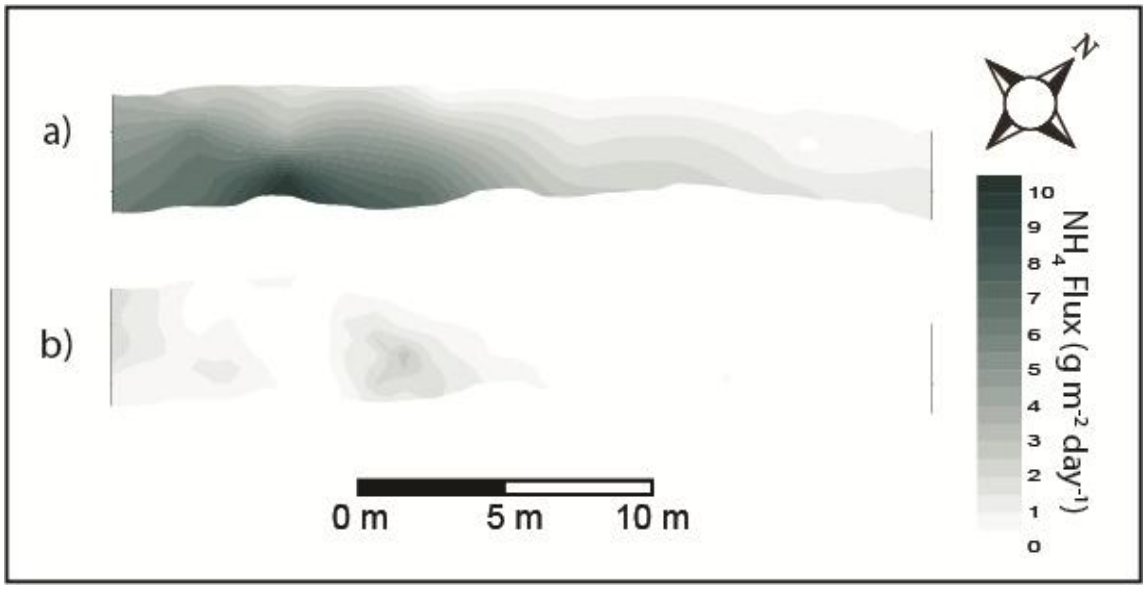

Figure 5.37: Interpolated maps for the **a)** maximum and **b)** minimum ammonium flux that can be calculated by the different combinations of concentration and water flux data collected in this study. Maximum flux is calculated using the June 2011 VFLUX data and the July 2011 piezometer data, while minimum flux is calculated using the January 2012 temperature grid data and the November 2011 peeper data.

5.5 Nutrient Mass Discharge at Site B

Shallow groundwater nutrient concentrations and hydraulic gradients were also measured along Dyment's Creek at Site B, although no water flux measurements were taken. This information provides some larger-scale context to the results derived from Site A, which covered only 28 m, a small percentage of the urban portion of Dyment's Creek. For instance, the Site B data will help reveal how representative the concentrations found at Site A might be of a larger reach of the stream, and provide further insight into potential nutrient sources and controlling factors. Finally, with this information a crude estimate of the nutrient mass discharge at Site B can be determined, applying the water flux data at Site A, for use in discussion of the broader implications to the nutrient budget of this stream and Lake Simcoe.

5.5.1 Site B Nutrient Concentrations

Shallow groundwater SRP, ammonium and nitrate concentrations along Dyment's Creek at Site B are shown in **Figures 5.38, 5.39,** and **5.40,** respectively. Samples were taken about 50 cm below the stream and 10 m apart along each bank (north and south). SRP concentrations ranged from 3 to 864 µg/L with a mean of 232 µg/L. These concentrations are similar to those observed in the piezometers installed at Site A (range 4 to 1201 µg/L), and the mean is well above the stream value. Site B shallow streambed ammonium values ranged from 0 to 16.7 mg/L, with a mean of 4.6 mg/L, which is lower than the range observed at Site A (0.1 to 38 mg/L). Several locations along Dyment's Creek at Site B had nitrate values much higher than those measured at Site A (range 0 to

2.4 mg/L) The maximum nitrate value was 57.2 mg/L and the mean value was 1.4 mg/L, although the majority of locations had very low (<0.05 mg/L) concentrations. Full contaminant data for Site B can be found in **Appendix F**.

As with Site A, SRP and ammonium concentrations at Site B appear driven by redox patterns, given that geochemically reducing areas were associated with higher SRP (**Figure 5.41**) and ammoniun was often found with other compounds commonly seen in reducing environments. Using the critera of **Table 5.13** to define redox conditions, the mean SRP concentrations of the oxic-suboxic-nitrate reducing locations (n=30) is 29 µg/L, the mean of the maganese and iron-sulphate reducing locations is 253 (n=7) µg/L, and the mean of the methanogenic locations (n=56) is 336 µg/L. However SRP and ammonium concentrations are also generally higher in locations adjacent to former landfills (indicated by the arrows on **Figures 5.38** and **5.39**). The mean SRP concentration for the samples located by a historic landfills was 315 µg/L compared to 120 µg/L for areas not located near a landfill, and the mean ammonium concentrations were 6.8 mg/L and 1.7 mg/L, respectively. As the distribution of nutrients appear partially controlled by landfills, this is evidence that these landfills may either be a source of nutrients or a cause for the redox conditions that may promote the release of nutrients from sediments. This distribution is also evidence that groundwater is entering the stream from both banks, as opposed to groundwater discharge from one side of the stream being sourced from a deeper flowpath from the opposite bank.

5.5.2 Site B Hydraulic Gradients

Potentiomanometer results along Site B (**Figure 5.42**), taken at depths ranging from 16 to 50 cm, from positions directly in the stream, showed positive hydraulic gradients ranging from 0.01 to 0.16. This indicates that groundwater was flowing upwards towards the stream at all 16 locations. There were no apparent patterns with the gradient with regards to location along the stream, the side of the stream, or nearby stream geomorphic features such as meanders, although the spatial extent of the data is limited. This variation may reflect differences in the shallow subsurface, as there may be a heterogeneous mix of fine and coarse grained material similar to those observed at Site A shown in section **5.1**. The data set suggests that Dyment's Creek is generally a gaining stream throughout the Site B reach, like Site A.

5.5.3 Site B Nutrient Fluxes and Discharges

Although water flux data was not collected for Site B, a crude estimate of the nutrient fluxes and discharges were determined using the water flux calculations from Site A. More specifically, the highest and lowest water flux values measured in section **5.2,** the June 2011 VFLUX data and the January 2012 temperature grid data, respectively, were used to give a maximum and minimum measured nutrient flux. The total groundwater discharge value for Site A was divided by 28 (length of the reach in m) to obtain a water flux value per metre of stream reach, and then multiplied by 10 as the samples taken at Site B were roughly 10 m apart. Since nutrient concentration measurements were taken on both sides of the stream, this was then divided by 2

resulting in an average water flux value for one half of a 10 m reach. These values were multiplied by the average nutrient concentrations to calculate nutrient fluxes.

This method requires several significant assumptions, such as that the flux per metre of reach was constant along and for both sides of Dyment's Creek at Site B and was similar to that measured at Site A. The width of the stream does not change significantly, and the stream bottom sediments at Site B are similar to the range found along the stream at Site A. There is some topographic variation, such as a concrete wall along part of the reach, though its effect on groundwater discharge is unclear. Hydraulic gradients are generally lower than those along Site A, but this may be due to the gradient measurements being taken directly in the streambed as opposed to in wells on the stream banks. In section **5.4,** nutrient levels were found to have more variation than water flux and were the primary driver of nutrient flux variability, so if this same pattern holds for Site B then erroneous flux values will likely have less of an impact than incorrect concentration data.

This method also assumes the concentration of nutrients at the depths measured (20-145 cm) were representative of the concentrations reaching the streambed interface. As shown in section **5.3**, groundwater SRP and ammonium concentrations generally decreased with depth at Site A. Thus, given the similar hydrologic and, likely, nutrient source conditions, it it probable that the concentrations along Site B at shallower depths in discharging groundwater are at least as high as the ones measured in this study.

The maximum measured water flux values (June 2011 VFLUX data) applied over Site B results in an estimated groundwater discharge of about 450 000 L/d, which would represent 12 % of the highest base flow measurements (outside of spring snowmelt) and 50% of the lowest base flow measurements for stream discharge at Site A. Therefore, these maximum water flux values are overestimates during times of low base flow, and maybe even high base flow. Using the mimimum measured flux values (January 2011 temperature grid) the total groundwater discharge would be about 200 000 L/d, which would result in 5% and 22% of the highest and lowest base flow measurements, respectively.

Using the minimum flux values, the calculated SRP discharge is 38 g/d. We can calculate the estimated increase in stream concentrations by dividing this groundwater discharge by the sum of the stream discharge just upstream of Site B with the estimated contribution of groundwater. This leads to an expected increase in stream SRP concentration of 12 µg/L in high base flow conditions, and 40 µg/L in low base flow conditons. However, the average measured difference between Site A and Site B stream SRP concentrations was 5 µg/L. There are multiple possibilities for this discrepancy. As stated earlier, the assumption that the water flux values in Site A could be extrapolated to Site B may not be correct, such as the maximum groundwater discharge value during times of low baseflow. As shown in section **5.3,** the SRP concentrations at the depths measured may not be representative of concentrations at the streambed interface, although evidence from Site A indicated that shallower concentrations may be higher. It is also possible that changing redox conditions remove some of the SRP. As previously

mentioned, Jarvie et al (2008) found that highly oxic conditions at the streambed interface create an "oxic cap" that allows SRP to re-sorb onto the sediment. However, the phosphorus may still enter the stream in biologically available colloidal or particulate forms, and slight perturbations to the oxic cap may cause a pulse of SRP to be relased to the stream.

The calculated ammonium discharge along Site B was 760 g/d. Using the method described above for SRP, this would lead to an increase in stream concentrations of 0.8 mg/L during low base flow conditions and 0.2 mg/L during high base flow conditions. The average difference in stream concentration between Site A and Site B was 0.3 mg/L. As with SRP, these discrepancies may be due to erroneous water flux values or the measured ammonium concentration may not be representative of the concentrations at the streambed interface.

Unlike at Site A, there were locations along Site B where the groundwater nitrate concentration was above the measured stream concentrations, indicating that groundwater discharge may be contributing to nitrate loading at Dyment's Creek. The total nitrate discharge calculated was 230 g/d, which would lead to an increase in stream nitrate concentrations of 0.3 mg/L in low base flow conditions and 0.1 mg/L in high base flow conditions. However, the average groundwater concentration of nitrate is lower than the average stream concentration, so it is possible that the influx of groundwater is actually having a dilution effect on Dyment's Creek, and therefore it is not an important contributor of nitrate at this location.

While it may be tempting to extrapolate the nutrient fluxes from Site A to the broader Site B reach, this would lead to higher estimations of the total mass discharges. For example, by multiplying the results from section 5.4 by the relative difference in reach length, we get a range of 43 to 181 g/d for SRP and 1786 to 4821 g/d for ammonium. This leads to an overestimation compared to the previously calculated value for both SRP and ammonium, by up to 75% for SRP and 136% for ammonium. This calculation is effective at this site for a "quick and dirty" estimate, though it would be best to collect nutrient concentration data if possible.

Stream SRP and ammonium concentrations in Dyment's Creek approach or exceed aquatic guideline levels, and groundwater represents a major loading of nutrients to the creek. Even the low estimates of SRP and ammonium discharges represent a significant input of nutrients. As watershed streams are the largest source of phosphorus to Lake Simcoe (Ministry of the Environment, Ontario, 2009) the potential contribution of groundwater cannot be overlooked. This work may be especially applicable to Bunker's Creek, which is located just north of Dyment's Creek in central Barrie and is also bordered by historic landfills.

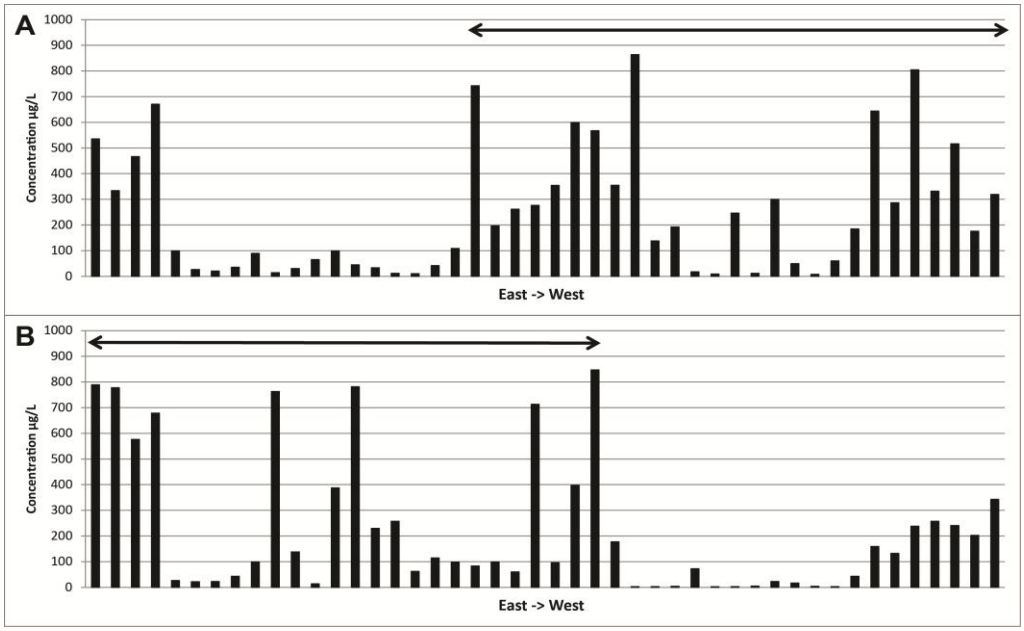

Figure 5.38: Shallow groundwater SRP concentrations at Site B along the A) northern and B) southern shores. Samples were taken about 10 m apart. Arrow along the top indicates location of former landfill. Mean Site A stream concentration was 23 µg/L.

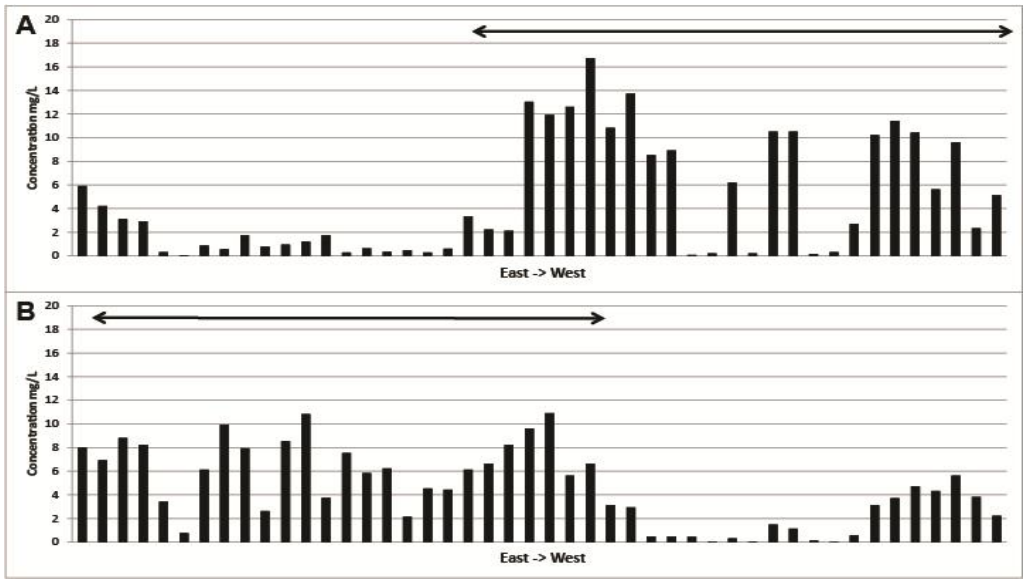

Figure 5.39: Shallow groundwater ammonium concentrations at Site B along the A) northern and B) southern shores. Samples were taken about 10 m apart. Arrow along the top indicates location of former landfill. Mean Site A stream concentration was 0.4 mg/L.

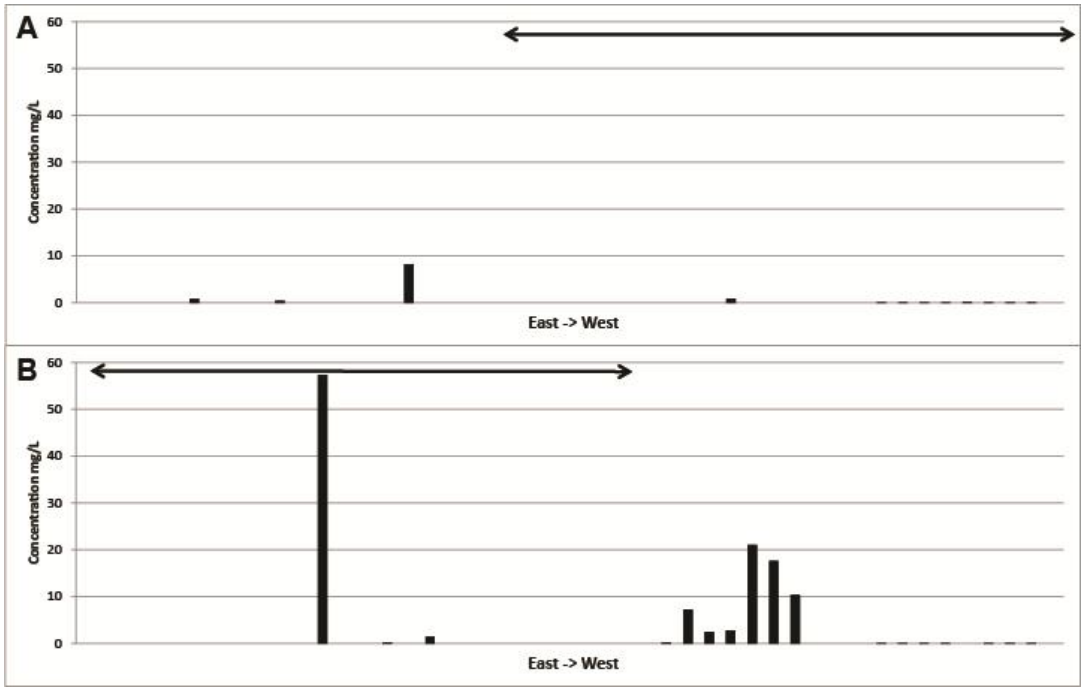

Figure 5.40: Shallow groundwater nitrate concentrations at Site B along the A) northern and B) southern shores. Samples were taken about 10 m apart. Arrow along the top indicates location of former landfill. Mean Site A stream concentration was 2.8 mg/L.

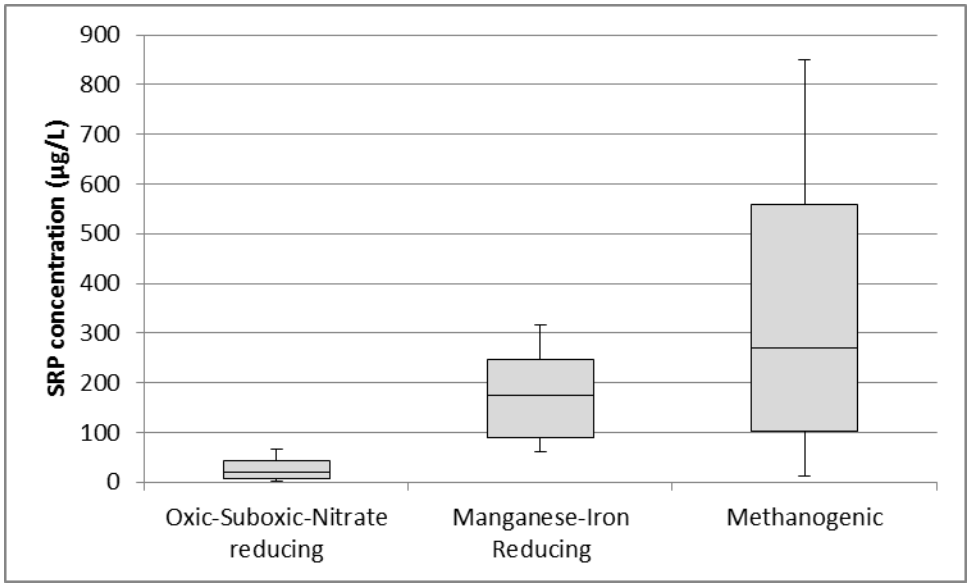

Figure 5.41: Box-whisper plot of SRP concentration and redox classification for groundwater samples at Site B.

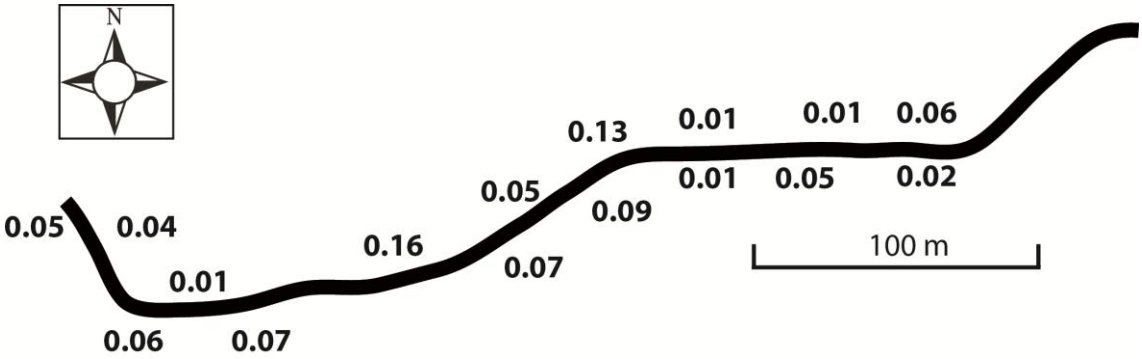

Figure 5.42: Vertical hydraulic gradients measured with a potentiomanometer at16 locations along Dyment's Creek at Site B. Positive values indicate gradients towards the stream.

6. Conclusions

6.1 Results Summary

Lake Simcoe suffers from eutrophication due to an excess of nutrients, especially phosphorus, and this is affecting the local environment and economy. Watershed streams are reported to be the largest source of phosphorus to the lake (Ministry of the Environment, Ontario, 2009). Groundwater may be a contributor to stream nutrient concentrations, including phosphorus, although its transport in groundwater is commonly assumed negligible. This study was undertaken to determine if groundwater may be an important pathway for nutrient loading to Dyment's Creek, an urban stream located in the Lake Simcoe watershed. There were five main parts to this study, the results of which are summarized below:

1. Hydraulic gradients were positive during base flow throughout the study period at Site A. This indicates that local groundwater was flowing towards the stream, and that this section is likely a groundwater discharge area, so elevated nutrient concentrations in the groundwater could make it a source of nutrients to the stream. Sediments at Site A were heterogeneous, with layers of sand and an organic silty peat, thus groundwater flow paths are likely non-ideal.

2. All four methods used to quantify streambed flux showed discharging conditions throughout the study area. The heat tracer flux results were reasoned to be the most accurate, given the robustness of the temperature measurement, although these measurements were limited to spring and summer. Darcy-based flux

measurements were not limited in that way so they provided a more complete temporal description of the groundwater flux. This data set suggested there were no major seasonal changes in streambed flux. Streambed flux (from thermal method) was spatially variable, with average flux values ranging between 0 and 34 m/d. This variability and range of values is commonly observed in the literature.

3. Stream SRP concentrations were higher than provincial guidelines for being considered eutrophic at some times during the study period (maximum value of 46 μg/L), and ammonium concentrations approached guideline values (maximum value of 0.72 mg/L), indicating that nutrients are a problem in Dyment's Creek. Shallow piezometers showed higher SRP (maximum: 1154 μg/L) and ammonium (maximum: 34.5 mg/L) concentrations than the stream at Site A, signifying that under the discharging conditions measured groundwater will further impair stream water quality, unless nutrient removal mechanisms are present in the stream or shallow sediments. Shallow groundwater nitrate concentrations were lower than Site A stream concentrations, so groundwater addition of nitrate was not a concern at Site A

Correlations with redox sensitive species along Dyment's Creek, such as Fe^{2+}, Mn^{2+}, and SO_4^{2-}, indicated that the SRP concentrations in the streambed were controlled by redox conditions, with the highest SRP concentrations found in the most reducing areas along Dyment's Creek at both Site A and B.

Differences between piezometer (flow sampler) and peeper (diffusion sampler) determined SRP values suggest that the phosphorus may be sourced from the organic-rich sediments. Ammonium concentrations were correlated with saccharin concentrations at Site A, indicating a potential landfill source. These were not as well correlated with SRP, again supporting a different source for SRP. Along Site B, both SRP and ammonium concentrations were generally higher adjacent to former landfills. We suspect that the landfill may be altering groundwater redox conditions that then lead to phosphorus release from sediments.

4. As there was evidence of both discharging conditions and higher nutrient concentrations in the groundwater than the stream water, there is likely nutrient flux to the streambed of Dyment's Creek from groundwater. This mass flux was calculated by combining both the concentration data and the water flux data. Nutrient flux for Site A varied depending on which methods were used to calculate water flux, with VFLUX resulting in higher values. The SRP discharge for the 28 m reach ranged from 2.7 to 11.3 g/d. This would represent 0.6 to 3% of the mass discharge in the stream during high base flow and 13 to 50% during low base flow. The calculated ammonium discharge ranged from 52 to 346 g/d. These are significant values as Site A is less than 1% of the stream total length. If these values are applicable to a larger reach of the stream, it is possible that groundwater discharge may be responsible for much of the stream nutrient concentrations.

5. Shallow groundwater nutrient concentrations along Site B were generally similar to those measured at Site A, indicating that results from Site A may be applicable to the larger, 450 m reach of Site B. Maximum measured shallow groundwater SRP was 864 µg/L, and maximum measured ammonium was 16.7 mg/L. Unlike Site A, portions of Site B showed nitrate values above stream concentrations, although the net effect of groundwater on stream nitrate concentrations is likely dilution. Nutrient fluxes along the larger 450 m reach were estimated by combining the Site B groundwater concentration data with water flux (range for 2 thermal-based calculations) measured at Site A. These ranged from 38 to 100 g/d for SRP and 760 and 2000 mg/L for ammonium. This total estimated SRP mass discharge from groundwater along Site B is similar to the total stream SRP mass discharge in Dyment's Creek. This suggests that the water flux differs at Site B from Site A, or that phosphorus removal or transformation is occurring.

This study shows that groundwater contributes a significant loading of nutrients to the streambed interface of Dyment's Creek. If the phosphorus from discharging groundwater along Sites A and B traveled though the streambed interface unimpeded, then groundwater could be the source of most of the SRP measured in Dyment's Creek at the downstream end of the study area. However, it may be that a portion is retained in the streambed interface, in an "oxic cap" as described by Jarive et al (2008). As the dissolved phosphorus and iron meet the oxygenated stream water, iron oxidation occurs, stripping phosphorus through sorption mechanisms (Fetter, 1999). If this is the case, then perturbations of this oxic cap (i.e. changing redox conditions) may release a pulse of SRP

in the stream water. Another possibility is the phosphorus travelling downstream in colloidal or particulate forms (Lapworth et al, 2011), which would not be measured by our stream water measurements. In both scenarios, this still represents a large loading of phosphorus to Dyment's Creek, and ultimately Lake Simcoe.

6.2 Implications

This study shows that groundwater should be considered in nutrient budgets for all of the Lake Simcoe watershed streams. The findings are especially relevant to the other urban streams bordering historic landfills, such as Bunker's Creek in central Barrie, and likely to other urban areas within the Lake Simcoe watershed, such as Orillia, Newmarket, and Bradford. However, if natural organic-rich sediments are indeed a major source of phosphorus to discharging groundwater as is the case in Dyment's Creek, then groundwater may represent a large annual loading to Lake Simcoe streams that will not be easily addressed. This may present a difficulty for restoration, as it is then not possible to remove the phosphorus source, although. However, cleaning up the nearby landfills may help if the groundwater switches to oxidizing conditions, rather than the reducing conditions that are allowing phosphorus to desorb from the sediment. Removing fill from the adjacent landfills may reduce the ammonium concentrations. This is a costly option for a restoration effort that may not have the desired effect.

The SRP flux results from this study (23-96 mg m^{-2} d^{-1}) are within the range of values found in other studies (0.03 – 933 mg m^{-2} d^{-1} **Table 6.1**). Such a large range likely reflects the range in scales and sources, as some locations are heavily impacted by

anthropogenic sources such as sewage. The SRP flux at Dyment's Creek is most similar to that found by Spruill and Bratton (2008), for groundwater discharging to an estuary in North Carolina. Flux at that location was measured by combining piezometer concentrations with water flux data, both of which had values similar to those found at Dyment's Creek. Contaminated sediments were a possible source of SRP to groundwater at that site. As with our study, the nutrient flux measured by Spruill and Bratton (2008) was spatially variable, although the data were on a much larger scale. The flux values from Dyment's Creek were also similar to those observed by McCobb et al. (2003), who calculated the phosphorus contribution sourced from a sewage plume to the shoreline of a lake. Unlike in Dyment's Creek, shallow lakebed sediments were oxic, and dissolved oxygen decreased with depth. Water flux from flow model was based on wells placed up to 36 m below the water table. Dissolved phosphorus concentrations decrease as the groundwater moves though the oxic zone, although high concentrations are still observed.

Much lower flux values were calculated by Belanger and Mikutel (1985) and Shaw et al (1990) for groundwater entering small lakes, likely due to lower groundwater phosphorus concentrations. There was no mention of the potential source of phosphorus at either site and streambed redox conditions were not reported. Lower phosphorus flux values were also calculated by Jarvie et al (2008) for a streambed heavily impacted by sewage and agriculture. They used vertical P profiles determined with DET gel probles, and then analyzed the results with analytical diffusion equations. The low flux results are likely due to the method used, which calculates diffusive, not advective, flux. Under

discharging conditions, groundwater may be a much larger flux of nutrients through the streambed at this site.

Table 6.1: Comparison of studies that measured phosphorus mass flux from groundwater or sediment pore water to a surface water body. Phosphorus measure indicated – SRP – Soluble reactive phosphorus, TP – Total phosphorus, TDP – Total dissolved phosphorus, Orthto-P - Orthophosphate. Methods of calculating and/or measuring the mass flux are given; these generally combine measure of water flux and groundwater phosphorus concentration.

Study	Phosphorus flux (mg m^{-2} d^{-1})	Possible source	Methods used	Scale
This study (Site A)	Mean value of 23-96, depending on method (SRP)	Organic-rich sediments, maybe landfills	Heat tracer methods combined with piezometers and peepers	115 m^2 streambed
Belanger and Mikutel, 1985	Mean value of 0.13 (TP)	Unknown	Seepage meters combined with piezometer data	$4.67*10^7$ m^2 lake
Shaw et al, 1990	Mean values of 0.06 to 0.16, depending on method (SRP, TDP)	Unknown	Water balance, seepage meters and Darcy's law combined with piezometer concentrations	$1.1*10^6$ m^2 lake
McCobb et al, 2003	Mean value of 142 (P)	Sewage treatment plant	Groundwater flow model combined with groundwater concentrations	6100 m^2 shoreline
Jarvie et al, 2008	Mean values of 0.03 to 0.84, depending on location (SRP)	Sewage, agriculture	DET probes, measures diffusive flux	3 sites, catchment areas up to $5.59*10^8$ m^2
Spruill and Bratton, 2008	Range of 0-86, mean value of 19 (Ortho-P)	Organic-rich sediments	Mass balance, seepage meters and Darcy's law combined with piezometer concentrations	$4.55*10^8$ m^2 estuary
Rivett et al, 2011	Mean values of 323 to 933 (PO_4), depending on method	Urban and industrial	Combining baseflow values with piezometer concentrations	88800 m^2 river

The highest phosphorus fluxes values were determined by Rivett et al (2011) for groundwater discharging to a 7.4 km reach of the River Tame in Birmingham, UK. These values are four order of magnitude higher the results seen by Shaw et al (1990). This study was on a larger scale, with the distance between piezometer transects ranging from 100 m to 1 km. These high flux values may be attributed to historically heavy industrialization and seepage of untreated sewage. Concerns about the groundwater quality date back to the 19th century, however, the authors did not discuss possible sources and potential long-term trends in phosphorus flux. Although these phosphorus flux values are higher than observed at Dyment's Creek, groundwater was not considered to have a large impact on the river's water quality.

While there are just a few studies on SRP flux, elevated levels of shallow groundwater SRP (Carlyle and Hill, 2001; Banaszuk et al, 2005; Jarvie et al, 2008; Schilling and Jacobson, 2008; Flores-Lopez et al, 2011) are not uncommon in the literature. In addition, the potential sources of nutrients to the groundwater at Dyment's Creek, i.e. landfills and sediments under reducing conditions, are not unique to this stream. Thus, the findings at Dyment's Creek may be more broadly applicable.

This study was the first to measure nutrient flux in groundwater through a streambed of an urban stream a combination of heat tracer methods for measuring water flux and nutrient concentrations. An advantage of heat tracer methods is that they are a quick and inexpensive way to measure streambed water flux. Using a simpler heat tracer method, such as Turcotte and Schubert (1982), allowed sampling on a very fine sub-

metre scale. Combining this method with a more robust one, such as Hatch et al (2006) using VFLUX, provided greater confidence in the result. Using local hydraulic gradients to calculate flux using Darcy's Law was very useful to fill in temporal gaps at times when the heat tracer methods could not be used. Another unique aspect of this study was the fine scale of the data. While there have been fine scale studies of both water flux and concentrations, this is the first study to calculate nutrient flux on a sub-metre scale. This study showed that nutrient flux can be highly spatially variable, changing by orders of magnitude in less than 5 metres. When determining nutrient flux for a larger area, care must be taken to not miss localized areas of high discharge or solely capture these areas, as this may lead to inaccurate calculations of total mass discharge.

This method of combing heat tracers to measure water flux and nutrient concentration data can be applied to more streams in the Lake Simcoe watershed and elsewhere to estimate the contribution of groundwater to nutrient concentrations of those streams. While nutrient flux was the focus of Dyment's Creek, this method could also be used to measure the flux of other dissolved groundwater species of interest. An advantage of this method is that the only continuous data required are streambed temperature and pollutant concentration. Unlike mass balance discharge calculations, this method allows "hotspots" of nutrient flux to be identified, which can then be the focus of possible restoration efforts

7. References

Abe, Y., Aravena, R., Zopfi, J., Parker, B., & Hunkler, D. (2009). Evaluating the fate of chlorinated ethenes in streambed sediments by combining stable isotope, geochemical and microbial methods. *Journal of Contaminant Hydrology, 107*, 10-21. doi:10.1016/j.jconhyd.2009.03.002

Anderson, M. (2005). Heat as a ground water tracer. *Ground Water*(43), 951-968.

Anibas, C., Buis, K., Verhoeven, R., Meire, P., & Batelaan, O. (2011). A simple thermal mapping method for seasonal spatial patterns of groundwater--surface water interaction. *Journal of Hydrology, 397*, 93-104. doi:10.1016/j.jhydrol.2010.11.036

Anibas, C., Fleckenstein, J., Volze, N., Buis, K., Verhoeven, R., Meire, P., & Batelaan, O. (2009). Transient or steady-state? Using vertical temperature profiles to quantify groundwater --surface water exchange. *Hydrological Processes, 23*, 2165-2177.

Banaszuk, P., & Wysocka-Czubaszek, A. (2005). Phosphorus dynamics and fluxes in a lowland river: The Narew Anastomosing River System, NE Poland. *Ecological Engineering, 25*, 429-441. doi:10.1016/j.ecoleng.2005.06.013

Banaszuk, P., Wysocka-Czubaszek, & Kondratiuk, P. (2005). Spatial and temporal patterns of groundwater chemistry in the river riparian zone. *Agriculture Ecosystems & Environment, 107*, 167-179. doi:10.1016/j.agee.2004.11.004

Baresel, C., & Destouni, G. (2009). Diffuse subsurface zinc loads from mining areas in the Dala¨ lven River Basin, Sweden. *Hydrology Research, 40*, 445-544. doi:doi: 10.2166/nh.2009.013

Belanger, T. V., & Mikutel, D. F. (1985). On the use of seepage meters to estimate groundwater nutrient loading to lakes. *Water Resources Bulletin, 21*, 265-272.

Barrett, M. H., Hiscock, K. M., Pedley, S., Lerner, D. N., Tellam, J. H., & French, M. J. (1999). Marker Species for Identifying Urban Groundwater Recharge Sources: A Review and Case Study in Nottingham, UK. *Water Research, 33*, 3083-397.

Brady, N. C., & Weil, R. R. (2004). *The Elements of Nature and Properties of Soils* (Second Edition ed.). Upper Saddle River, New Jersey: Pearson Prentice-Hall.

Bredeheoft, J., & Papadopulos, I. (1965). Rates of Vertical Groundwater Movement Estimated from the Earth's Thermal Profile. *Water Resources Research, 1*, 325-328.

Briggs, M. A., Lautz, L. K., McKenzie, J. M., Gordon, R. P., & Harre, D. K. (2012). Using high-resolution distributed temperature sensing to quantify spatial and temporal variability in vertical hyporheic flux. *Water Resources Research, 48,* 1-16. doi:10.1029/2011WR011227

Brokelmann, A., Zamfirescu, D., Ptak, T., Grathwohl, P., & Teutsch, G. (2003). Quantification of mass fluxes and natural attenuation rates at an industrial site with a limited monitoring network: a case study. *Journal of Contaminant Hydrology, 60,* Journal of Contaminant Hydrology. Retrieved from www.elsevier.com/locate/jconhyd

Burkholder BK, Grant GE, Haggerty R, Khangaonkar T, & Wampler PJ. (2008). Influence of hyporheic flow and geomorphology on temperature of a large, gravel-bed river, Clackamas River, Oregon, USA. *Hydrological Processes* **22**: 941–953

Canadian Council of Ministers of the Environment. (2004). *Canadian water quality guidelines for the protection of aquatic life: Phosphorus: Canadian Guidance Framework for the Management of Freshwater Systems. In: Canadian environmental quality guidelines.* Gatineau, QC: Environment Canada. Retrieved from http://www.ec.gc.ca

Canadian Council of Ministers of the Environment. (2010). *Canadian water quality guidelines for the protection of aquatic life: Ammonia. In: Canadian environmental quality guidelines.* Gatineau, QC: Environment Canada. Retrieved from http://www.ec.gc.ca/ceqg-rcqe

Canadian Council of Ministers of the Environment. (2012). *Canadian water quality guidelines for the protection of aquatic life: Nitrate. In: Canadian environmental quality guidelines.* Gatineau, QC: Environment Canada. Retrieved from http://ceqg-rcqe.ccme.ca

Cardenas, M. B., Wilson, J. L., & Zlotnik, V. A. (2004). Impact of heterogeneity, bed forms, and stream curvature on subchannel hyporheic exchange. *Water Resources Research, 40,* 1-13. doi:10.1029/2004WR003008

Cardenas, B. (2010). *Thermal skin effect of pipes in streambeds and its implications on groundwater flux estimation using diurnal temperature signals.* doi:W03536, doi:10.1029/2009WR008528

Carlyle, G., & Hill, A. R. (2001). Groundwater Phosphate Dynamics in a River Riparian Zone: Effects of Hydrologic Flowpaths, Lithology and Redox Chemist. *Journal of Hydrology, 247*, 151-168.

Chambers, P. A., Guy, M., Roberts, E. S., Chariton, M. N., Kent, R., Gagnon, C., . . . Foster, N. (2001). *Nutrients and Their Impact on the Canadian Environment.* Agriculture and Agri-Food Canada, Environment Canada, Fisheries and Oceans Canada, Health Canada, and Natural Resources Canada.

Chang, K.-t. (2008). *Introduction to Geographic Information Systems* (Fourth Edition ed.). Toronto: McGraw-Hill.

Chapman, S. W., Parker, B. L., Cherry, J. A., Aravena, R., & Humkeler, D. (2007). Groundwater-surface water interaction and its role on TCE groundwater plume attenuation. *Journal of Contaminant Hydrology, 91*, 203-232.

Christensen, T. H., Bjerg, P. L., Banwart, S. A., Jakobsen, R., Heron, G., & Albrechtsen, H.-J. (2000). Characterization of redox conditions in groundwater contaminant plumes. *Journal of Contaminant Hydrology, 45*, 165–241.

Claret, C., & Boulton, A. J. (2009). Integrating hydraulic conductivity with biogeochemical gradients and microbial activity along river–groundwater exchange zones in a subtropical stream. *Hydrogeology Journal, 17*, 151-160. doi:10.1007/s10040-008-0373-3

Conant, B. J. (2004). Delineating and Quantifying Ground Water Discharge Zones Using Streambed Temperatures. *Ground Water, 41*, 647-656.

Conant, B. J., Cherry, J. A., & Gillham, R. W. (2004). A PCE groundwater plume discharging to a river: influence of the streambed and near-river zone on contaminant distribution. *Journal of Contaminant Hydrology, 73*, 249-279.

Constantz, J. (2008). *Heat as a tracer to determine streambed water exchanges.* doi:10.1029/2008WR006996

Constantz, J., Cox, M., & Su, G. (2003). Comparison of Heat and Bromide as Ground Water Tracers Near Streams. *Ground Water, 41*, 647-656.

Constantz, J., Stewart, A., Niswonger, R., & Sarma, L. (2002). Analysis of temperature profiles for investigating stream losses beneath ephemeral channels. *Water Resources Research, 38*, 1-13. doi:10.1029/2001WR001221

Coyne, A., Schafer, J., Dabrin, A., Girardot, N., & Blanc, G. (2007). Groundwater contributions to metal transport in a small river affected by mining and smelting waste. *Water Research, 41*, 3420 – 3428.

Cuthbert, M., MacKay, R., Durand, V., Aller, M.-F., Greswell, R. B., & Rivett, M. O. (2010). Effect of horizontal heat and fluid flow on the vertical temperature distribution in a semiconfining layer. *Advances in Water Resources, 13*, 1347-1358. doi:10.1016/j.advwatres.2010.09.014

Dale, R. K., & Miller, D. C. (2007). Spatial and temporal patterns of salinity and temperature at an intertidal groundwater seep. *Estuarine, Coastal and Shelf Science, 72*, 283-298. doi:10.1016/j.ecss.2006.10.024

DeVries, D. A. (1963). Thermal properties of soils. In W. R. Van Wijk (Ed.), *Physics of Plant Environment Second Edition* (pp. 210-235). Amsterdam, Netherlands: North-Holland Publishing Co. doi:10.1002/qj.49709038628

Dickman, M., & Rygiel, G. (1998). Municipal landfill impacts on a natural stream located in an urban wetland in Regional Niagara, Ontario. *Canadian Field-Naturalist, 112*, 619-630.

Dubrovsky, N. N., Burow, K. R., Clark, G. M., Gronberg, J. A., Hamilton, P. A., Hitt, K. J., and Wilber, W. G. (2010). The Quality of Our Nation's Water— Nutrients in the Nation's Streams and Groundwater, 1992–2004. *National Water Quality Assessment Program Circular 1350*, 174p.

Eisen, C., & Anderson, M.P. (1979). The Effects of Urbanization on Ground-Water Quality -- A Case Study. *Ground Water, 17*, 456-452.

Ellis, P. A., & Rivett, M. O. (2007). Assessing the impact of VOC-contaminated groundwater on surface water at the city scale. *Journal of Contaminant Hydrology, 91*, 107-127.

Fanelli, R., & Lautz, L. (2008). Patterns of Water, Heat, and Solute Flux through Streambeds around Small Dams. *Ground Water, 46*, 671-687. doi:10.1111/j.1745-6584.2008.00461.x

Fetter, C. W. (1999). *Contaminant Hydrogeology.* Waveland Press, Inc: Long Grove, IL

Flores-Lopez, F., Easton, Z. M., Geohring, L. D., & Steenhuis, T. S. (2011). Factors Affecting Dissolved Phosphorus and Nitrate Concentrations in Ground and Surface Water for a Valley Dairy Farm in the Northeastern United States. *Water Environment Research, 83,* 116-127. doi:10.2175/106143010X12681059116770

Freeze, R. A., & Cherry, J. A. (1979). *Groundwater.* Toronto: Prentice-Hall of Canada.

Fritz, B. G., & Arntzen, E. V. (2007). Effect of Rapidly Changing River Stage on Uranium Flux through the Hyporheic Zone. *Ground Water, 45,* 753–760. doi:10.1111/j.1745-6584.2007.00365.x

Fryar, A. E., Wallin, E. J., & Brown, D. L. (2000). Spatial and Temporal Variability in Seepage Between a Contaminated Aquifer and Tributaries to the Ohio River. *Ground Water Monitoring & Remediation, 20,* 129–146. doi:10.1111/j.1745-6592.2000.tb00279.x

Gardner, K. M., & Royer, T. V. (2010). Effect of Road Salt Application on Seasonal Chloride Concentrations and Toxicity in South-Central Indiana Streams. *Journal of Environmental Quality, 39,* 1036-1042. doi:10.2134/jeq2009.0402

Google. 2012. "Barrie, Ontario." Generated by Alex Fitzgerald; using Google Maps; < https://maps.google.ca/>. (September 20, 2012.

Gordon, R. P., Lauta, L. K., Briggs, M. A., & McKenzie, J. M. (2012). Automated calculation of vertical pore-water flux from field temperature time series using the VFLUX method and computer program. *Journal of Hydrology, 420-421,* 142-158. doi:10.1016/j.jhydrol.2011.11.053

Goto, S., Yamano, M., & Kinoshita, M. (2005). Thermal response of sediment with vertical fluid flow to periodic temperature variation at the surface. *Journal of Geophysical Research, 110,* 1-11. doi::10.1029/2004JB003419

Gougeon, R., Spidel, M., Lee, K., & Field, C. J. (2004). Canadian Diabetes Association National Nutrition Committee Technical Review: Non-nutritive Intense Sweeteners in Diabetes Management. *Canadian Journal of Diabetes, 28,* 385-399.

Hamonts, K., Kuhn, T., Maesen, M., Bonders, J., Lookman, R., Kalka, H., . . . DeJonghe, W. (2009). Factors Determining the Attenuation of Chlorinated Aliphatic Hydrocarbons in Eutrophic River Sediment Impacted by Discharging Polluted Groundwater. *Environmental Science and Technology, 43,* 5270–5275. doi:10.1021/es8035994

Harte, P. T., & Trowbridge, P. R. (2010). Mapping of road-salt-contaminated groundwater discharge and estimation of chloride load to a small stream in southern New Hampshire, USA. *Hydrological Processes, 24*, 2349–2368. doi:10.1002/hyp.7645

Harvey, J. W., & Bencala, K. E. (1993). The Effect of Streambed Topography on Surface-Subsurface Water Exchange in Mountain Catchments. *Water Resourses Research, 29*, 89-98.

Harvey, J. W., & Nuttle, W. (1995). 1. Fluxes of water and solute in a coastal wetland sediment. 2. Effect of micropores on solute exchange with surface water. *Journal of Hydrology, 64*, 109-125.

Harvey, J. W., Chambers, R. M., & Hoelscher, J. R. (1995). Preferential Flow and Segregation of Porewater Solutes in Wetland Sediment. *Estuaries , 18*, 568-578.

Hatch, C., Fischer, A., Revenaugh, J., & Reuhi, C. (2006). Quantifying surface water--groundwater interactions using time series analysis of thermal records: Method Development. doi:W10410, doi:10.1029/2005WR004787

Hatch, C., Fischer, A., Ruehl, C., & Stemler, G. (2010). Spatial and temporal variations in streambed hydraulic conductivity quantified with time-series thermal methods. *Journal of Hydrology, 389*, 276-288.

Hatt, B. E., Fletcher, T. D., Walsh, C. J., & Taylor, S. L. (2004). The Influence of Urban Density and Drainage Infrastructure on the Concentrations and Loads of Pollutants in Small Streams. *Environmental Management, 34*, 112-124. doi:10.1007/s00267-004-0221-8

Hazen, A. 1. (1911). Discussion—dams of sand foundations. *Transactions, 73*.

Healy, R. W., & Ronan, A. D. (1996). *Documentation of the computer program VS2DH for simulation of energy transport in variably saturated porous media-modification of the U.S. Geological Survey's computer program VS2DT.* U.S. Geological Survey.

Heeren, D. M., Fox, G. A., Miller, R. B., Storm, D. E., Fox, A. K., Penn, C. J., . . . Mittelstet, A. R. (2011). Stage-dependent transient storage of phosphorus in alluvial floodplains. *Hydrological Processes, 25*, 3230–3243. doi:10.1002/hyp.8054

Hesslein, R. H. (1976). An in Situ Sampler for Close Interval Pore Water Studies. *Limnology and Oceanography, 21*, 912-914. Howard, K. W., & Beck, P. J. (1993). Hydrogeochemical implications of groundwater contamination by road de-icing chemicals. *Journal of Contaminant Hydrology, 12*, 245-268.

Howard, K. W., Eyles, N., & Livingstone, S. (1996). Minicipal Landfilling Practice and Its Impact on Ground Water Resources in and Around Urban Toronto Canada. *Hydrology Journal, 4*, 64-79.

Howard, K. W., & Livingstone, S. (2000). Transport of urban contaminants into Lake Ontario via sub-surface flow. *Urban Water, 2*, 183-195.

Hubbart, J., Link, T., Campbell, c., & Cobos, D. (2005). Evaluation of a low-cost temperature measurement system for environmental applications. *Hydrological Processes, 19*, 1517-1523.

Hunt, R. J., Krabbenhoft, D. P., & Anderson, M. P. (1997). Assessing hydrogeochemical heterogeneity in natural and constructed wetlands. *Biogeochemistry, 39*, 271–293.

Hunt, R. J., Strand, M., & Walker, J. F. (2006). Measuring groundwater–surface water interaction and its effect on wetland stream benthic productivity, Trout Lake watershed, northern Wisconsin, USA. *Journal of Hydrology, 320*, 370–384. doi::10.1016/j.jhydrol.2005.07.029

Hvorslev, M. J. (1951). *Time lag and soil permeabilityin groundwater observations, Waterways Experimental StationBulletin No. 36.* Vicksburg, Miss.: U.S. Army Corps of Engineers.

Jarvie, H. P., Robert, J. G., Palmer-Feldgate, E. J., Quintom, K. S., Harman, S. A., & Carbo, P. (2008). Measurement of soluble reactive phosphorus concentration profiles and fluxes in river-bed sediments using DET gel probes. *Journal of Hydrology, 350*, 261– 273. doi:10.1016/j.jhydrol.2007.10.041

Johnson, A., Boer, B., Woessner, W., Stanford, J., Poole, G., Thomas, S., & O'Daniel, S. (2005). Evaluation of an Inexpensive Small-Diameter Temperature Logger for Documenting Ground Water-River Interactions. *Ground Water Monitoring & Remediation, 25*, 68–74.

Kalbus, E., Reinstorf, F., & Schirmer, M. (2006). Measuring methods for groundwater--surface water interactions: a review. *Ground Water Monitoring & Remediation, 10*, 68–74.

Kalbus, E., Schmidt, C., Beyer-Raich, M., Leschik, S., Reinstorf, F., Balcke, G., & Schirmer, M. (2007). New methodology to investigate potential contaminant mass fluxes at the stream--aquifer interface by combining integral pumping tests and streambed temperatures. *Environmental Pollution, 148*, 808-816.

Kannel, P. R., Lee, S., & Lee, Y.-S. (2008). Assessment of spatial–temporal patterns of surface and ground water qualities and factors influencing management strategy of groundwater system in an urban river corridor of Nepal. *Journal of Environmental Management, 86*, 595-604. doi:10.1016/j.jenvman.2006.12.021

Keery, J., Binley, A., Crook, N., & Smith, J. (2007). Temporal and spatial variability of groundwater--surface water fluxes: Development and application of an analytical method using temperature time series. *Journal of Hydrology, 336*, 1-16.

Kelly, V. J., Lynch, D. D., & Rounds, S. A. (1999). *Sources and Transport of Phosphorus and Nitrogen During Low-Flow Conditions in the Tualatin River, Oregon,1991-93.* U.S. Geological Survey Water-Supply Paper 2465-C.

Kelly, V. R., Lovett, G. M., Weathers, K. C., Findlay, S. E., Strayner, D. L., Burns, D. J., & Likens, G. E. (2008). Long-Term Sodium Chloride Retention in a Rural Watershed: Legacy Effects of Road Salt on. *Environmental Science and Technology, 42*, 410-415. doi:10.1021/es071391l

Kelly, W. R., Panno, S. V., Hackley, K. C., Hwang, H.-H., & Martinsek, A. T. (2010). Using chloride and other ions to trace sewage and road salt in the Illinois Waterway. *Applied Geochemistry, 25*, 661-673. doi:0.1016/j.apgeochem.2010.01.020

Kim, H., & Hemond, H. F. (1998). Natural Discharge of Volatile Organic Compounds from Contaminated Aquifer to Surface Waters. *Journal of Environmental Engineering, 124*, 744-751.

Krause, S., Blume, T., & Cassidy, T. J. (2010). Investigating patterns and controls of groundwater up-welling in a lowland river by combining Fibre-optic Distributed Temperature Sensing with observations of vertical hydraulic gradients. *Hydrology and Earth System Sciences, 16*, 1775–1792. doi:10.5194/hess-16-1775-2012

Krause, S., Hannah, D. M., Fleckenstein, J. H., Heppell, C. M., Kaeser, D., Pickup, R., & Wood, P. J. (2010). Inter-disciplinary perspectives on processes in the hyporheic zone. *Ecohydrology, 2010*. doi:0.1002/eco.176

Landmeyer, J. E., Bradley, P. M., Trego, D. A., Hale, K. G., & Haas, J. E. (2010). MTBE, TBA, and TAME Attenuation in Diverse Hyporheic Zones. *Ground Water, 48*, 30*41. doi:10.1111/j.1745-6584.2009.00608.x

Lapham, W. W. (1989). *Use of Temperature Profiles Beneath Streams to Determine Rates of Vertical Ground-Water Flow and Vertical Hydraulic Conductivity.* Denver, Co: U.S. Geological Survey - Water Supply Paper; 2337.

Lapworth, D. J., Gooddy, D. C., and Jarvie, H. P. (2011). Understanding Phosphorus Mobility and Bioavailability in the Hyporheic Zone of a Chalk Stream. *Water, Soil, and Air Pollution, 218, 213-226*

LaSage, d. M., Fryar, A. e., Mukherjee, A., Sturchio, N. C., & Heraty, L. J. (2008). Groundwater-derived contaminant fluxes along a channelized Coastal Plain stream. *Journal of Hydrology, 360*, 265– 280. doi:0.1016/j.jhydrol.2008.07.026

Lautz, L. (2010). Impacts of nonideal field conditions on vertical water velocity estimates from streambed temperature time series. *Water Resources Research, 46*. doi:W01509. doi:10.1029/2009WR007917

Lautz, L., Kranes, N., & Siegel, D. (2010). Heat tracing of hetergeneous hyporheic exchange adjacent to in-stream geomorphic features. *Hydrological Processes, 24*, 3074-3086. doi:10.1002/hyp.7723

Lee, R. (1977). A Device for Measuring Seepage Flux in Lakes and Estuaries. *Liminology and Oceanography, 22*, 140-147.

Lendvay, J. M., Sauck, W. A., McCormick, M. L., Barcelona, M. J., Kampbell, D. H., Wilson, J. T., & Adriaen, P. (1998). Geophysical characterization, redox zonation, and contaminant distribution at a groundwater/surface water interface. *Water Resources Research, 34*, 3545-3559,.

Lorah, M. M., Cozzarelli, I. M., & Bohkeet, J. K. (2009). Biogeochemistry at a wetland sediment-alluvial aquifer interface in a landfill leachate plume. *Journal of Contaminant Hydrology, 105*, 99-107. doi:10.1016/j.jconhyd.2008.11.008

Lorah, M. M., & Olsen, L. D. (1999). Natural attenuation of chlorinated volatile organic compounds in a freshwater tidal wetland: Field evidence of anaerobic biodegradation. *Water Rosources Research, 35*, 3811-3827.

Lu, N., & Ge, S. (1966). Effect of horizontal heat and fluid flow on the vertical temperature distribution in a semiconfining layer. *Water Resources Research, 52*, 1449-1453.

Lyford, F. P., Flight, L. E., Stone, J. R., & Clifford, S. (1999). *Distribution of Trichloroethylene and Geologic Controls on Contaminant Pathways near the Royal River, McKin Superfund Site Area, Grey, Maine.* U.S. Environmental Protection Agency. U.S. Geological Survey .

Maier, H. S., & Howard, K. W. (2011). Influence of Oscillating Flow on Hyporheic Zone Development. *Ground Water, 49*, 830-844. doi:10.1111/j.1745-6584.2010.00794.x

Mayes, W. M., Gozzard, E., Potter, H. A., & Jarvis, A. P. (2008). Quantifying the importance of diffuse minewater pollution in a historically heavily coal mined catchment. *Environmental Pollution, 151*, 165-175. doi:10.1016/j.envpol.2007.02.008

McCobb, T. D., Leblanc, D. R., Walter, D. A., Hess, K. M., Kent, D. B., & Smith, R. L. (2003). *Phosphorus in a Ground-Water Contaminant Plume Discharging to Ashumet Pond, Cape Cod, Massachusetts, 1999.* Toxic Substances Hydrology Program, U.S. Department of the Interior. U.S. Geological Survey.

McKnight, U. F. (2010). An integrated model for assessing the risk of TCE groundwater contamination to human receptors and surface water ecosystems. *Ecological Engineering, 36*, 1126-1137.

McMahon, P., B., & Chapelle, F. H. (2008). Redox Processes and Water Quality of Selected Principal Aquifer Systems. *Ground Water, 46*, 259–271. doi:10.1111/j.1745-6584.2007.00385.x

Melosevic, N., Thomsen, N. I., Juhler, R. K., Albrechtsen, H.-J., & Bjerg, P. L. (2012). Identification of discharge zones and quantification of contaminant mass discharges into a local stream from a landfill in a heterogeneous geologic setting. *Journal of Hydrology, 446-447*, 13-23. doi:10.1016/j.jhydrol.2012.04.012

Meriano, M., Eyles, N., & Howard, K. W. (2009). Hydrogeological impacts of road salt from Canada's busiest highway on a Lake Ontario watershed (Frenchman's Bay) and lagoon, City of Pickering. *Journal of Contaminant Hydrology, 107*, 66-81. doi:0.1016/j.jconhyd.2009.04.002

Meyer, J. L., Paul, M. J., & Taulbee, W. (2005). Stream ecosystem function in urbanizing landscapes. *The North American Benthological Society, 24*, 602-612.

Ministry of the Enviornment, Ontario. (2009). *Resources: Lake Simcoe Protection Plan.* Retrieved from Ministry of the Enviornmrnt, Ontario: http://www.ene.gov.on.ca/environment/en/resources/STD01_076301.html

Ministry of the Enviornment, Ontario. (2012). *Local Projects : Lake Simcoe Protection*. Retrieved from Ministry of the Enviornment, Ontario: http://www.ene.gov.on.ca/environment/en/local/lake_simcoe_protection/index.htm

Mullaney, J. R., Lorenz, D. L., & Arntson, A. D. (2009). Chloride in Groundwater and Surface Water in Areas Underlain by the Glacial Aquifer System, Northern United States. *U.S. Geological Survey Scientific Investigations Report, 5086*, 41p. Retrieved from http://www.usgs.gov/pubprod

Mutiti, S., & Levy, J. (2010). Using temperature modeling to investigate the temporal variability of riverbed hydraulic conductivity during storm events. *Journal of Hydrology, 2010*, 321-334.

Nagorsk, S. A., & Moore, J. N. (1999). Arsenic mobilization in the hyporheic zone of a contaminated stream. *Water Resources Research, 1999*, 3441-3450.

Nicholls, K. H. (1992). *Water Quality Trends in Lake Simcoe 1972-1990, Implications for Basin Planning and Limnological Research Needs.* Newmarket, Ontario.: Lake Simcoe Region Conservation Authority, .

Null, K. A., Corbett, D. R., DeMaster, D. J., Burkholder, J. M., Thomas, C. J., & Reed, R. E. (2011). Porewater advection of ammonium into the Neuse River Estuary, North Carolina, USA. *Estuarine, Coastal and Shelf Science, 95*, 314-325. doi:10.1016/j.ecss.2011.09.016

Orghidan, O. (1955). A new habitat of subsurface waters: the hyporheic biotope (translation, 2010). *Archiv fur Hydrobiologie (Germany), 176*, 291-302. doi:10.1127/1863-9135/2010/0176-0291

Palmer-Felgate, E. J., Jarvie, H. P., Williams, R. J., Mortimer, R. J., Loewenthal, M., & Neal, c. (2008). Phosphorus dynamics and productivity in a sewage-impacted lowland chalk stream. *Journal of Hydrology, 351*, 87-97. doi:10.1016/j.jhydrol.2007.11.036

Palmer-Felgaqte, E. J., Mortimer, R. J., Krom, M. D., & Jarvie, H. P. (2010). Impact of Point-Source Pollution on Phosphorus and Nitrogen Cycling in Stream-Bed Sediments. *Environmental Science and Technology, 44*, 908–914. doi:10.1021/es902706r

Parsons, M. L. (1970). Groundwater thermal regime in a glacial complex. *Water Resources Research, 6*, 1701–1720.

Paul, M. J., & Meyer, J. L. (2001). Streams in the Urban Landscape. *Annual Review of Ecology and Systematics, 32*, 333-365.

Pretty, J. L., Hildrew, A. G., & Trimmer, M. (2006). Nutrient dynamics in relation to surface–subsurface hydrological exchange in a groundwater fed chalk stream. *Journal of Hydrology, 330*, 84– 100. doi:10.1016/j.jhydrol.2006.04.013

Ptacek, C. J. (1998). Geochemistry of a septic-system plume in a coastal barrier bar, Point Pelee, Ontario, Canada. *Journal of Contaminant Hydrology, 33*, 293-312.

Qian, J., Wang, L., Zhan, H., & Chen, Z. (2011). Urban land-use effects on groundwater phosphate distribution. *Hydrogeology Journal, 19*, 1431-1442. doi:10.1007/s10040-011-0770-x

Rau, G., Andersen, M., McCallum, A., & Acworth, R. (2010). Analytical methods that use natural heat as a tracer to quantify surface water-groundwater exchange, evaluated using field temperature records. *Hydrogeology Journal, 18*, 1093-1110.

Reay, G. W., Gallagher, D. L., & Simmons, G. M. (1992). Groundwater Discharge and its Impact on Surface Water Quality in a Chesapeake Bay Inlet. *Water Resources Bulletin, 28*, 1121-1134.

Revil, A. (2000). Thermal conductivity of unconsolidated sediments with geophysical applications. *The Journal of Geophysical Research, 105*, 16,749-16,768.

Rivett, M. O., Ellis, P. A., & Mackay, R. (2011). Urban groundwater baseflow influence upon inorganic river-water quality: The River Tame headwaters catchment in the City of Birmingham, UK. *Journal of Hydrology, 400*, 206-222. Retrieved from www.elsevier.com/locate/jhydrol

Robertson, A. L., & Wood, P. J. (2010). Ecology of the hyporheic zone: origins, current knowledge and future directions. *Fundamental and Applied Limnology, Archiv für Hydrobiologie, 176/4*, 279-289. doi:10.1127/1863-9135/2010/0176-0279

Rosenberry, D. O., & LaBaugh, J. W. (2008). *Field techniques for estimating water fluxes between surface water and ground water* (Vols. Techniques and Methods 4–D2). (D. a. Rosenberry, Ed.) U.S. Geological Survey.

Rosenberry, D. O., & Pitlick, J. (2009). Effects of sediment transport and seepage direction on hydraulic properties at the sediment–water interface of hyporheic settings. *Journal of Hydrology, 373*, 377–391. doi:10.1016/j.jhydrol.2009.04.030

Roshan, H., Rau, G. C., Andersen, M. S., & Acworth, I. R. (2012). Use of heat as tracer to quantify vertical streambed flow in a two-dimensional flow field. *Water Resources Research, 48, 1-16. doi:10.1029/2012WR011918*

Roy, J. W., & Bickerton, G. (2010). Proactive Screening Approach for Detecting Groundwater Contaminants along Urban Streams at the Reach-Scale. *Environmental Science and Technology, 44*, 6088–6094. doi:10.1021/es101492x

Roy, J. W., & Bickerton, G. (2012). Toxic Groundwater Contaminants: An Overlooked Contributor to Urban Stream Syndrome? *Environmental Science and Technology, 46*, 729-736. doi:10.1021/es2034137

Roy, J. W., Robillard, J. M., Watson, S. B., & Hayashi, M. (2009). Non-intrusive characterization methods for wastewater-affected groundwater plumes discharging to an alpine lake. *Environmental Montoring and Assessment, 149*, 201–211. doi:10.1007/s10661-008-0194-9

Roy, J. W., Zaitlin, B., Hayashi, M., & Watson, S. B. (2010). Influence of groundwater spring discharge on small-scale spatial variation of an apline stream ecosystem. *Ecohydrology, 4*, 661–670. doi:10.1002/eco.156

Rozemeijer, J. v. (2010). Direct measurements of the tile drain and groundwater flow route contributions to surface water contamination: From field-scale concentration patterns in groundwater to catchment-scale surface water quality. *Environmental Pollution, 158*, 3571-3579.

Ryan, R. W. (2010). Natural Discharge of Volatile Organic Compounds from Contaminated Aquifer to Surface Waters. *Journal of Hydrology, 392*, 1-11.

Schilling, K. E., & Jacobson, P. (2008). Groundwater nutrient concentrations near an incised midwestern stream: eVects of Xoodplain lithology and land management. *Biogeochemistry, 87*, 199-216.

Schmidt, C., Bayer-Raich, M., & Schirmer, M. (2006). Characterization of spatial heterogeneity of groundwater-stream water interactions using multiple depth streambed temperature measurements at the reach scale. *Hydrology and Earth System Science Discussion, 3*, Hydrology and Earth System Science Discussion.

Schmidt, C., Conant, J. B., Bayer-Raich, M., & Schirmer, M. (2007). Evaluation and field-scale application of an analytical method to quantify groundwater discharge using mapped streambed temperatures. *Evaluation and field-scale application of an analytical method to quantify groundwater discharge using mapped streambed temperatures., 3*, 1419-1446.

Schmidt, C., Martienssen, M., & Kalbus, E. (2011). Influence of water flux and redox conditions on chlorobenzene concentrations in a contaminated streambed. *Hydrological Processes, 25*, 234-245. doi:10.1002/hyp.7839

Shaw, J. F., & Prepas, E. E. (1989). Temporal and Spatial Patterns of Porewater Phosphorus in Shallow Sediments, and its Potential Transport into Narrow Lake, Alberta. *Canadian Journal of Fisheries and Aquatic Sciences, 46*, 981-988.

Shaw, R. D., Shaw, J. F., Fricker, H., & Prepas, E. E. (1990). An integrated approach to quantify groundwater transport of phosphorus to Narrow Lake, Alberta. *Limnology and Oceanography, 35*, 870-886.

Sheldrick, B. H., & Wang, C. (2007). Particle Size Distribution. In M. R. Carter, E. G. Gregorich, M. R. Carter, & ,. E. Gregorich (Eds.), *Soil Sampling and Methods of Analysis, Second Edition* (pp. 713-725). Boca Raton, Florida: CRC Press, Taylor & Francis Group, Informa.

Shepherd, K. A., Ellis, P. A., & Rivett, M. O. (2006). Integrated Understanding of urban land, groundwater, baseflow, and surface-water quality—The City of Birmingham, UK. *Science of the Total Environment, 306*, 180-195. doi:10.1016/j.scitotenv.2005.08.052

Silliman, S., & Booth, D. (1993). Analysis of time-series measurements of sediment temperature for identification of gaining vs losing portions of Juday Creek, Indiana. *Journal of Hydrology, 146*, 131-148.

Silliman, S., Ramirez, J., & McCabe, R. (1995). Quantifying downflow through creek sediments using temperature time series: one-dimensional solution incorporating measured surface temperature. *Journal of Hydrology, 167*, 99-119.

Smith, J. a. (2008). Geomorphic control on pollutant retardation at the groundwater-surface water interface. *Hydrological Processes, 22*, 4679-4694.

Smolders, A. J., Lucassen, E. C., Bobink, R., Roelofs, J. G., & Lamers, L. P. (2010). How nitrate leaching from agricultural lands provokes phosphate eutrophication in groundwater fed wetlands: the sulphur bridge *Biogeochemistry, 98, 1-7.* doi:10.1007/s10533-009-9387-8

Soulsby, C., Tetzlaff, D., van den Bedem, N., Malcolm, I. A., Bacon, P. J., & Youngson, a. F. (2007). Inferring groundwater influences on surface water in montane catchments from hydrochemical surveys of springs and streamwaters. *Journal of Hydrology, 333*, 199-213. doi:10.1016/j.jhydrol.2006.08.016

Spruill, T. B., & Bratton, J. F. (2008). Estimation of Groundwater and Nutrient Fluxes to the Neuse River Estuary, North Carolina. *US Geological Survey, Estuaries and Coasts, 31*, 501–520. doi:10.1007/s12237-008-9040-0

Stallman, R. (1965). Steady One-Dimensional Fluid Flow in a Semi-Infinite Porous Medium with Sinusoidal Surface Temperature. *Journal of Geophysical Research, 70*, 2821-2827.

Stelzer, R. S., Bartsc, L. S., Richardson, W. B., & Strauss, E. A. (2011). The dark side of the hyporheic zone: depth profiles of nitrogen and its processing in stream sediments. *Freshwater Biology, 56*, 2021-2033. doi:10.1111/j.1365-2427.2011.02632.x

Stonestrom, D., & Constantz, J. (2003). *Heat as a tool for studying the movement of ground water nears streams.* U.S. Geological Survey.

Suzuki, S. (1960). Percolation Measurements Based on Heat Flow Through Soil with Special Reference to Paddy Fields. *Journal of Geophysical Research , 64*, 2821-2827.

Triska, F. J., Kennedy, V. C., Avanzino, R. J., Zellweger, G. W., & Bencala, K. E. (1989). Retention and Transport of Nutrients in a Third-Order Stream in Northwestern California: Hyporheic Processes. *70*, 1893-1905. Retrieved from http://www.jstor.org/stable/1938120 .

Turcott, D., & Schubert, G. (1982). *Geodynamics: Applications of Continuum Physics to Geological Problems.* Toronto: John Wiley and Sons:.

Turnipseed, D.P., and Sauer, V.B. (2010). Discharge measurements at gaging stations: U.S. Geological Survey Techniques and Methods book 3, chap. A8, 87p.

Van Stempvoort, D. R., Roy, R. W., Brown, S. J., & Bickerton, G. (2011). Artificial sweeteners as potential tracers in groundwater in urban environments. *Journal of Hydrology, 40*, 126–133. doi:10.1016/j.jhydrol.2011.02.013

Vazquez-Sune, E., Sanchez-Vila, X., & Carrera, J. (2005). Introductory review of specific factors influencing urban groundwater, an emerging branch of hydrogeology, with reference to Barcelona, Spain. *Hydrogeology Journal*, *13*, 522-533.

Vogt, T., Schneider, P., Hahn-Woernle, L., & Cirpka, O. A. (2010). Estimation of seepage rates in a losing stream by means of fiber-optic high-resolution vertical temperature profiling. *Journal of Hydrology, 380*, 154-164. doi::10.1016/j.jhydrol.2009.10.033

Vroblesky, D. A., Lorah, M. M., & Trimble, S. P. (1991). Mapping Zones of Contaminated Ground-Water Discharge Using Creek-Bottom_Sediment Vapour Samplers, Aberdeen Proving Ground, Maryland. *Ground Water, 1*, 1-12.

Vroblesky, D. A., Rhodes, L. C., Robertson, J. F., & Harrigan, J. A. (1996). Locatinf VOC Contamination in a Fractured-Rock Aquifer at the Ground-Water/Surface-WaterInterface Using Passive Vapour Coolers. *Ground Water, 34*, 223-230.

Walsh, C. J., Roy, A. H., Feminella, J. W., Cottingham, P. D., Groffman, P. M., & Morgan II, R. P. (2005). The urban stream syndrome: current knowledge and the search for a cure. *Journal of the North American Benthological Society, 34*, 706-723.

Williams, D. D., Williams, N. E., & Cao, Y. (1999). Road salt contamination of groundwater in a major metropolitan area and development of a biological index to monitor its impact. *Water Research, 34*, 127-138.

Winde, F., & van der Walt, I. J. (2004). The significance of groundwater–stream interactions and fluctuating stream chemistry on waterborne uranium contamination of streams—a case study from a gold mining site in South Africa. *Journal of Hydrology, 287*, 178-196. doi:10.1016/j.jhydrol.2003.10.004

Winter, T. C., Harvey, J. W., Framke, O. L., & Alley, W. M. (1998). *Ground Water and Surface Water A Single Resource.* U.S. GEOLOGICAL SURVEY.

Woessner, W. (2000). Stream and Fluvial Plain Ground Water Interactions: Rescaling Hydrogeologic Thought. *Ground Water, 38*, 423-429.

Young, P. C., Pedregal, D. J., & Tych, W. (1999). Dynamic Harmonic Regression. *Journal of Forecasting, 18*, 369-394.